AD-A055 721 DAVID W TAYLOR NAVAL SHIP RESEARCH AND DEVELOPMENT CE--ETC F/G 14/2
ROTATING ARM EXPERIMENTS FOR THE STABLE SEMI-SUBMERGED PLATFORM--ETC(U)
SEP 77 J A FEIN

UNCLASSIFIED DTNSRDC/SPD-698-02

NL

1 OF 2
AD
A055721

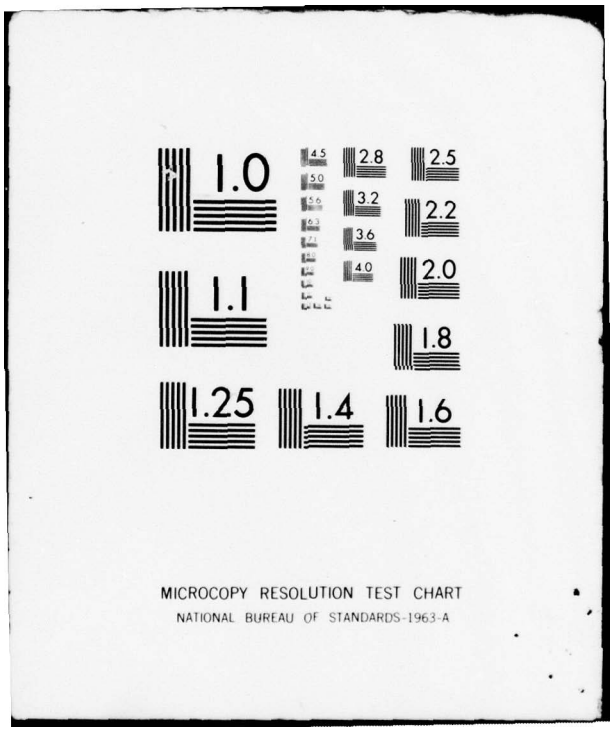
1.0
1.1
1.25
1.4
1.6
1.8
2.0
2.2
2.5
2.8
3.2
3.6
4.0
4.5
5.0
5.6
6.3
7.1
MICROCOPY RESOLUTION TEST CHART
NATIONAL BUREAU OF STANDARDS-1963-A

(12)

DAVID W. TAYLOR NAVAL SHIP RESEARCH AND DEVELOPMENT CENTER

Bethesda, Md. 20084

(6) ROTATING ARM EXPERIMENTS FOR THE STABLE SEMI-SUBMERGED PLATFORM (SSP) MANEUVERING PREDICTIONS,

by

(10) James A. Fein

APPROVED FOR PUBLIC RELEASE: DISTRIBUTION UNLIMITED

SHIP PERFORMANCE DEPARTMENT

(11) September 1977 (12) 137p. (14) DTNSRDC SPD-698-02

MAJOR DTNSRDC ORGANIZATIONAL COMPONENTS

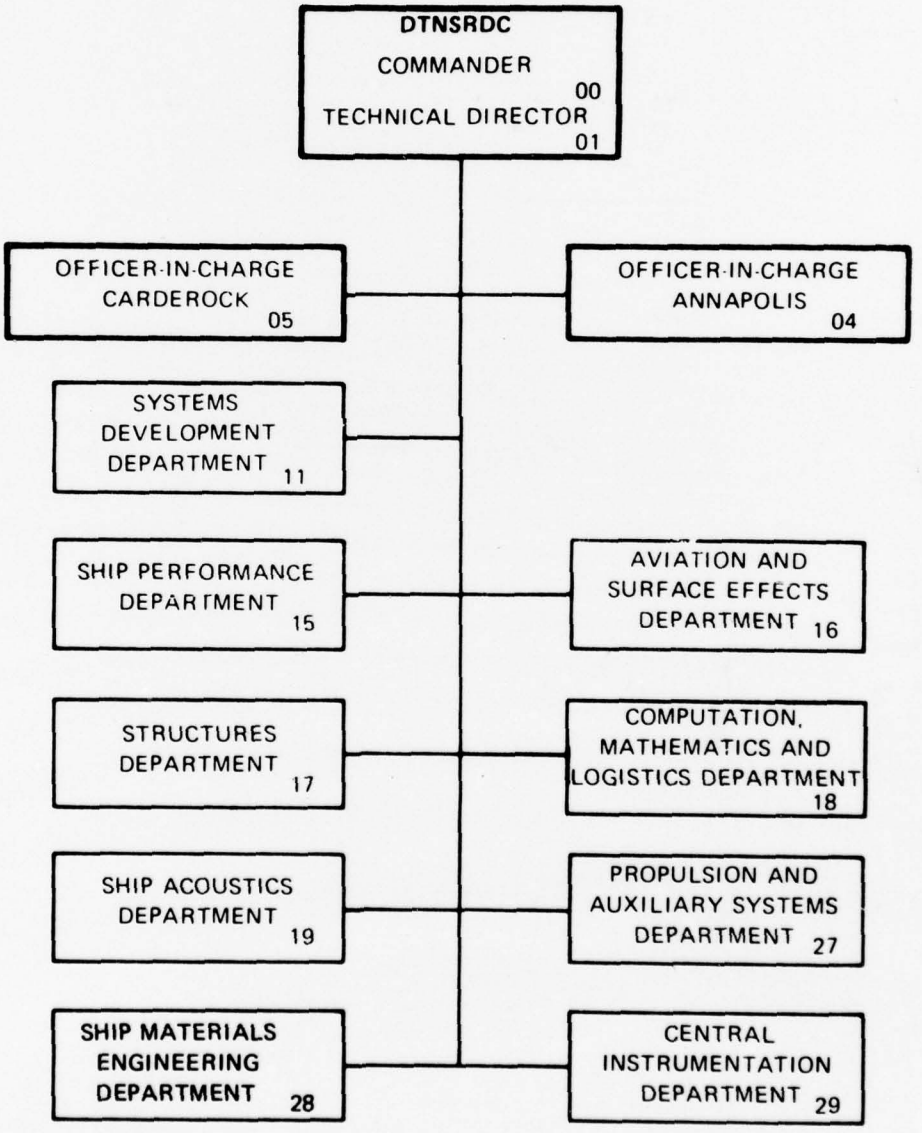

UNCLASSIFIED

SECURITY CLASSIFICATION OF THIS PAGE (When Data Entered)

REPORT DOCUMENTATION PAGE		READ INSTRUCTIONS BEFORE COMPLETING FORM
1. REPORT NUMBER SPD-698-02	2. GOVT ACCESSION NO.	3. RECIPIENT'S CATALOG NUMBER
4. TITLE (and Subtitle) ROTATING ARM EXPERIMENTS FOR THE STABLE SEMI-SUBMERGED PLATFORM (SSP) MANEUVERING PREDICTIONS		5. TYPE OF REPORT & PERIOD COVERED 6. PERFORMING ORG. REPORT NUMBER
7. AUTHOR(s) JAMES A. FEIN		8. CONTRACT OR GRANT NUMBER(s)
9. PERFORMING ORGANIZATION NAME AND ADDRESS David W. Taylor Naval Ship Research and Development Center Bethesda, Maryland 20084		10. PROGRAM ELEMENT, PROJECT, TASK AREA & WORK UNIT NUMBERS 1-1500-100-37
11. CONTROLLING OFFICE NAME AND ADDRESS NAVSEA, CODE 03		12. REPORT DATE September 1977 13. NUMBER OF PAGES 119
14. MONITORING AGENCY NAME & ADDRESS(if different from Controlling Office)		15. SECURITY CLASS. (of this report) 15a. DECLASSIFICATION/DOWNGRADING SCHEDULE
16. DISTRIBUTION STATEMENT (of this Report) APPROVED FOR PUBLIC RELEASE: DISTRIBUTION UNLIMITED		
17. DISTRIBUTION STATEMENT (of the abstract entered in Block 20, if different from Report)		
18. SUPPLEMENTARY NOTES		
19. KEY WORDS (Continue on reverse side if necessary and identify by block number) Maneuvering, Rotating Arm, SWATH		

20. ABSTRACT (Continue on reverse side if necessary and identify by block number)

This report contains the results of model experiments conducted on the rotating arm facility at the David W. Taylor Naval Ship Research and Development Center (DTNSRDC) in order to determine the horizontal plane characteristic of a Stable Semi-Submerged Platform (SSP). Nondimensional coefficients for the side force, yaw moment, and roll moment at a wide range of speed, drift angle, draft, roll angle, positive and negative yaw rate and rudder deflections are reported in graphical form. Also, comparisons with straight line

next page

DD FORM 1 JAN 73 1473 EDITION OF 1 NOV 65 IS OBSOLETE
S/N 0102-014-6601

UNCLASSIFIED
SECURITY CLASSIFICATION OF THIS PAGE (When Data Entered)

experiments are presented. The results presented privide a sufficient data base for simulation studies of craft turning.

TABLE OF CONTENTS

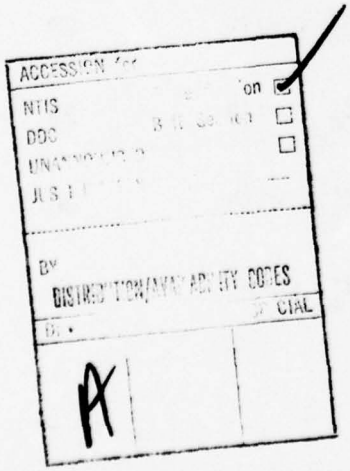

LIST OF FIGURES

LIST OF FIGURES (Cont'd)

LIST OF FIGURES (Cont'd)

LIST OF FIGURES (Cont'd)

LIST OF FIGURES (Cont'd)

LIST OF FIGURES (Cont'd)

LIST OF FIGURES (Cont'd)

LIST OF FIGURES (Cont'd)

LIST OF FIGURES (Cont'd)

LIST OF FIGURES (Cont'd)

NOMENCLATURE

Physical Quantities

ρ	density of water
L	length (overall)
U	linear velocity of craft
g	gravitational constant
R	radius of rotating arm
β	drift angle
ϕ	roll angle
δ_r	rudder angle
$r' = L/R$	nondimensional yaw rate
$v' = -\sin \beta$	nondimensional sway velocity

Nondimensional Body Axis Forces and Moments

$K' = \frac{K}{(\rho/2)\, L^3U^2}$	roll moment coefficient
$M' = \frac{M}{(\rho/2)\, L^3U^2}$	pitch moment coefficient
$N' = \frac{N}{(\rho/2)\, L^3U^2}$	yaw moment coefficient
$X' = \frac{X}{(\rho/2)\, L^2U^2}$	axial force coefficient
$Y' = \frac{Y}{(\rho/2)\, L^2U^2}$	lateral force coefficient
$Z' = \frac{Z}{(\rho/2)\, L^2U^2}$	vertical force coefficient

Nondimensional Derivatives

(The zero subscript indicates derivative is taken at point at which independent variable is zero).

$$N_r' = \left(\frac{\partial N'}{\partial r'}\right)_o$$

$$Y_r' = \left(\frac{\partial Y'}{\partial r'}\right)_o$$

$$K_r' = \left(\frac{\partial K'}{\partial r'}\right)_o$$

$$N_v' = \left(\frac{\partial N'}{\partial v'}\right)_o$$

$$Y_v' = \left(\frac{\partial Y'}{\partial v'}\right)_o$$

$$K_v' = \left(\frac{\partial K'}{\partial v'}\right)_o$$

$$N_{\delta_r}' = \left(\frac{\partial N'}{\partial \delta_{r'}}\right)_o$$

$$Y_{\delta_r}' = \left(\frac{\partial Y'}{\partial \delta_{r'}}\right)_o$$

$$K_{\delta_r}' = \left(\frac{\partial K'}{\partial \delta_{r'}}\right)_o$$

$$N_\phi' = \left(\frac{\partial N'}{\partial \delta_{r'}}\right)_o$$

$$Y_\phi' = \left(\frac{\partial Y'}{\partial \phi'}\right)_o$$

$$K_\phi' = \left(\frac{\partial K'}{\partial \phi'}\right)_o$$

ABSTRACT

This report contains the results of model experiments conducted on the rotating arm facility at the David W. Taylor Naval Ship Research and Development Center (DTNSRDC) in order to determine the horizontal plane characteristics of a Stable Semi-Submerged Platform (SSP). Nondimensional coefficients for the side force, yaw moment, and roll moment at a wide range of speed, drift angle, draft, roll angle, positive and negative yaw rate and rudder deflections are reported in graphical form. Also, comparisons with straight line experiments are presented. The results presented provide a sufficient data base for simulation studies of craft turning.

ADMINISTRATIVE INFORMATION

This work was supported by the Naval Seas Systems Command under the direction of Code 1507, at the David W. Taylor Naval Ship Research and Development Center, Work Unit Number 1-1500-100-37.

INTRODUCTION

An extensive rotating arm experimental program was conducted on the Stable Semi-submerged Platform (SSP KAIMALINO), a SWATH ship represented by a 1/7.8 scale model (DTNSRDC Model 5267). These experiments were conducted in order to evaluate the horizontal plane characteristics of the SSP KAIMALINO, an existing large scale SWATH, and to provide additional verification of the rotating arm experimental technique. Horizontal plane characteristics can be deduced from the experimental data measured. Verification of the rotating arm experimental procedures is demonstrated by the agreement between results for both positive and negative turn rates and by the agreement between rotating arm results extrapolated to zero turn rate and straight-line results from a previous experiment. The data from these experiments have been incorporated in a mathematical model that can be employed to predict turning capability.

Experiments were conducted at nondimensional yaw rates, ranging from -0.1316 to 0.4242 on the Rotating Arm Facility corresponding to speeds of 3 to 21 knots full scale. The craft was completely captive with respect to the towing rig throughout the experiment. Forces and moments were measured and recorded in all six degrees of freedom, with respect to the coordinate system illustrated in Figure 1. This report includes a description of the model, a discussion of test procedures, an analysis of the data, an interpretation of the test results and pertinent conclusions.

DESCRIPTION OF MODEL

Detailed geometric characteristics of the model of the SSP are given in Table 1. The configuration of the vehicle includes two parallel submerged bodies of revolution that provide buoyancy and house propulsion and other equipment. The bodies are connected aft by a hydrofoil which provides vertical stability and control. Photographs of bow, and a side view of the experimental model are illustrated in Figures 2 and 3 respectively. As illustrated by the photos, the

above-water platform is supported by two vertical surface-piercing struts attached to each pod. The model was constructed to a linear ratio of 7.8 according to drawings provided by the Naval Ocean Systems Center (NOSC), Hawaii. The prototype, which is described in detail in Reference 1*, is a workboat currently being used at NOSC, Hawaii. Fairly extensive full sclae trials have been conducted on SSP and are reported in References 2 and 3.

EXPERIMENTAL EQUIPMENT AND PROCEDURES

The model was completely captive with respect to the tow rig and was rigidly attached to a structural channel through spacer blocks at 2 points. Two gage assemblies were bolted to the channel, each containing three modular force balances oriented along the body axis to measure longitudinal, lateral, and normal force components. In addition, one modular force balance was mounted on the port side of the bridging structure at the LCG to measure roll force at a prescribed moment arm. Gage assembly locations are shown in Figure 4. A photograph of an experimental test is shown in Figure 5.

The three gage assemblies were connected to struts mounted on the surface ship towing beam of the Rotating Arm Towing Carriage. Each strut connection had a yaw, pitch, and roll pivot. In addition, each strut could be independently adjusted in the vertical direction to effect change in draft. This arrangement provided all force components at each of the struts attached to the channel and allowed pitching and yawing moments to be calculated about the reference point half-way between the two struts at the LCG. The moment arm for these calculations was the distance from the reference point to the center of the struts.

The roll angle of the model was set by adjusting the height of the strut which was attached to the roll force block gage at the edge of the bridging structure. This strut was adjusted each time the roll angle was changed so that only the body vertical-axis force was transmitted. For each run at a non-zero roll angle the gages were adjusted

*Complete list of References on Page 13.

to zero at standstill in order to cancel the roll moment due to buoyancy. Yaw angle was set by rotating the entire apparatus from above. The model was set at zero pitch angle throughout the experiments. Rudder angle was changed by a servo-actuator mounted on the model.

The force measurement outputs were integrated over a standard time of 6 seconds and multiple samples were taken. All forces, angle settings and carriage speed values were stored on stripcharts.

Centripetal tares were calculated using the model mass and the carriage rotational speed. Tares were removed and all forces and moments calculated about the reference point by the computer program described in the next section.

The design displacement was maintained at 395 kilograms (871 pounds) throughout the experimental program. This corresponds to a design draft of 59.7 centimeters (23.50 inches) model scale. A deep draft condition of 69.9 centimeters (27.50 inches) was also tested. The draft was set by screw jacks and measured optically at the beginning of each condition then checked periodically throughout the experimental program. The water level was carefully monitored and kept at the proper level.

The actual CG position of the model which was used in correcting the data was obtained from standstill measurements in water at various roll and trim angles.

The experimental program included variations of drift angle, roll angle, speed, draft, rudder deflection angle, propeller RPM, and radius, i.e., distance from center of the rotating arm. Also, some experiments were conducted at negative turn rates. The propeller RPM was adjusted to provide self propulsion of the model except at the highest speed where the maximum motor power was used. The RPM was varied from these values at various speeds in order to investigate propulsion effects on the hydrodynamic forces and moments. The ranges of all the variables were chosen to represent realistic operating conditions and to develop a data base for maneuvering predictions. Combinations of variables were often examined and repeat points were obtained. Radius was limited by the size of the Rotating Arm Facility

and the need to prevent interference and reflection from the beach. All data was collected during a single pass around the tank to avoid running into the model wake.

ANALYSIS AND PRESENTATION OF DATA

The raw test data was in the form of voltages which were read off the modular force balances. The signals were filtered and sent to stripchart recording devices and to the computer. A set of computer programs was utilized to convert the data into nondimensional coefficients and to correct for tares. The data analysis techniques are similar to those utilized in Reference 4.

The on-carriage Interdata computer program performed the following analysis tasks.

1. Conversion of voltages to engineering units
2. Correction of data for model CG location and centripetal tares
3. Calculation of resultant hydrodynamic forces and moments about the reference point
4. Tabulation of raw data and statistical measures of data consistency
5. Tabulation of resultant forces and moments in English and metric units
6. Nondimensionalization of the results and tabulation of the nondimensional quantities.

The program and printout provide the capability of identifying erroneous data points. Errors in carriage speed and angle settings were readily identifiable. The analysis of only part of a data record was often of use on the carriage to salvage valid data without repeating the run. The computer and the operating system on the arm were very helpful in the efficient performance of the experiments. Over 550 valid data points were obtained in less than 90 total hours of experimentation including the time required for rigging and frequent model changes.

The data was taken from a matrix of speeds, drift angles, roll angles and yaw rates (radii). The coupling between all the quantities was determined experimentally so that subsequent simulation would have an empirical basis. The ranges of the variables were determined from the expected operating envelope of the ship during turning maneuvers and low speed mine countermeasures missions.

Nondimensional data for the yaw moment (N'), side force (Y') and the roll moment (K') were plotted for each speed in three different series: against yaw rate for a family of drift angles, against rudder angle for a family of yaw rates and against roll angle for a family of yaw rates. These graphical representations of the experimental data are presented in the Appendices. An examination of other possible parametric curves, such as plots of forces against drift angle or roll angle for a family of rudder angles and plots of forces against drift angle for a family of roll angles, showed very little spread between the curves, i.e., very little coupling. Hence, these parametric plots are not presented. These coupling effects are included in the simulation data base that obtains values for N', Y', and K'.

The linear derivatives, plotted in Figures 6 through 16, are useful in understanding the results. The derivatives are slopes of straight lines drawn through the data. The sway velocity derivatives (N'_v, Y'_v and K'_v) were obtained from curves constructed from the intercepts of the yaw rate plots extrapolated to zero yaw rate, or in those cases for which negative yaw rates were tested, interpolated to zero yaw rate. As can be seen, the linearity of the data permitted reliable extrapolations, thus making it possible to obtain straight-line experimental results at a considerable savings in time and expense. The validity of the extrapolation process is further substantiated by Figures 18, 20, 21, 24, 27, 29 and 30 which contain data points obtained during straight-line experimental program previously conducted at DTNSRDC (Reference 5).

Figures 17 through 79, presented in Appendix A, contain data for the design draft condition. The yaw rate/drift angle effects for N', Y', and K' at various speeds are illustrated in Figures 17 through 42. In all these curves, the high degree of linearity of the data within the drift angle and yaw rate range of the experiment is apparent. The only noticeable nonlinear effects occur at the lowest speed (3 kts) for nondimensional turn rates larger than 0.3.

The SSP model tested employs two propellers that rotate in the same direction. Consequently, there are asymmetries in the experimental data. These asymmetries should be most apparent by nonzero values of N', Y', and K' at zero turn rate. However, an examination of these values shows that the asymmetries encountered are small.

Figures 43 through 66 give the yaw rate/rudder angle effects at the design draft. Rudder angles up to 40 degrees were investigated. Yaw moment due to the rudder peaked between 30 and 40 degrees of rudder deflection. The curves are very linear out to approximately 30 degrees at all speeds. The parametric curves at different yaw rates in these figures are almost parallel implying that the effect of yaw rate on yaw moment and side force due to the rudder is small. This enables the determination of moments at zero yaw rate (straight-line) from a parallel curve drawn through the origin of the plot. Figures 45 and 53 for 7 knots full scale show that the straight-line rudder data is indeed parallel to that obtained on the rotating arm.

Figures 67 through 79 show that the roll angle effect on the forces and moments are quite small and linear as might be expected for a craft having a small waterplane area. Roll angles of up to 6 degrees were considered. It should be noted that only hydrodynamic effects are illustrated here since hydrostatic effects were removed by zeroing the gages before the experimental run. The rudder angle and drift angle were held at zero for the data for this set of curves.

Appendix B contains data for the deep draft condition. Design draft is approximately 4.66 m full scale, whereas, deep draft is approximately 5.45 m. Since the waterplane area is small, and the rudders fully submerged, the differences in the data between deep and design draft values are small. For example, the difference in yaw moment at a rudder angle of 20 degrees, turn rate of 0.09, speed of 9 knots, at deep draft is approximately 10% greater than the yaw moment at design draft. Since the data are highly linear, the effects of changing draft can be analyzed using the plots of nondimensional coefficients shown in Figures 7 through 16.

Generally, the data for the entire SSP experimental program are well behaved and provide an extensive data base suitable for determining turning characteristics through the use of simulation models.

DISCUSSION OF RESULTS

A considerable amount of data was generated during this experiment, too much to permit detailed consideration of each experimental point. A full treatise regarding turning circles and stability characteristics must await implementation of the maneuvering simulation presently under development at DTNSRDC. However, general observations regarding the nature of the data, and the effect of speed and draft on the directional stability are presented in this section.

An examination of the data as presented by the curves in Figures 17 through 101 indicate a high degree of linearity. Small nonlinearities with respect to turn rate occur at low speeds (such as 3 kts) for the higher turn rates (r' greater than 0.3) as illustrated in Figures 25, 27, and 34. These nonlinearities are not likely to be due to non-turbulent flow, since sand strips on the forward strut and hull were used to trip the flow. Also, at rudder angles greater than 30 degrees small nonlinearities appear that are attributable to stall effects. It should be noted that the nonlinearities are retained in the data base for simulation purposes.

Since the data exhibits such a high degree of linearity with respect to r', δ_r and ϕ, it is convenient to continue the analysis using the

linear derivatives of the data. The derivatives considered in this report are described in detail in Reference 6.

The first significant observation to be made is that the various derivatives considered display noticeable nonlinearities with respect to ship speed. The derivatives N'_r, Y'_r, K'_r, N'_v, K'_v, $Y_{\delta r}'$, $K_{\delta r}'$, and Y_{ϕ}' have peaks between 6 and 11 kts (see Figures 6, 7, 8, 9, 11, 13, 14, and 16). Although these maximums and minimums are not very pronounced, the broad peaks are quite noticeable. This behavior may be due to the interaction between the rudders and the propellers and in some cases to the effects of passing through wave drag hump at 11 knots.

The yaw moment-yaw rate damping coefficient N'_r, is shown in Figure 6. The most negative value of N'_r, occurs at approximately 7 knots. The least negative value occurs at the higher speeds tested. In all cases N'_r is less than zero indicating probable directional stability. Also, the values of N'_r for the deep draft condition are always more negative than the design draft condition implying greater directional stability at deeper drafts. The actual effect of draft on turn diameter must be explored via simulation studies since on the average the changes in N'_r are not very large, and the other forces and moments that may affect turn diameter are dependent on the draft.

The derivative Y'_r is positive for the SSP as it is for conventional ships. Although the variations in Y'_r are not large, it does decrease as the speed increases which would tend to increase the turning diameter at higher speeds.

K'_r, illustrated in Figure 8, is negative and not strongly dependent on speed. In the vicinity of hump speed, 9-11 kts, a deeper draft causes a noticeable change in K'_r toward more negative values.

Plots of the coefficients N'_v, Y'_v and K'_v are presented in Figures 9, 10, and 11 respectively. These coefficients exhibit only a small dependence on speed. However, the effect of hump on N'_v and Y'_v is quite evident as can be seen at 10 kts in Figures 9 and 10.

The nondimensional coefficient, N'_{δ_r} , is plotted in Figure 12. The SSP rudder is fully submerged and located in the propeller slip stream. The speed effect is very small, i.e., N'_{δ_r} remains relatively constant. The effect of draft on N'_{δ_r} is minor since the rudder is fully submerged.

The nondimensional coefficient, Y'_{δ_r} , given in Figure 13, is positive and exhibits a strong dependence on speed. The maximum occurs at approximately 9 kts which is just before hump speed. This behavior is attributed to variation in flow patterns as hump speed is passed. Speed dependence of rudder derivatives was also found in Reference 4 for other SWATH configurations.

The variation of K'_{δ_r} with speed is small, although its magnitude is large. Since its value is large, and the sign is negative it is quite likely that predicted roll angles will be directed into the turn. Roll angles into the turn have been observed during full scale trials (see Reference 2).

The hydrodynamic roll derivatives N_ϕ and Y_ϕ are given in Figures 15 and 16. N_ϕ drops off as speed increase in a linear fashion. Y_ϕ is not strongly dependent on speed. However, a small peak appears in the vicinity of hump speed (approximately 10 kts).

Although considerable understanding of the physical system at hand is possible by analyzing the derivatives as done above, the analysis is relevant only in the region over which linear approximations are valid. In order to fully determine maneuvering characteristics a simulation model employing the full data base containing all nonlinearities must be used.

CONCLUSIONS AND RECOMMENDATIONS

Several significant conclusions can be made regarding the experimental program reported here. These are summarized below.

1. The rotating arm experimental technique can be utilized to provide all static derivatives involved with the prediction of maneuvering performance. This can be accomplished with the ship type considered without performing straight line experiments by extrapolating or interpolating the results to infinite radius, thus saving time and expense. These extrapolation procedures have been verified by comparing results with

straight line experiments. The rotating arm with the current computer system allowing for analysis during the experimental program can be operated as an efficient and accurate experimental facility for evaluating turning and straight line performance of surface ships. This technique is more straight-forward than the horizontal planar-motion-mechanism approach as it does not require that attention be given to frequency effects, though acceleration-dependent derivatives must be obtained analytically.

2. The experimental data from the rotating arm experiments on SSP are linear with yaw rate except for large yaw rates and large rudder angles. This allows a full characterization of the forces and moments by a small data base. Also, the linearity implies that tractable theoretical formulations could be developed with respect to roll, drift, and possibly yaw rate dependencies. On the other hand, the strong dependency of the forces and moments on speed imply that the development of theoretical models for the speed effects may be difficult.
3. The SSP design is statically stable in yaw with the linear derivatives always possessing the sign expected from conventional displacement-type of ship work.
4. Accurate experimental data can be taken on the rotating arm for negative turn rates. Such testing can be used to determine ship model asymmetries and allow interpolation to be used to determine straight line results.
5. Rudder effectiveness does not increase significantly as draft increases. However, the detailed effects of draft on turning performance must await simulation studies.

ACKNOWLEDGMENTS

Special thanks are extended to R. Thomas Waters, Lawrence Murray, J. Brooks Peters and William B. Dixon, Jr., all of DTNSRDC, for their assistance during the experimental program. The support and advice of

Margaret D. Ochi and D. Cieslowski of DTNSRDC is greatly appreciated as is the contractual support provided by ORI, Inc., in particular that of Dr. J. E. Whalen.

REFERENCES

1. Lang, T. G., J. D. Hightower and A. T. Strickland, "Design and Development of the 190-Ton Stable Semisubmerged Platform (SSP)", Journal of Engineering for Industry, November 1974.

2. Stenson, R. J., "Full Scale Powering Trials of the Stable Semi Submerged Platform, SSP Kaimalino", SPD Report 650-01, April 1976.

3. Fein, J. A. and R. T. Waters, "Control Response Trials of the Stable Semi-Submerged Platform (SSP Kaimalino)", SPD Report 650-02, April 1976.

4. Fein, J. A. and R. T. Waters, "Rotating Arm Experiments for SWATH 6A Maneuvering Predictions", SPD Report 698-01, July 1976.

5. Fein, J. A. and J. P. Feldman, "Controllability of the Stable Semi-Submerged Ship". Paper 1XB-3 Third Ship Control Systems Symposium, Bath, England, 1972.

6. Comstock, J. P., Ed., Principles of Naval Architecture, SNAME 1967.

TABLE 1

GEOMETRIC AND PHYSICAL CHARACTERISTICS OF
THE STABLE SEMI-SUBMERGED PLATFORM

	Model	Ship
Linear Ratio	7.8	
Length (overall)	3.386 m	26.41 m
Submerged length	3.126 m	24.38 m
Maximum beam	1.817 m	14.17 m
Transverse strut separation (centerline to centerline)	1.562 m	12.19 m
Model Weight	0.482 MTFW	-------
Displacement, design draft	0.395 MTFW	193.0 MTSW
Displacement, deep draft	0.413 MTFW	201.6 MTSW
Vertical distance, baseline to design waterline	0.597 m	4.66 m
Vertical distance, baseline to deep waterline	0.699 m	5.45 m
Vertical distance baseline to center of gravity model (reference point)	0.709 m	--------
Vertical distance baseline to longitudinal distance of the ship	0.601 m	4.69 m
Longitudinal distance, nose to center of gravity (reference point)	1.479 m	11.54 m
Diameter of submerged hull, each	0.253 m	1.97 m
Forward strut, each:		
Height	0.576 m	4.49 m
Chord at design WL	1.036 m	8.08 m
Chord at deep WL	1.086 m	8.47 m

	Model	Ship
Section	Lenticular	
Maximum thickness to chord ratio	.15	.15
Aft strut, each:		
Length	0.78 m	6.09 m
Section	Lenticular	
Maximum thickness to chord ratio	.15	.15
Propellers, each:		
Diameter	0.2286 m	1.778 m
Pitch-diameter ratio	1.1	variable
Number of blades	4	4
Direction of rotation	R. H.	R. H.
Vertical distance, propeller axis to baseline	0.128 m	1.00 m
Canards, each:		
Section profile, NACA	64-015	
Span	0.235 m	1.83 m
Longitudinal distance from CG to hinge axis	1.097 m	8.56 m
Longitudinal distance from trailing edge to hinge axis	0.192 m	1.50 m
Vertical distance from baseline to hinge axis	0.128 m	1.00 m
Stern Foil		
Chord	0.305 m	2.378 m
Span at leading edge	1.353 m	10.56 m
Section profile, modified NACA (wedge shaped trailing edge)	64-021	

	Model	Ship
Longitudinal distance from CG to 25 percent chord	1.182 m	9.22 m
Chord, flaps	0.076 m	0.59 m
Span, flaps, total	1.353 m	10.56 m
Height from baseline to chordline	0.128 m	1.00 m
Rudders, each:		
Chord, trailing edge to hinge axis	0.113 m	0.88 m
Span	0.567 m	4.42 m
Maximum thickness	0.0196 m	0.153 m
Transverse distance from centerline to hinge axis	0.780 m	6.09 m
Longitudinal distance from CG to hinge axis	1.536 m	11.98 m

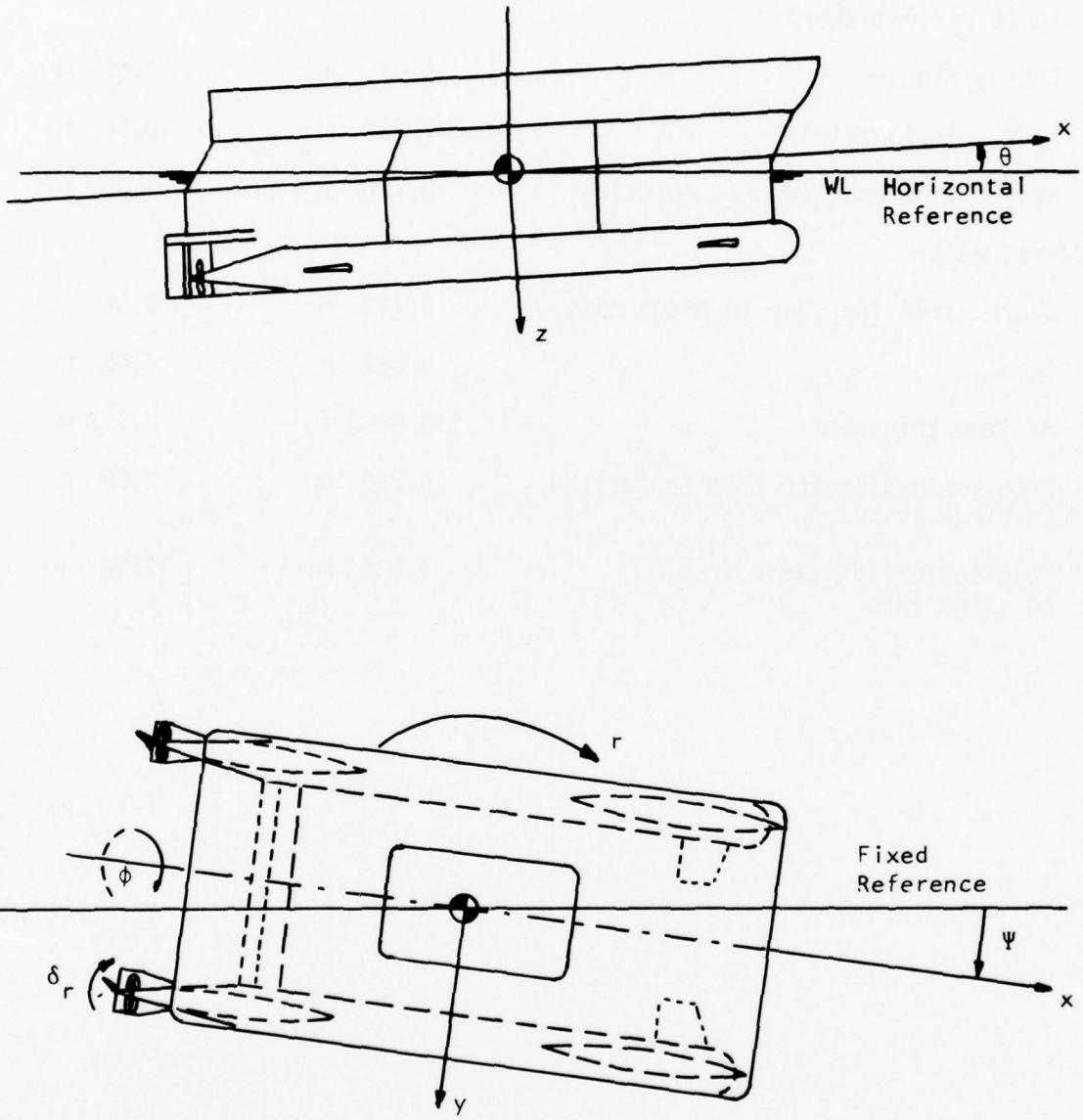

Figure 1 - Schematic Indicating Coordinate Systems and Positive Directions of Measured Quantities

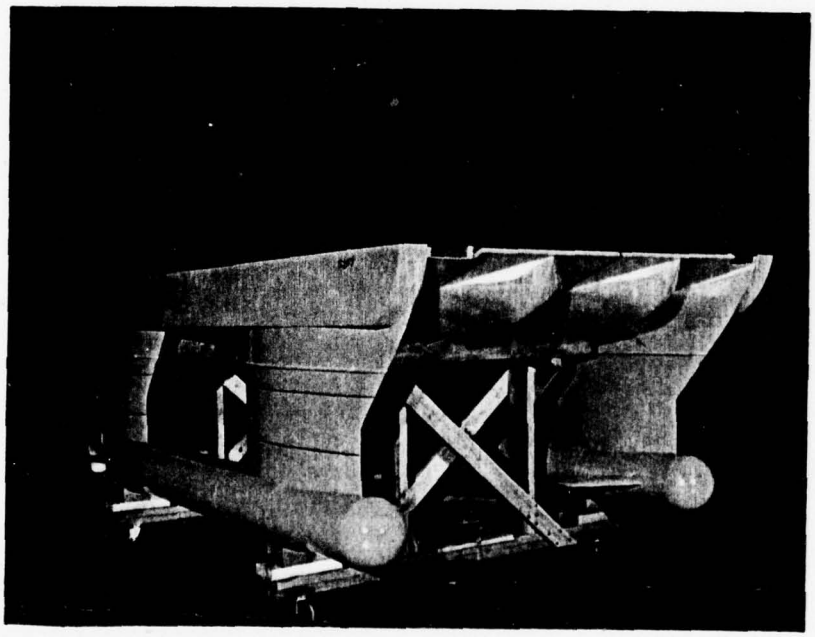

Figure 2 - Photograph of a Bow View of the Experimental Model

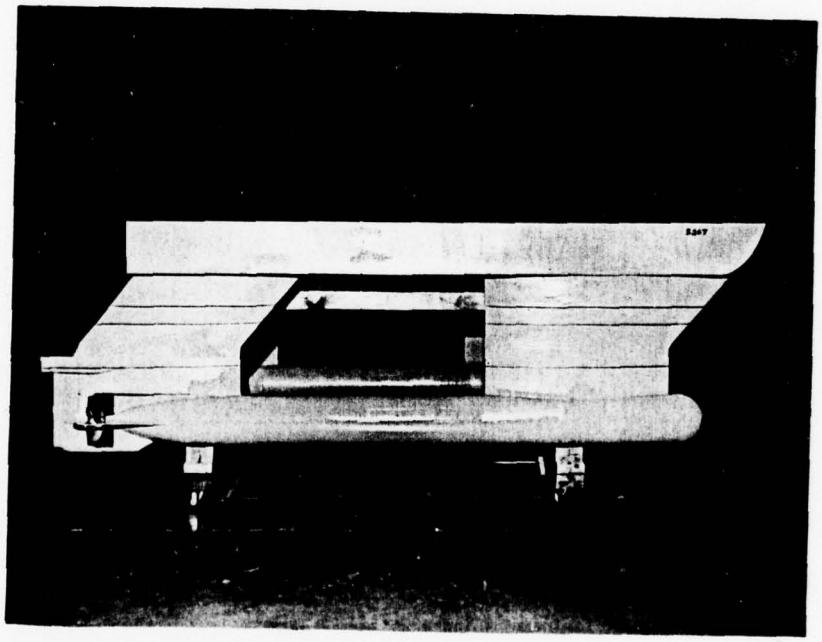

Figure 3 - Photograph of a Side View of the Experimental Model

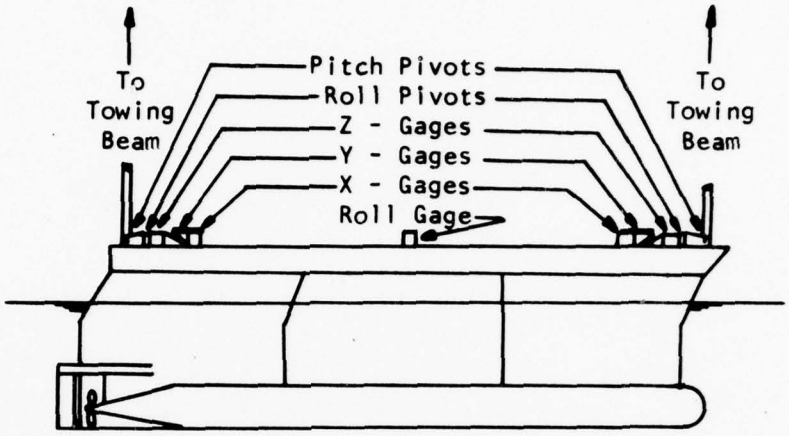

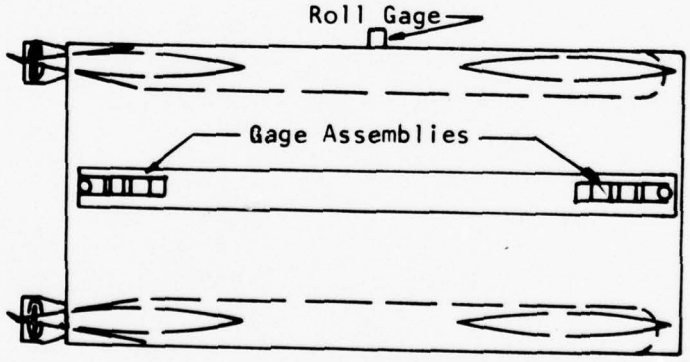

Figure 4 - Schematic Showing Locations of the Gage Assemblies

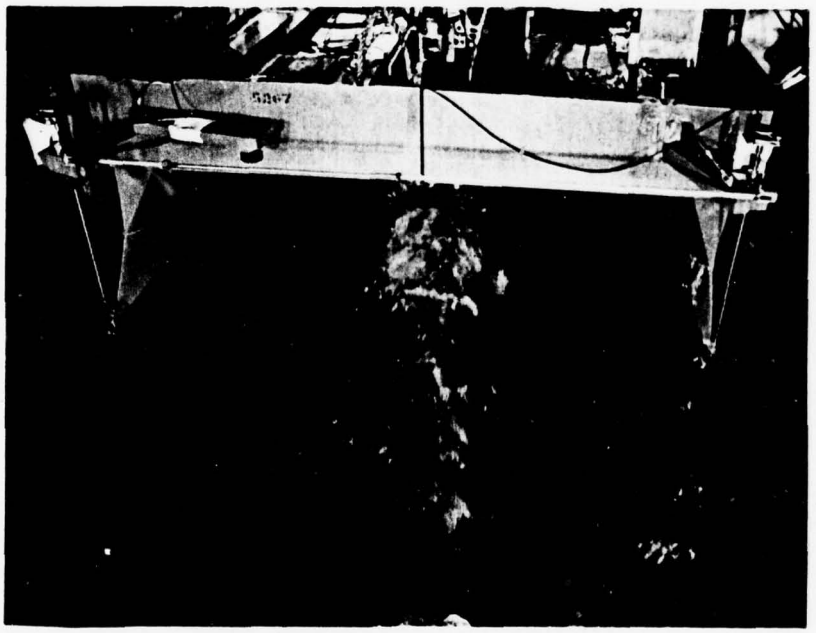

Figure 5 - A Photograph Showing the Stern During an Experimental Test Run

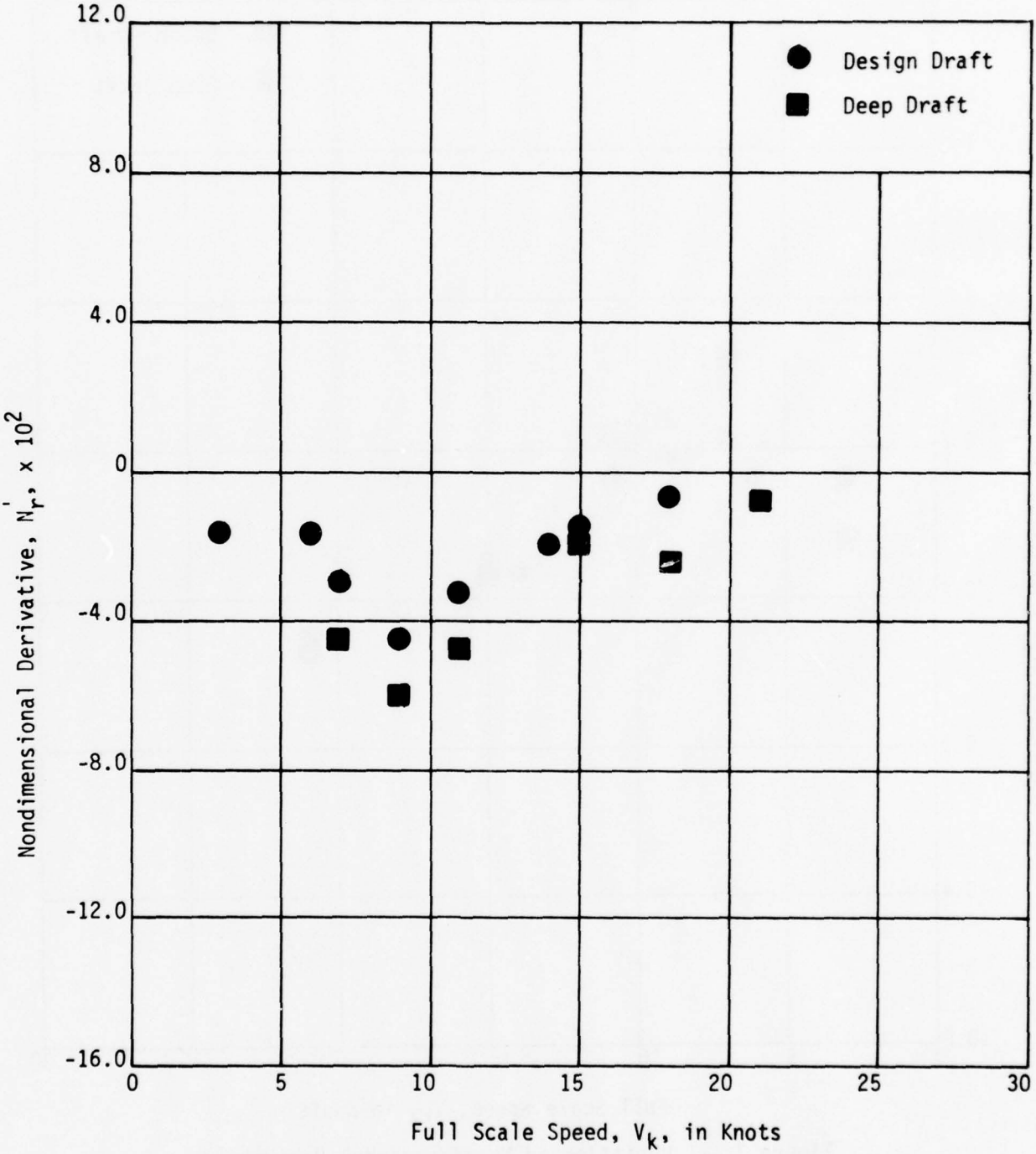

Figure 6 - Variation of Nondimensional Derivative, N_r', with Full Scale Speed for Two Different Drafts

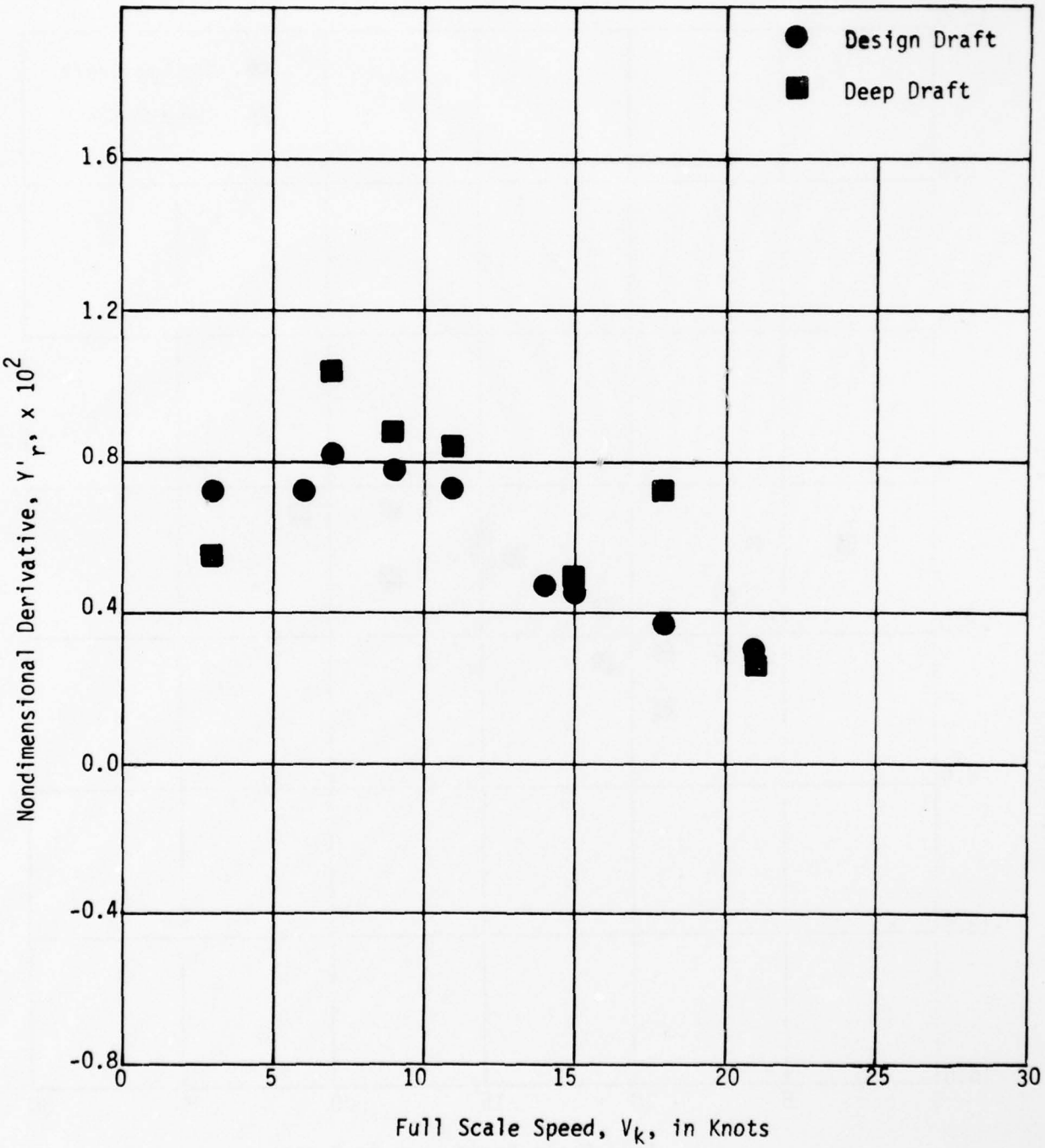

Figure 7 - Variation of Nondimensional Derivative, Y'_r with Full Scale Speed for Two Different Drafts

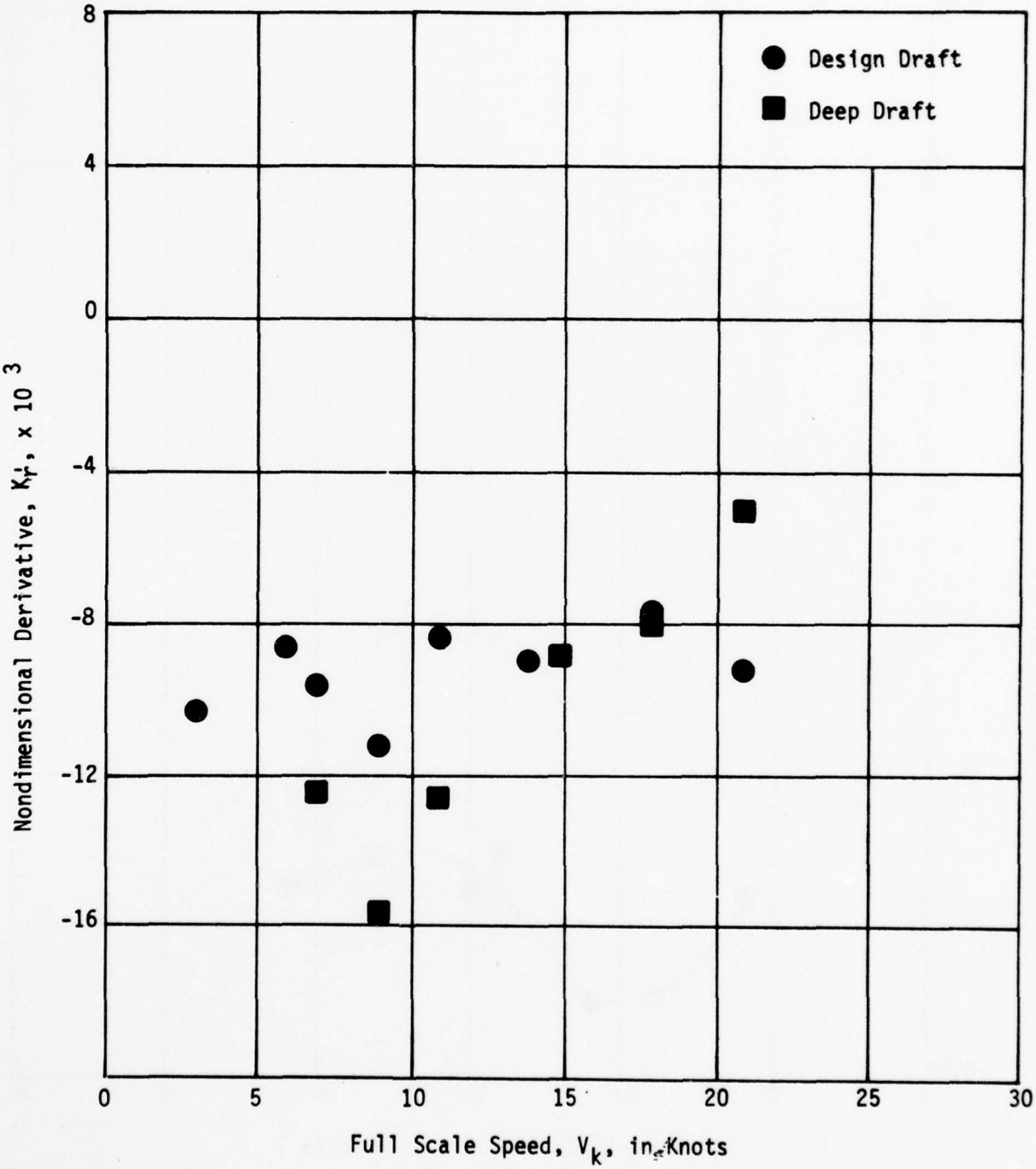

Figure 8 - Variation of Nondimensional Derivative, K'_r, with Full Scale Speed for Two Different Drafts

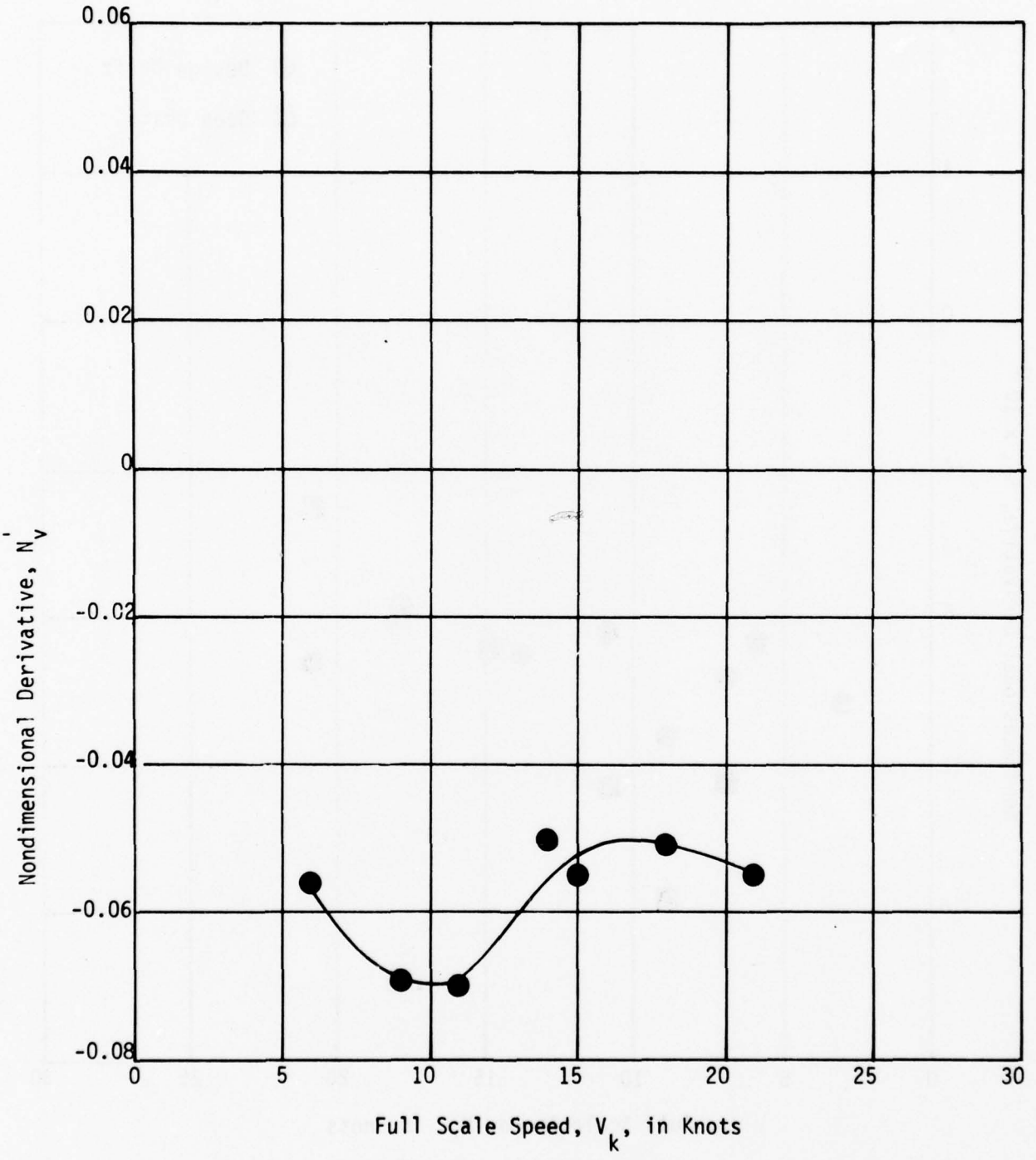

Figure 9 - Variation of Nondimensional Derivative, N_v', with Full Scale Speed

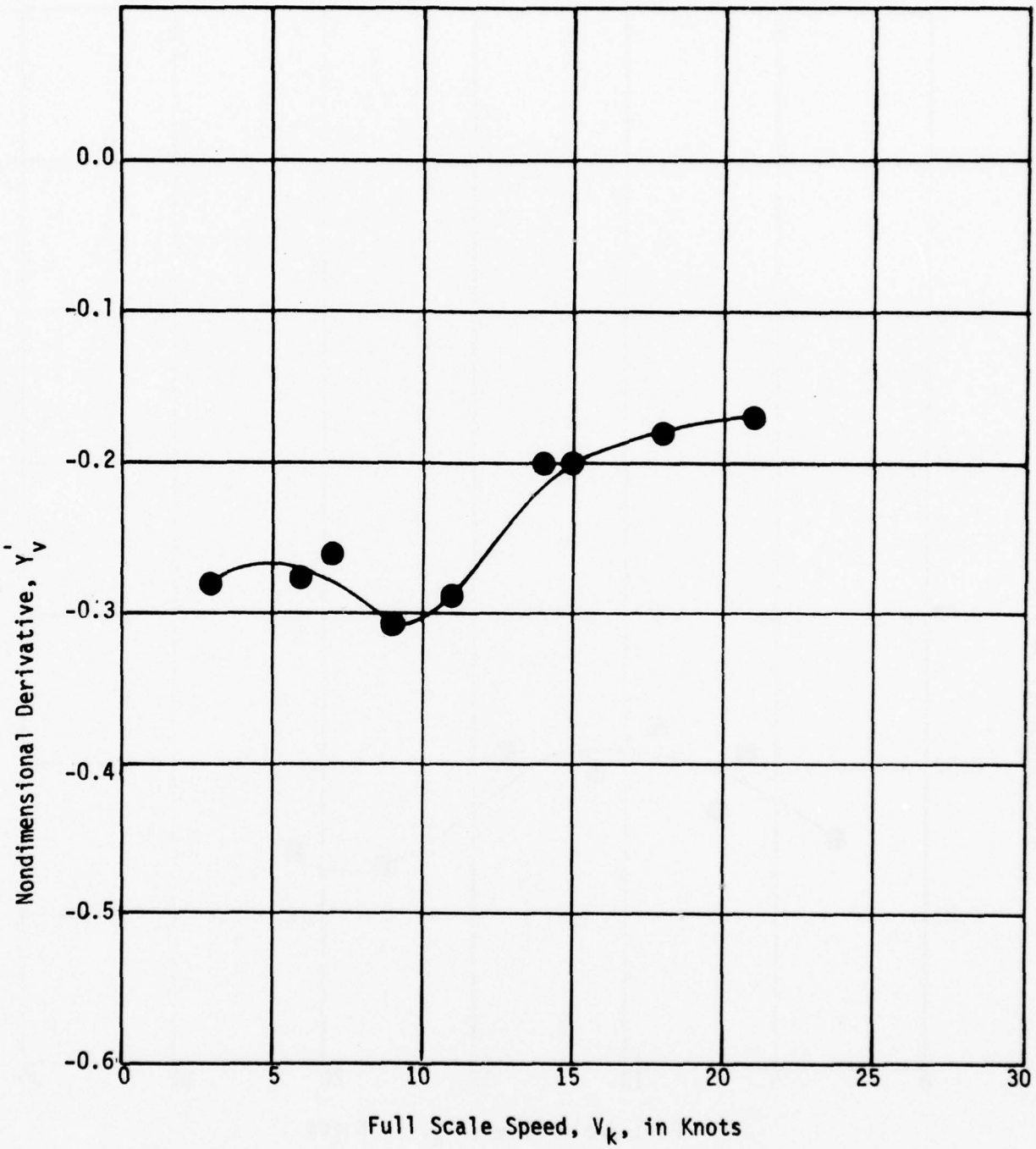

Figure 10 - Variation of Nondimensional Derivative, Y_v', with Full Scale Speed

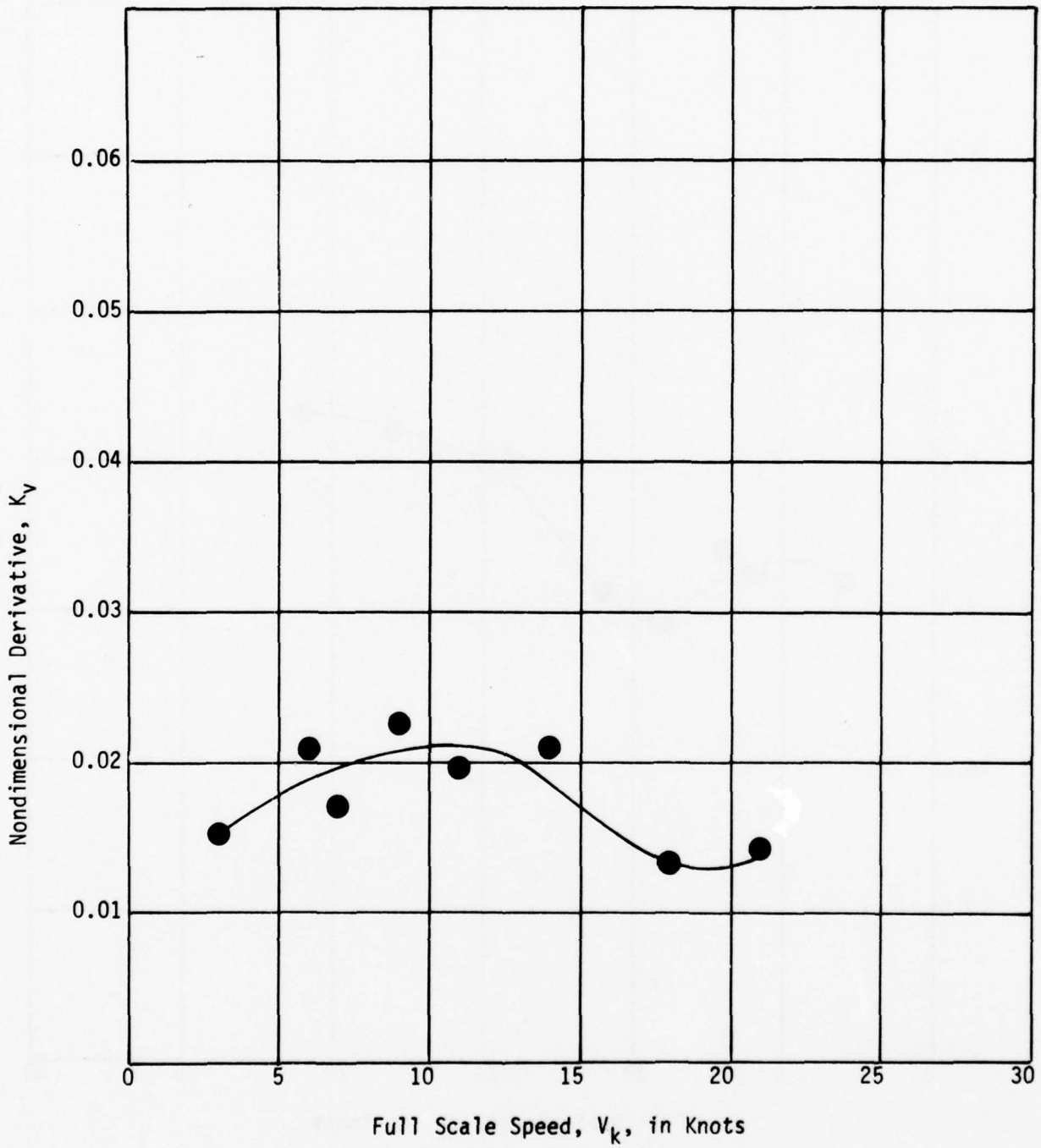

Figure 11 - Variation of Nondimensional Derivative, K_v', with Full Scale Speed

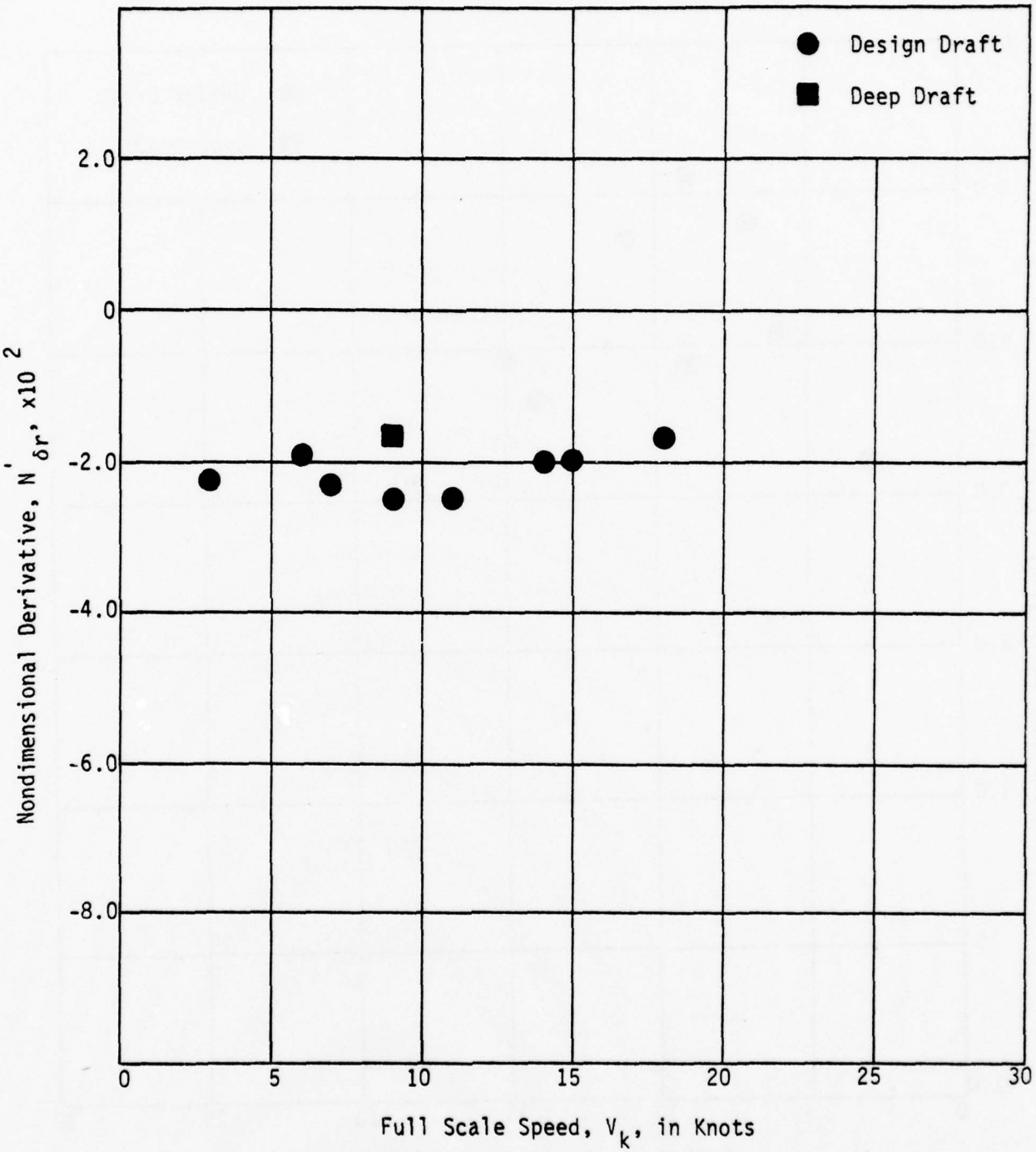

Figure 12 - Variation of Nondimensional Derivative, $N'_{\delta r}$, with Full Scale Speed

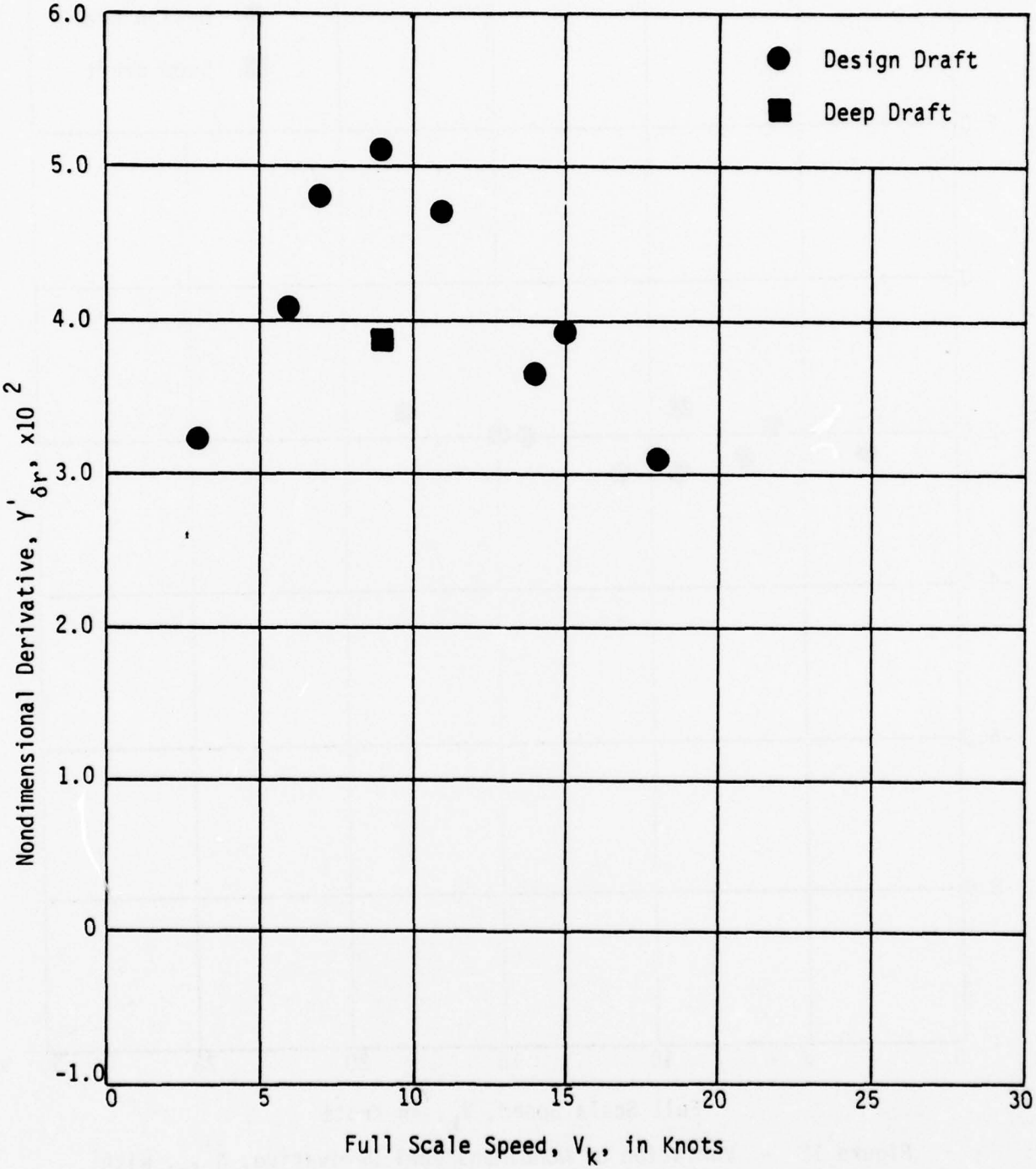

Figure 13 - Variation of Nondimensional Derivative, $Y'_{\delta r}$, with Full Scale Speed

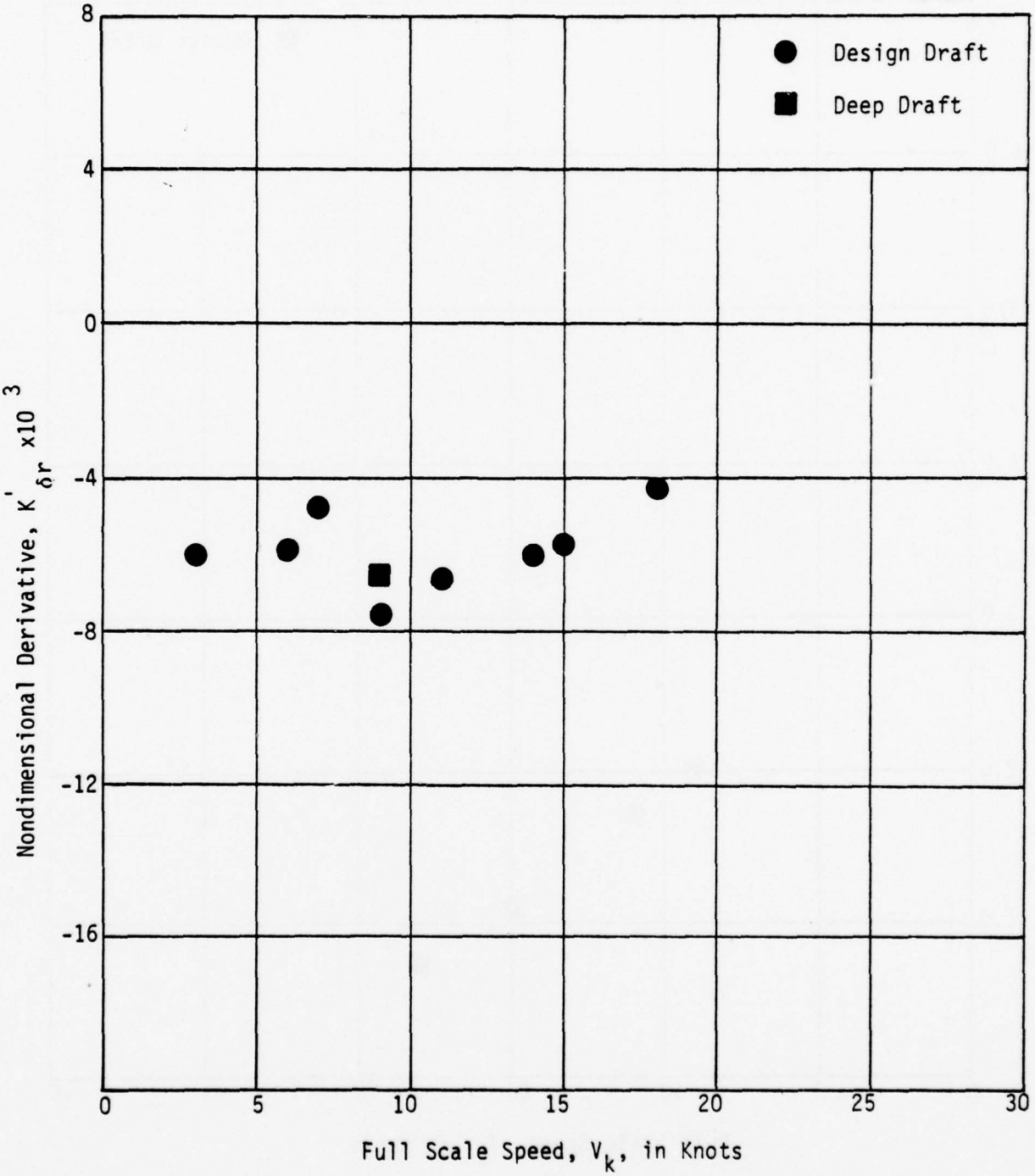

Figure 14 - Variation of Nondimensional Derivative, $K'_{\delta r}$, with Full Scale Speed

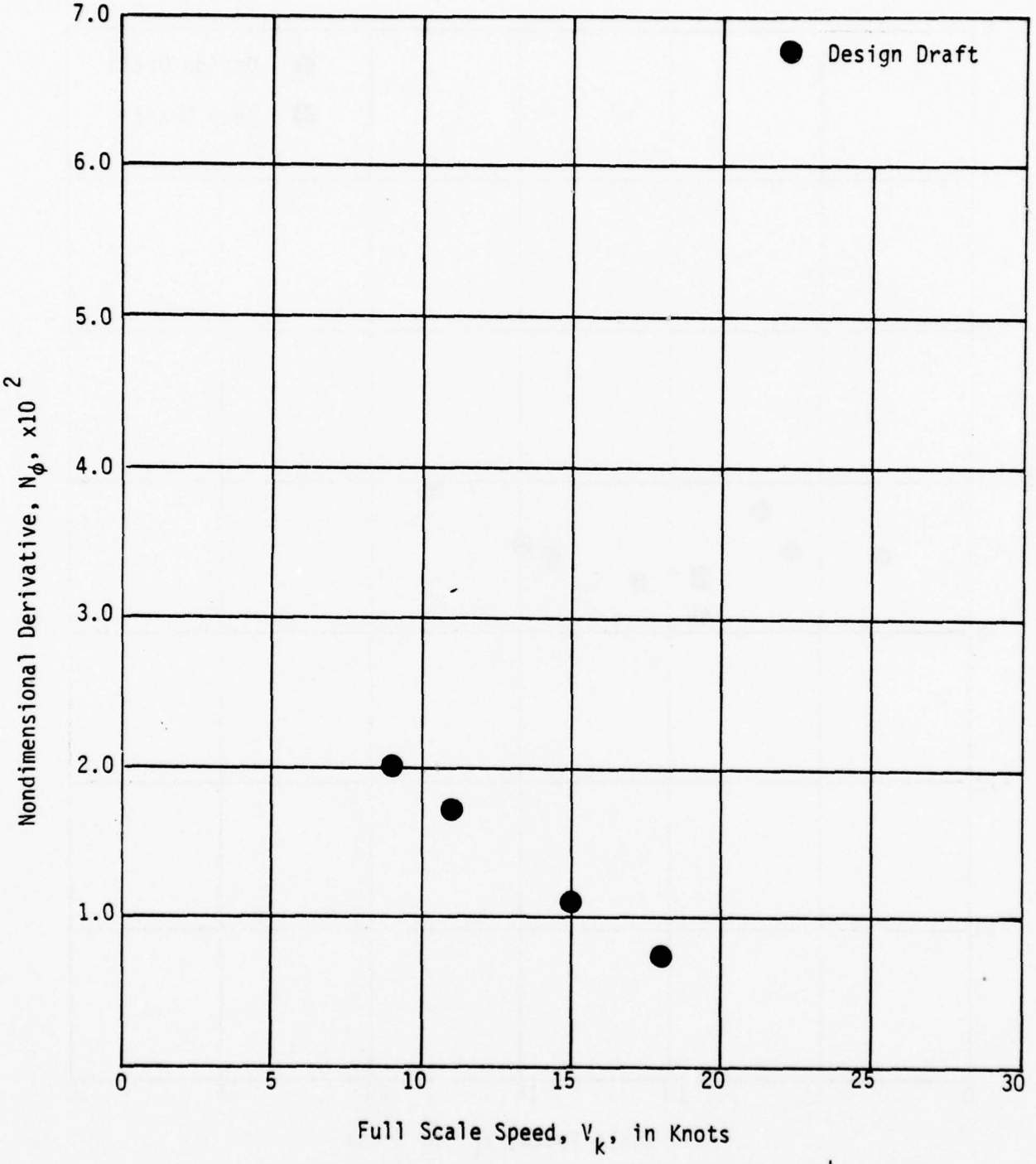

Figure 15 - Variation of Nondimensional Derivative, N'_ϕ, with Full Scale Speed

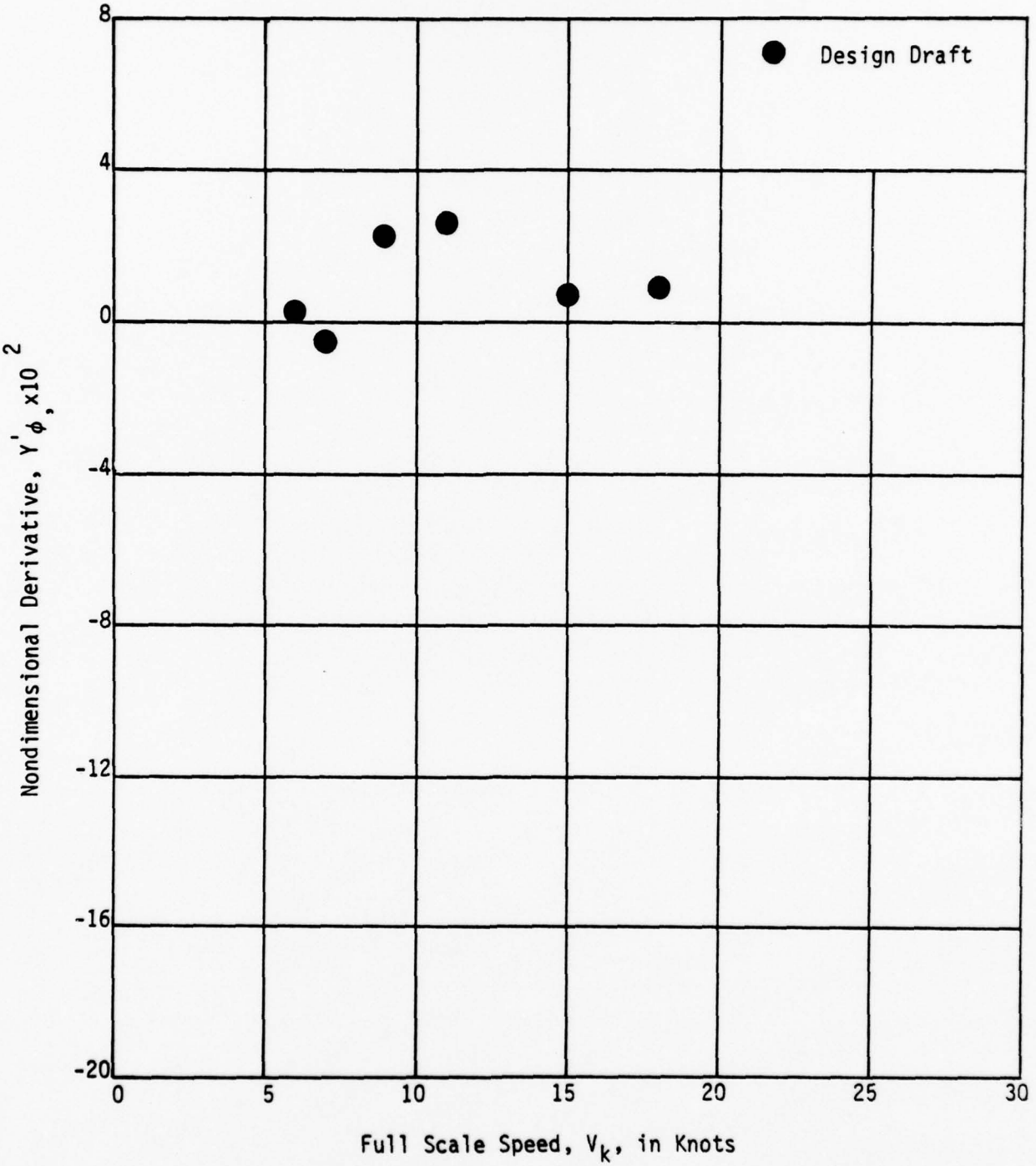

Figure 16 - Variation of Nondimensional Derivative, Y'_ϕ, with Full Scale Speed

Appendix A
(Figures 17 through 79)

NONDIMENSIONAL DATA CURVES FOR DESIGN DRAFT

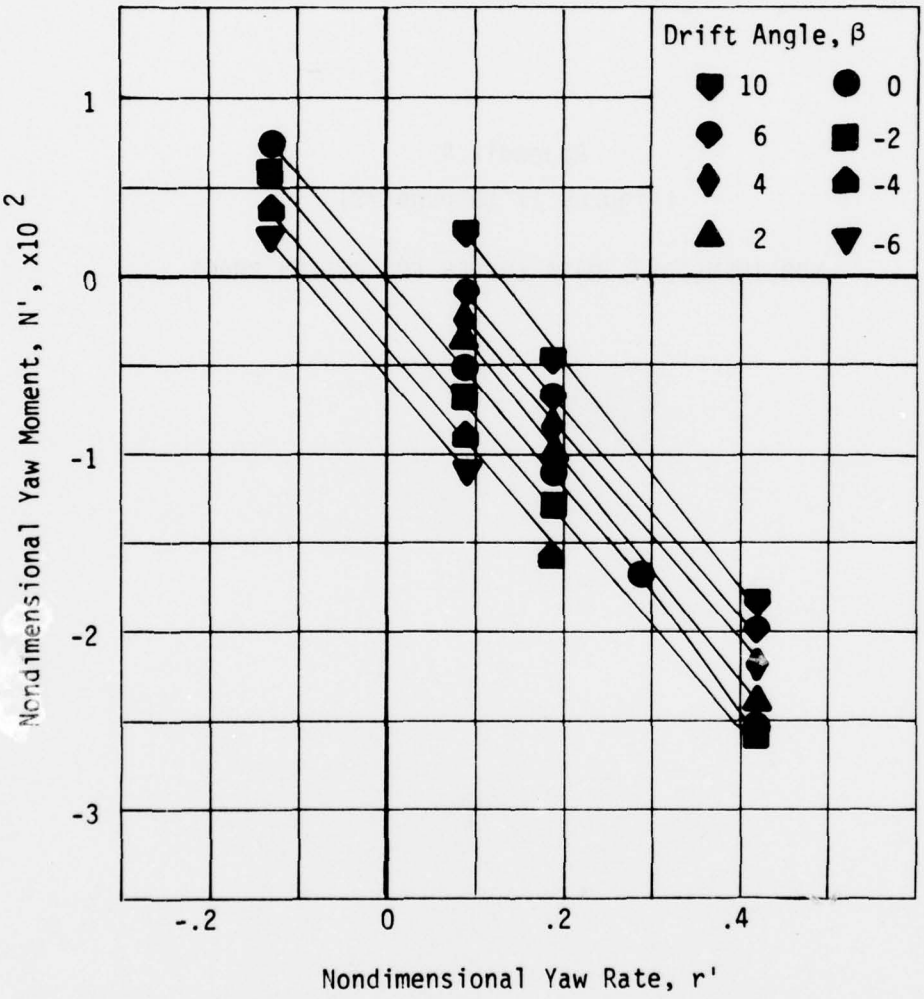

Figure 17 - Variation of Nondimensional Yaw Moment with Nondimensional Yaw Rate for a Series of Drift Angles at a Full Scale Speed of 6 Knots at Design Draft

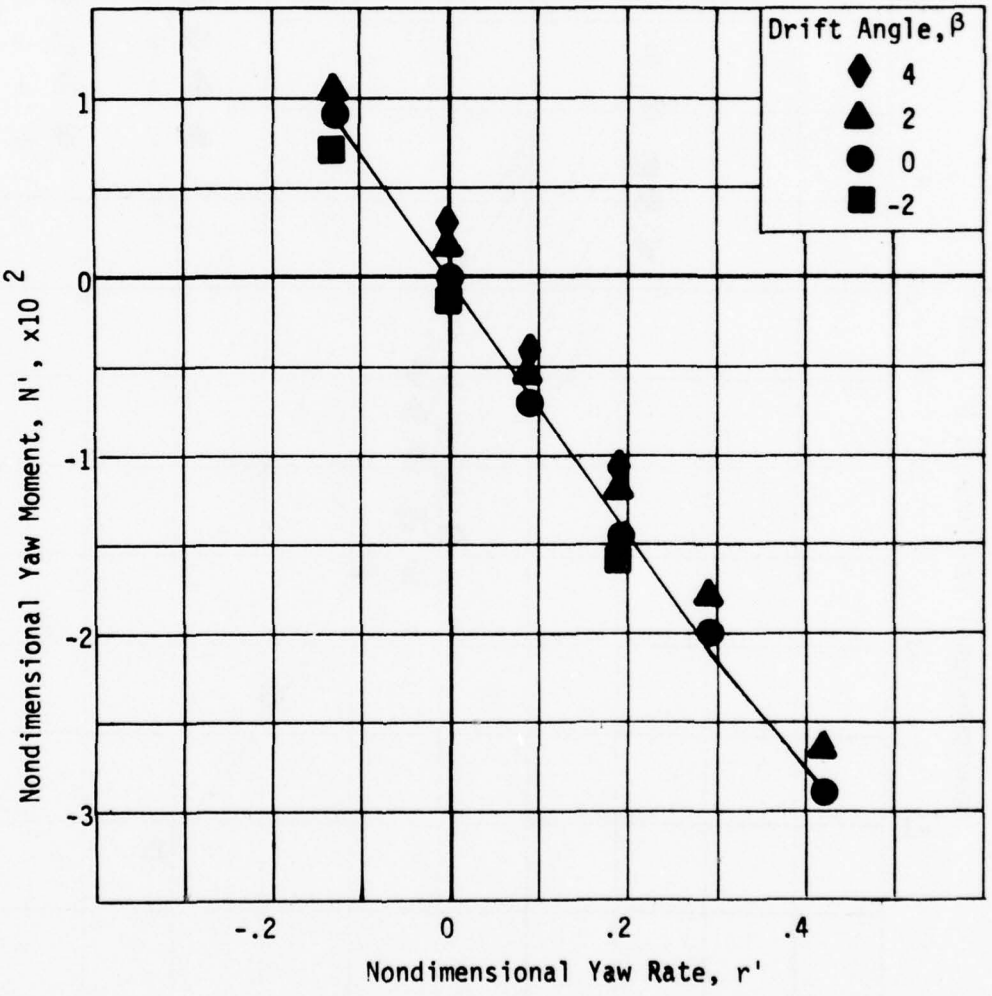

Figure 18 - Variation of Nondimensional Yaw Moment with Nondimensional Yaw Rate for a Series of Drift Angles at a Full Scale Speed of 7 Knots at Design Draft

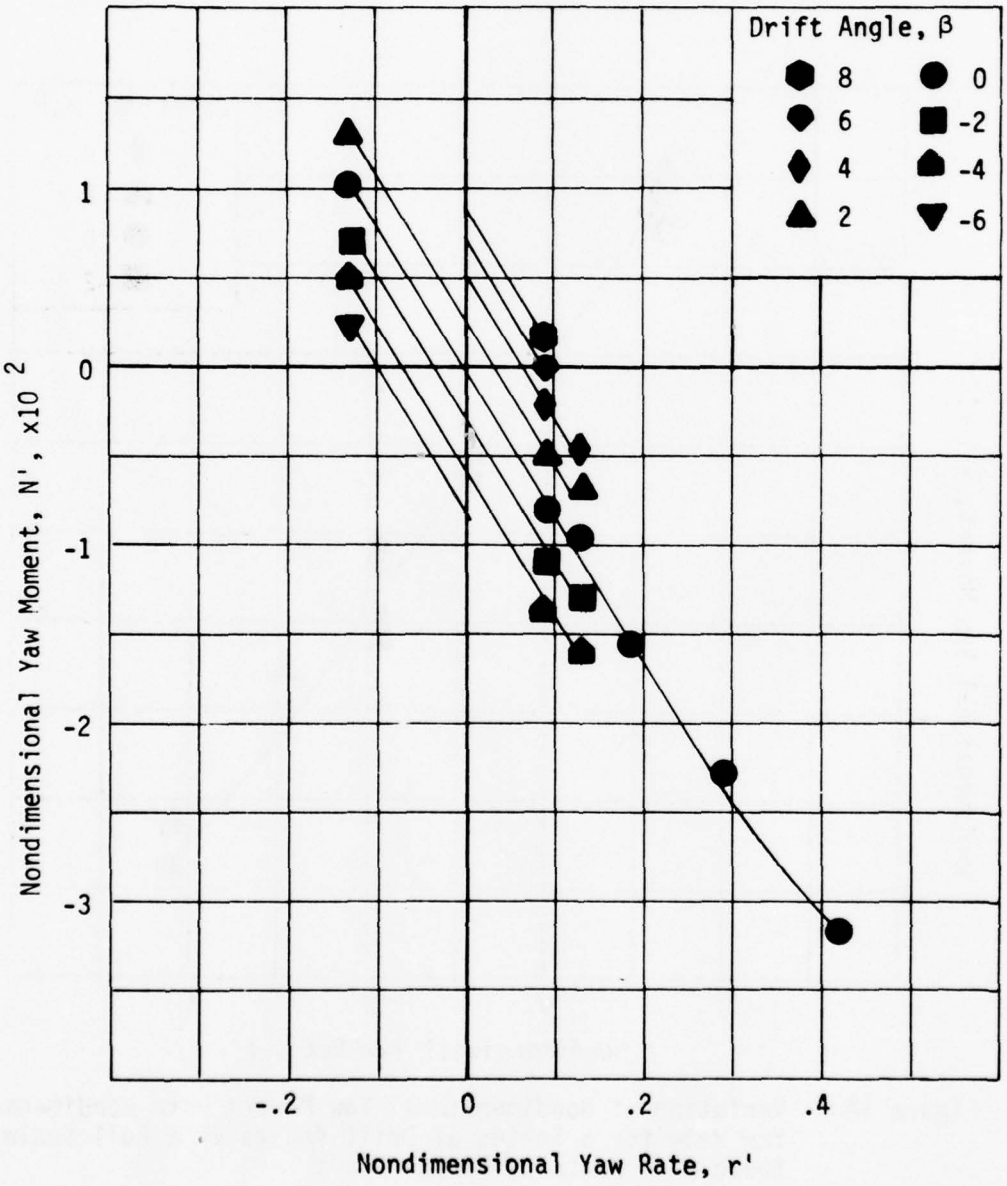

Figure 19 - Variation of Nondimensional Yaw Moment with Nondimensional Yaw Rate for a Series of Drift Angles at a Full Scale Speed of 9 Knots at Design Draft

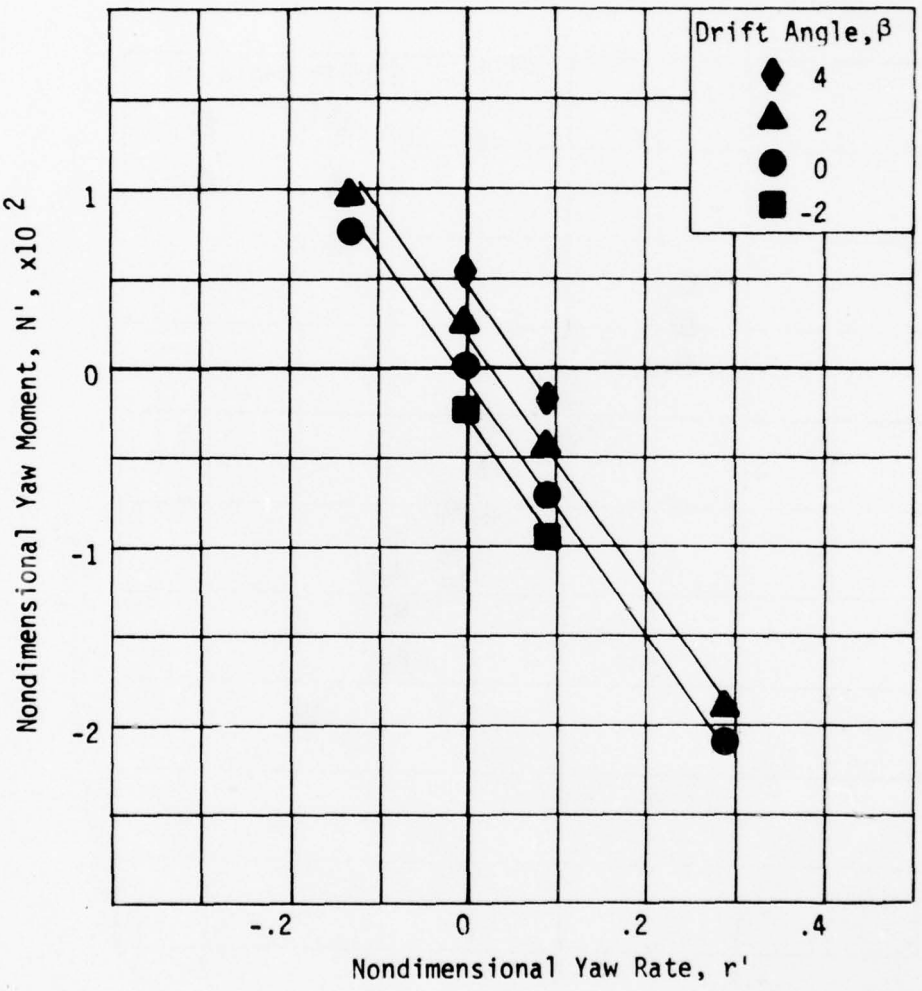

Figure 20 - Variation of Nondimensional Yaw Moment with Nondimensional Yaw Rate for a Series of Drift Angles at a Full Scale Speed of 11 Knots at Design Draft

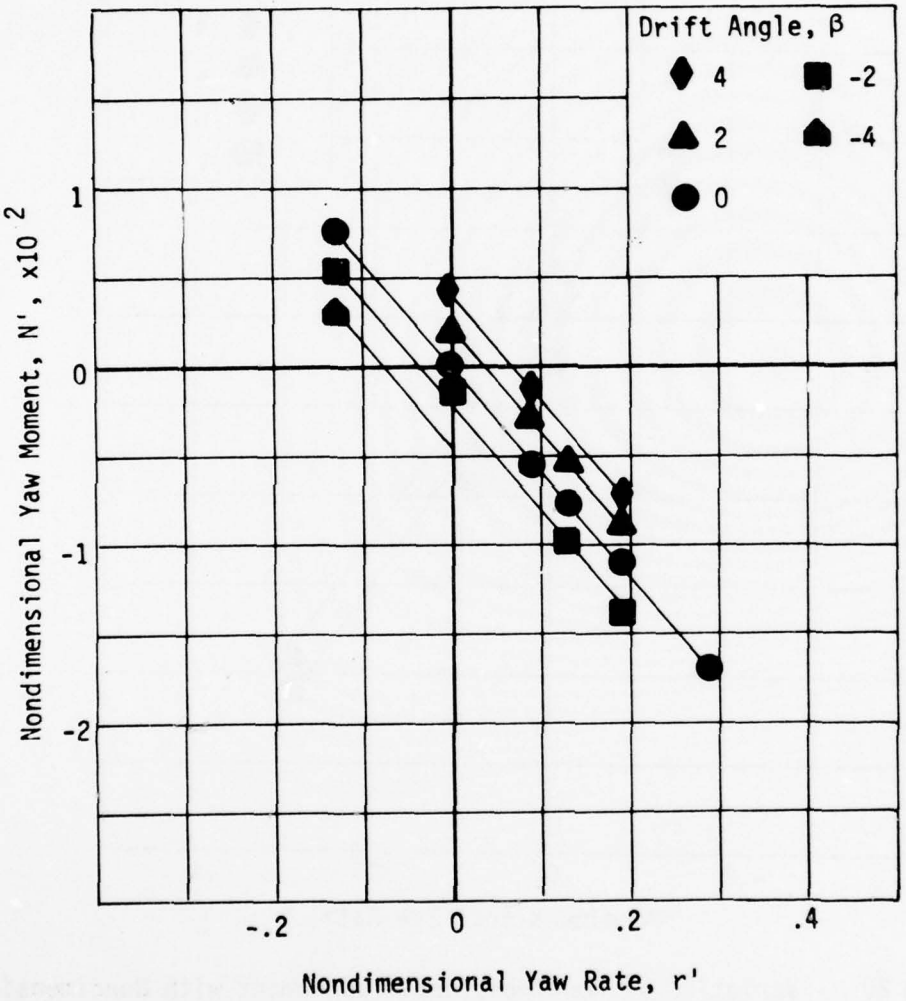

Figure 21 - Variation of Nondimensional Yaw Moment with Nondimensional Yaw Rate for a Series of Drift Angles at a Full Scale Speed of 14 Knots at Design Draft

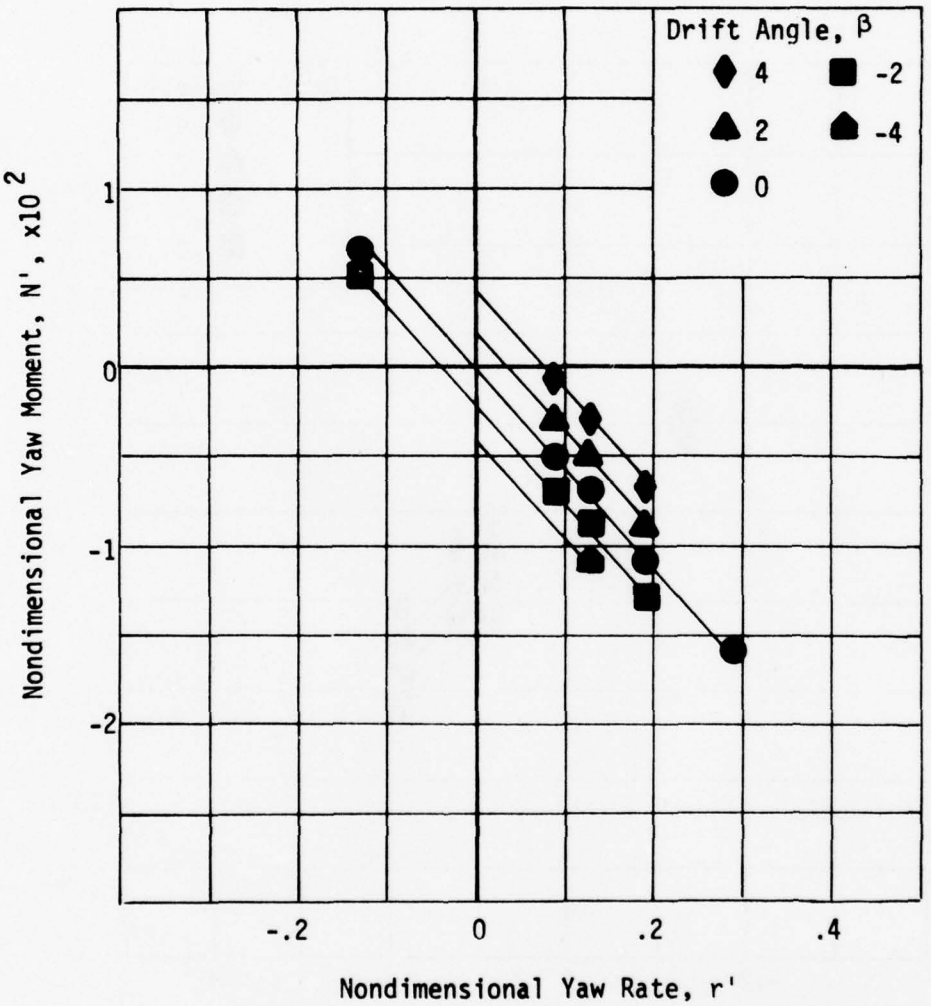

Figure 22 - Variation of Nondimensional Yaw Moment with Nondimensional Yaw Rate for a Series of Drift Angles at a Full Scale Speed of 15 Knots at Design Draft

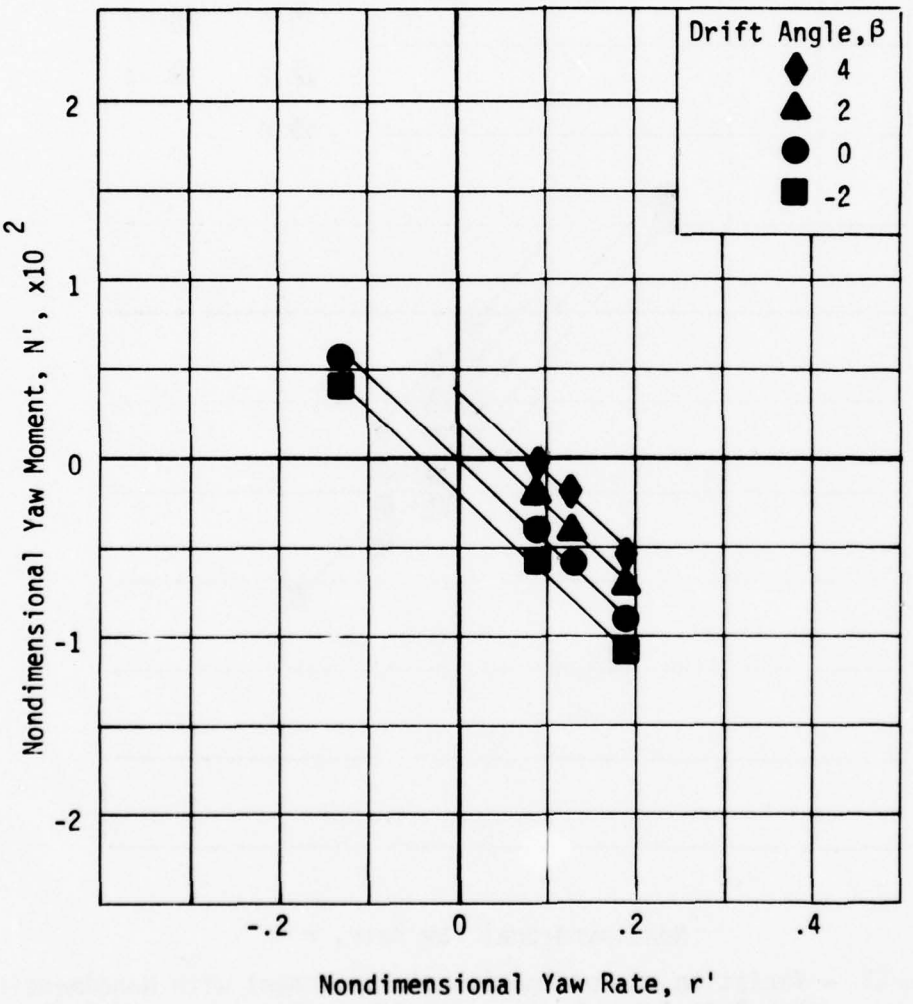

Figure 23 - Variation of Nondimensional Yaw Moment with Nondimensional Yaw Rate for a Series of Drift Angles at a Full Scale Speed of 18 Knots at Design Draft

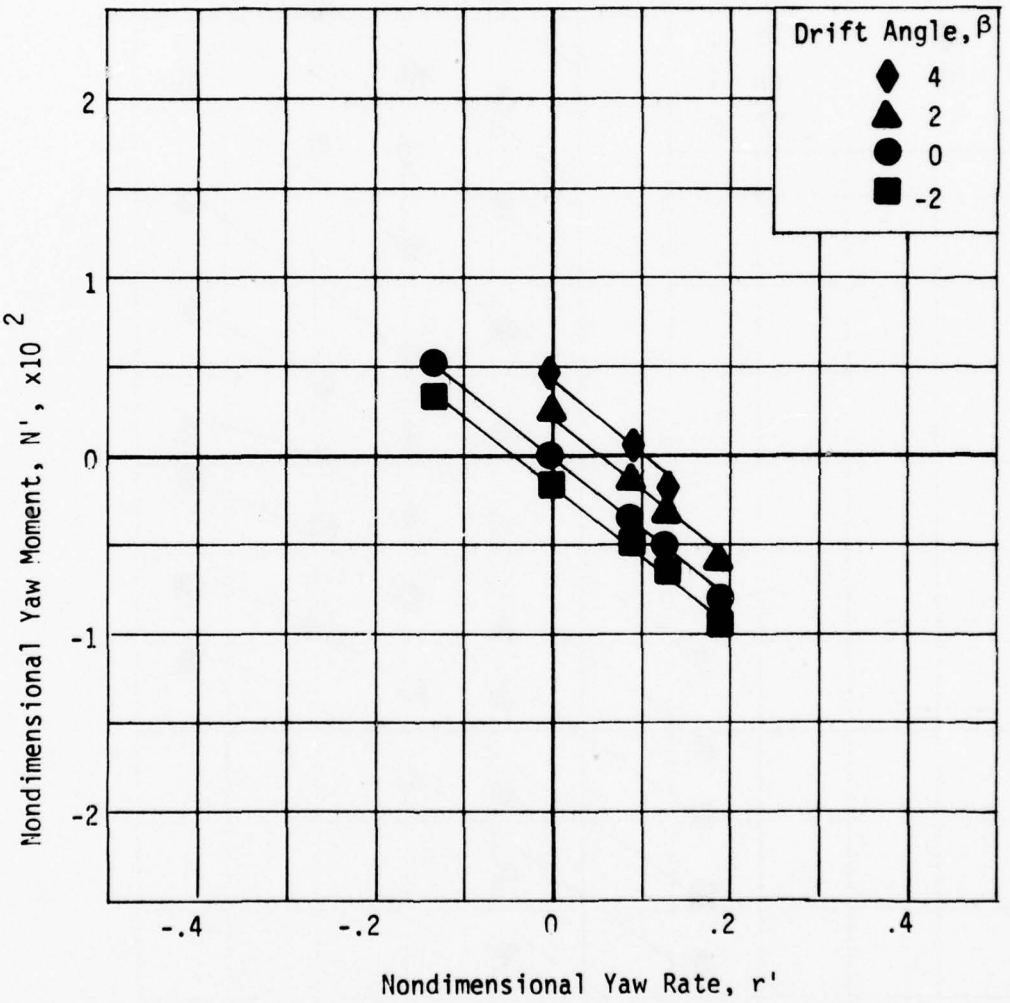

Figure 24 - Variation of Nondimensional Yaw Moment with Nondimensional Yaw Rate for a Series of Drift Angles at a Full Scale Speed of 21 Knots at Design Draft

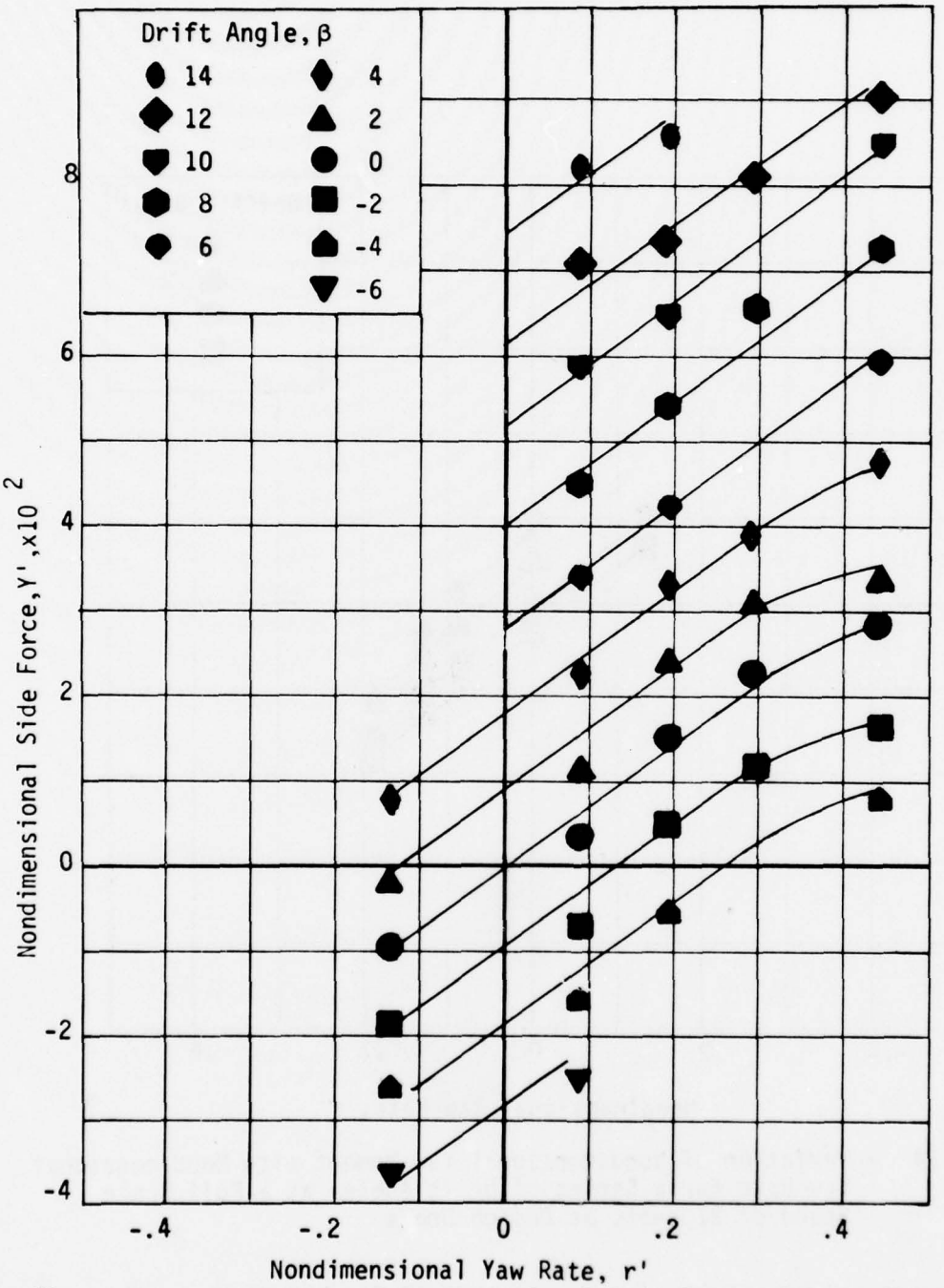

Figure 25 - Variation of Nondimensional Side Force with Nondimensional Yaw Rate for a Series of Drift Angles at a Full Scale Speed of 3 Knots at Design Draft

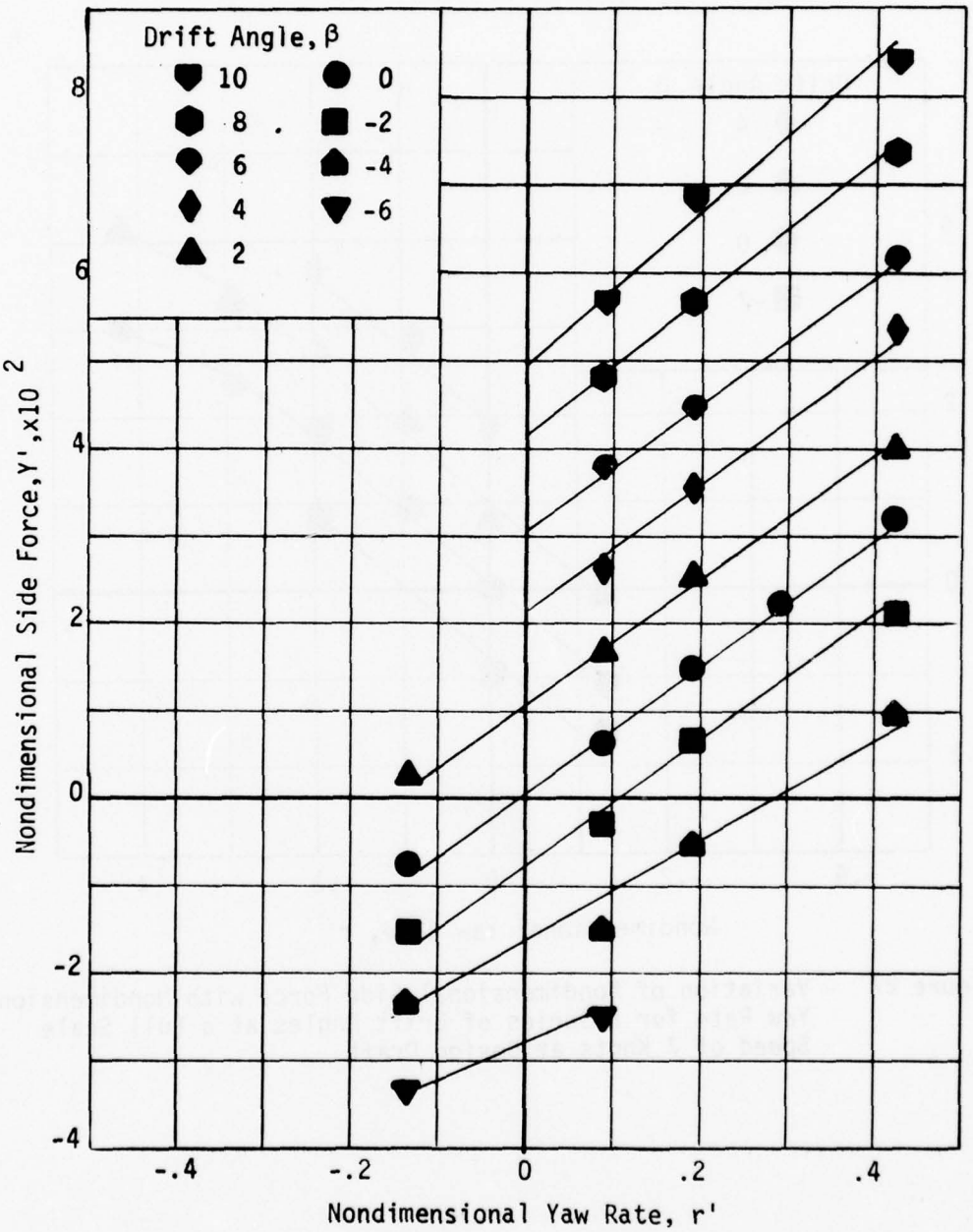

Figure 26 - Variation of Nondimensional Side Force with Nondimensional Yaw Rate for a Series of Drift Angles at a Full Scale Speed of 6 Knots at Design Draft

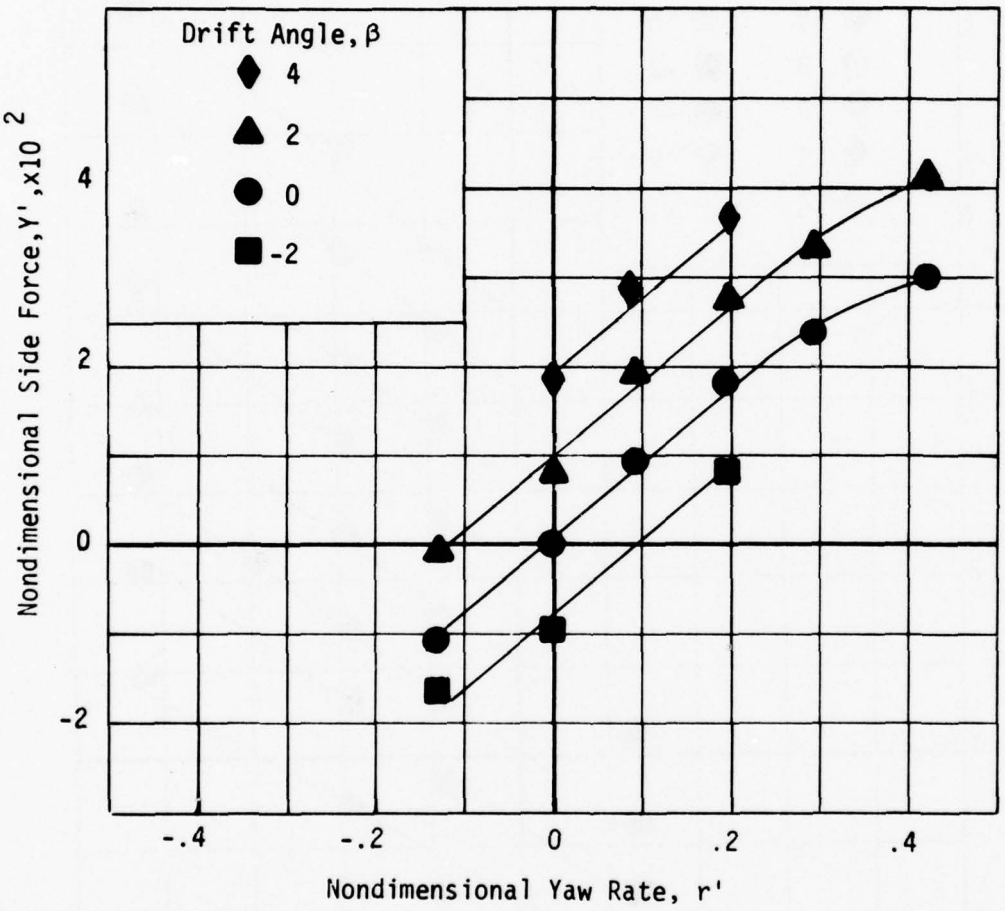

Figure 27 - Variation of Nondimensional Side Force with Nondimensional Yaw Rate for a Series of Drift Angles at a Full Scale Speed of 7 Knots at Design Draft

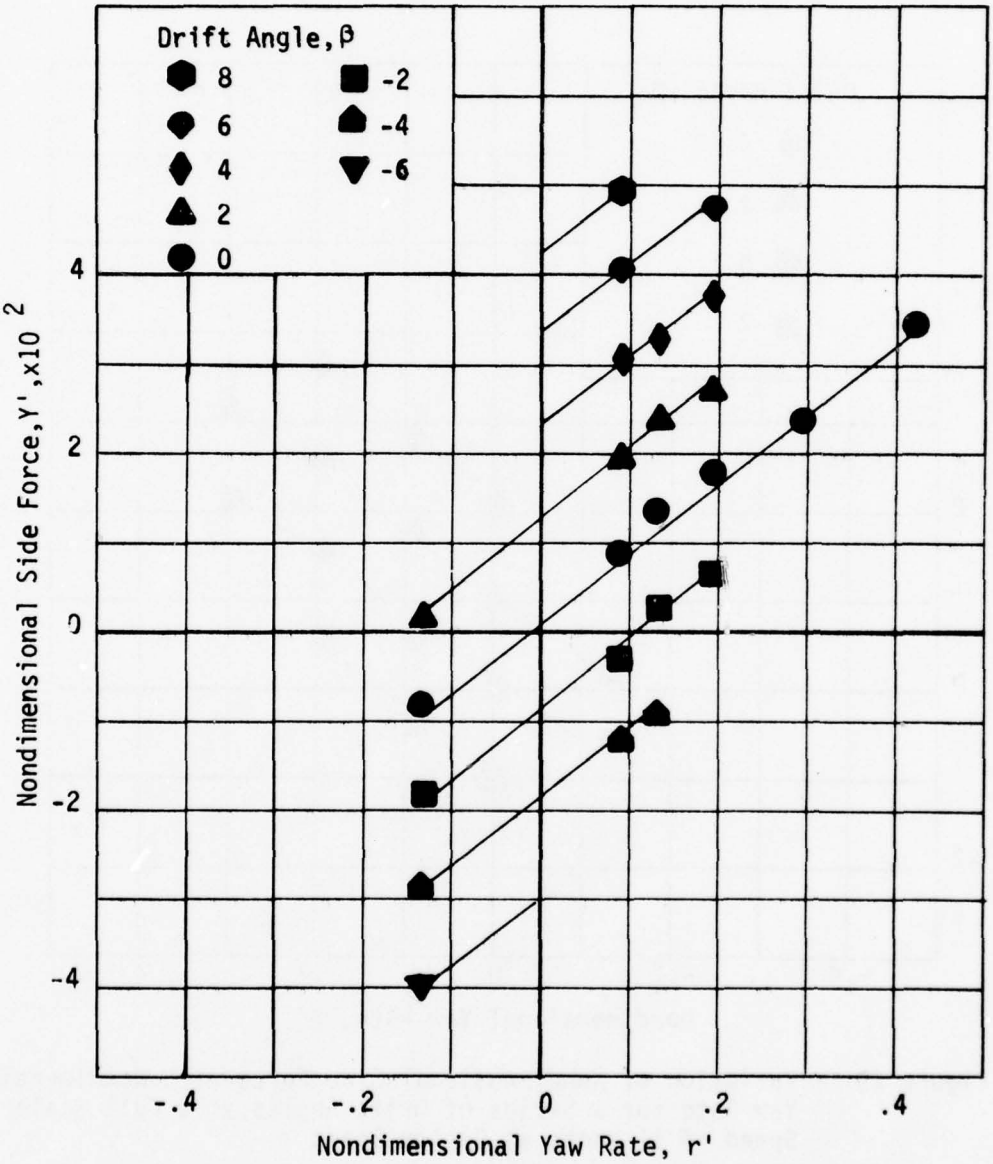

Figure 28 - Variation of Nondimensional Side Force with Nondimensional Yaw Rate for a Series of Drift Angles at a Full Scale Speed of 9 Knots at Design Draft

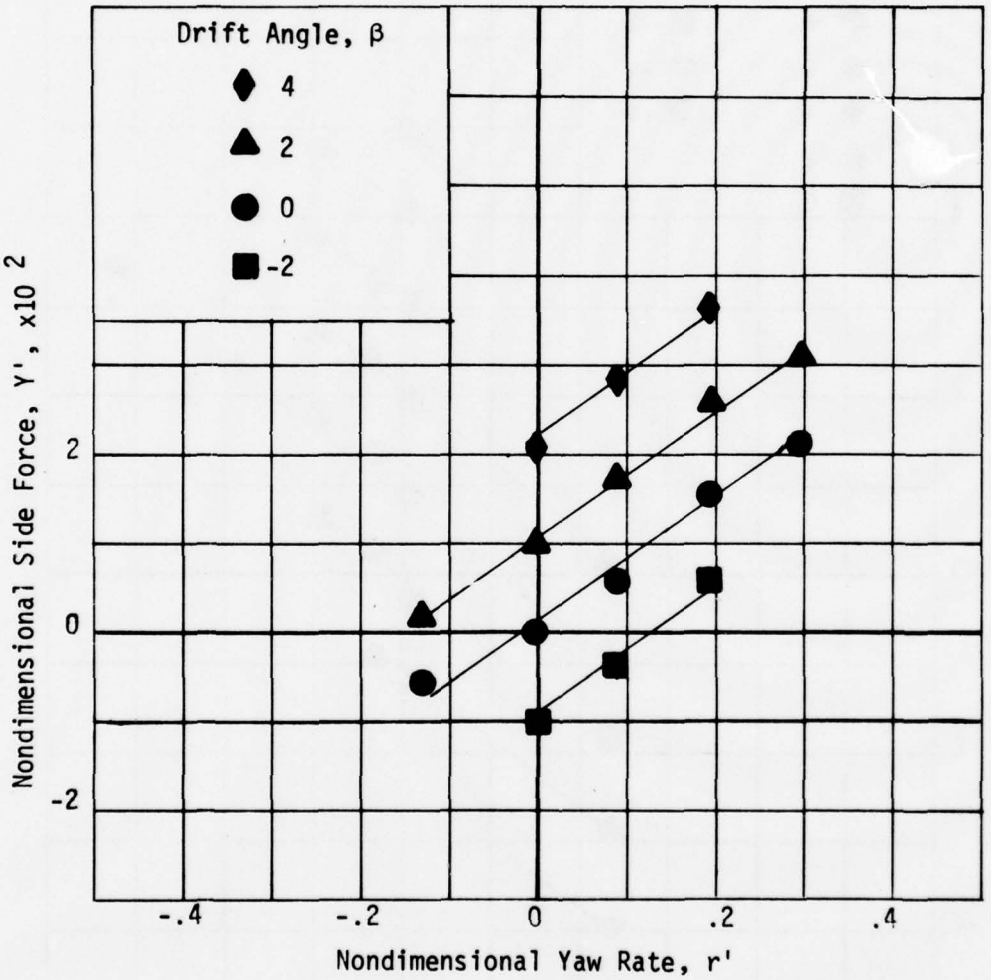

Figure 29 - Variation of Nondimensional Side Force with Nondimensional Yaw Rate for a Series of Drift Angles at a Full Scale Speed of 11 Knots at Design Draft

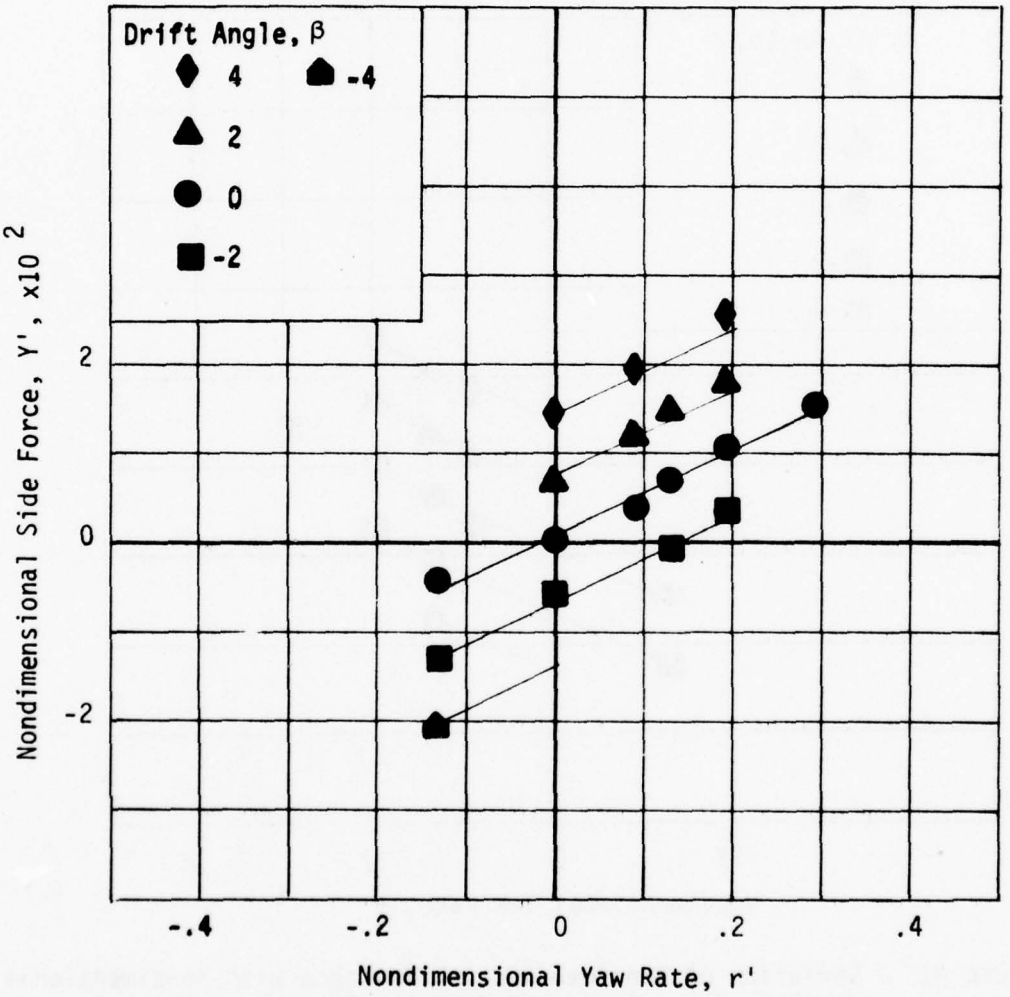

Figure 30 - Variation of Nondimensional Side Force with Nondimensional Yaw Rate for a Series of Drift Angles at a Full Scale Speed of 14 Knots at Design Draft

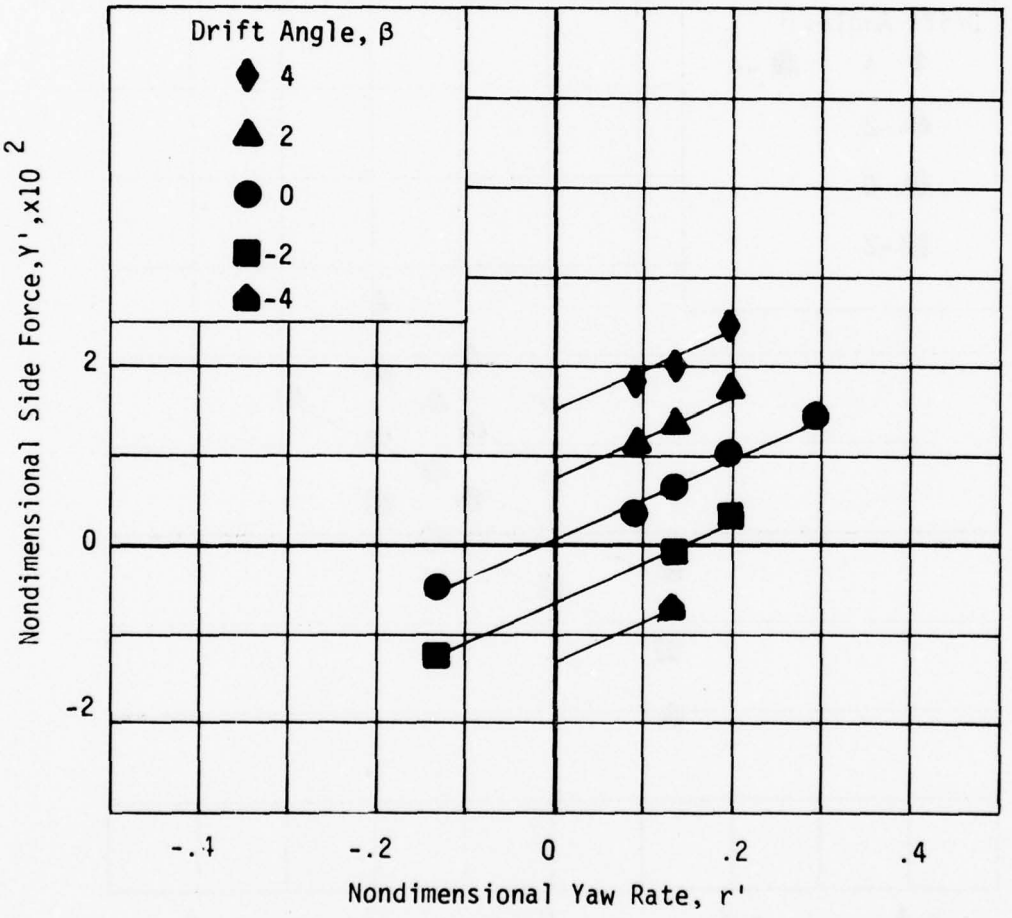

Figure 31 - Variation of Nondimensional Side Force with Nondimensional Yaw Rate for a Series of Drift Angles at a Full Scale Speed of 15 Knots at Design Draft

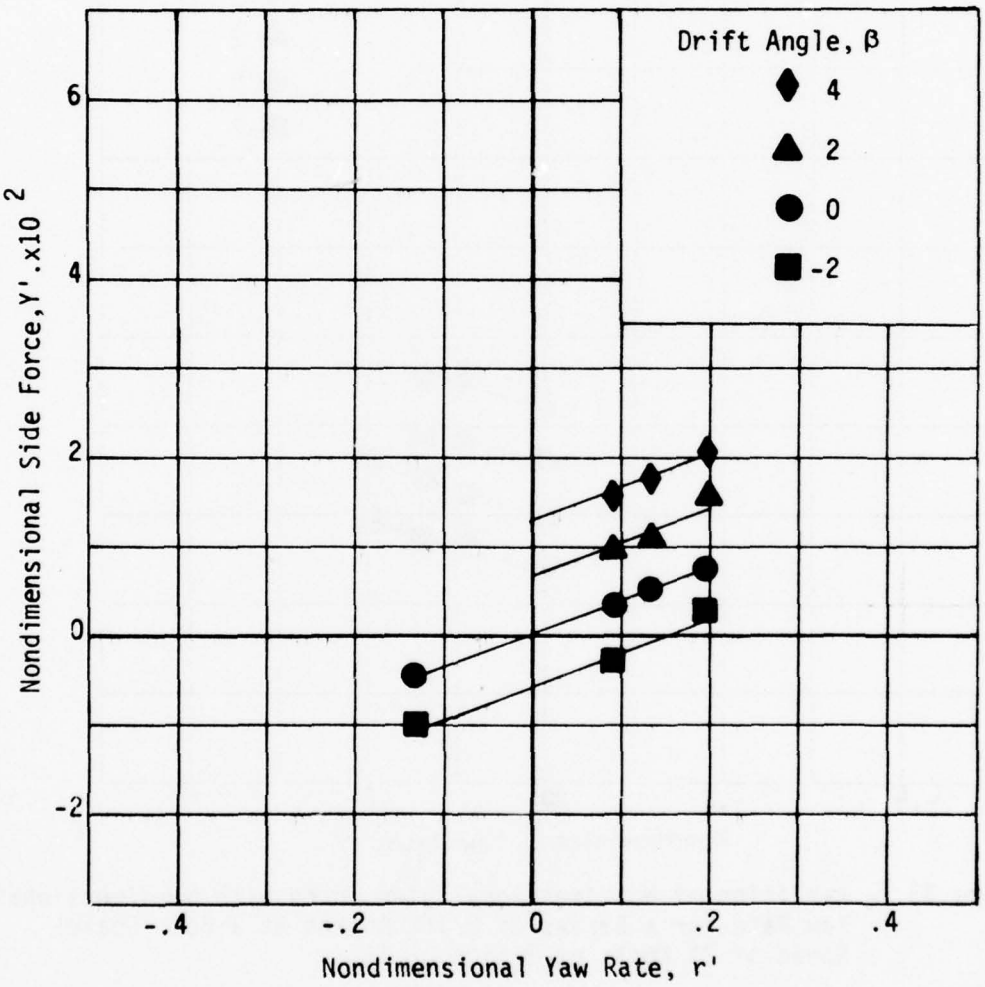

Figure 32 - Variation of Nondimensional Side Force with Nondimensional Yaw Rate for a Series of Drift Angles at a Full Scale Speed of 18 Knots at Design Draft

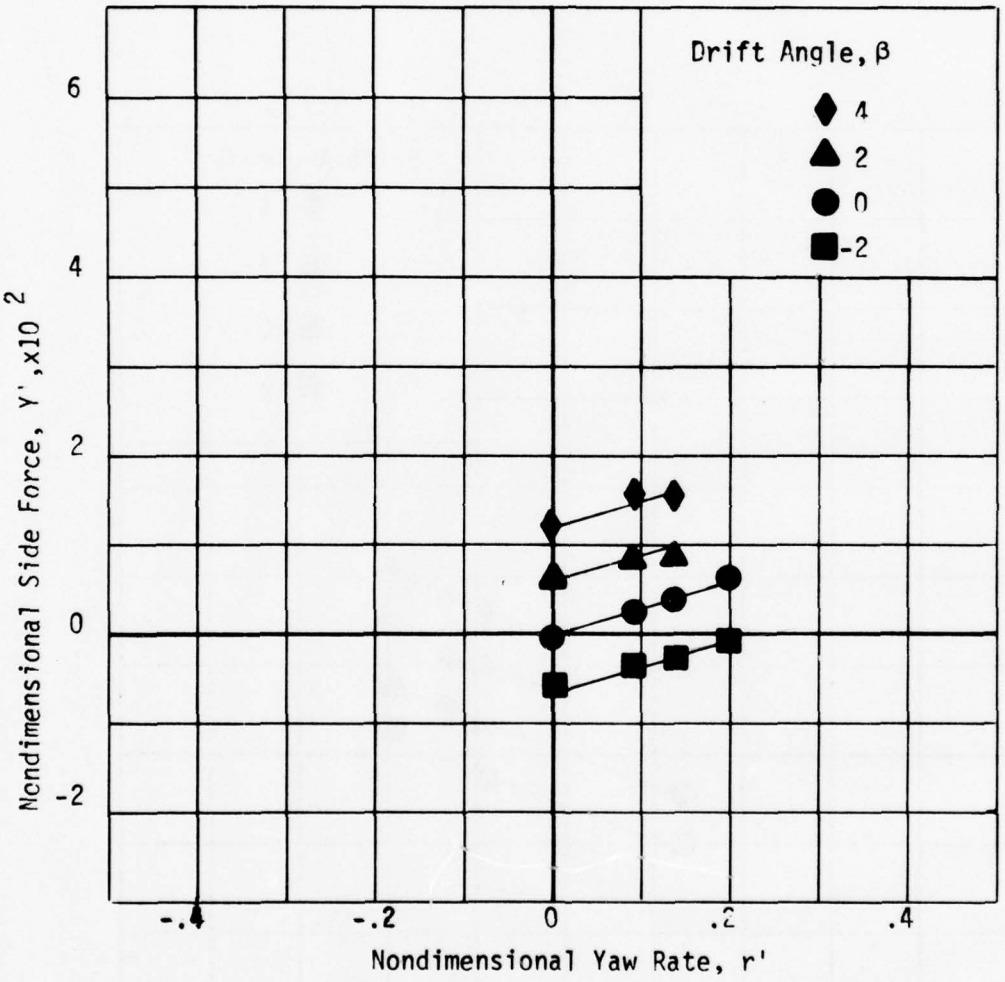

Figure 33 - Variation of Nondimensional Side Force with Nondimensional Yaw Rate for a Series of Drift Angles at a Full Scale Speed of 21 Knots at Design Draft

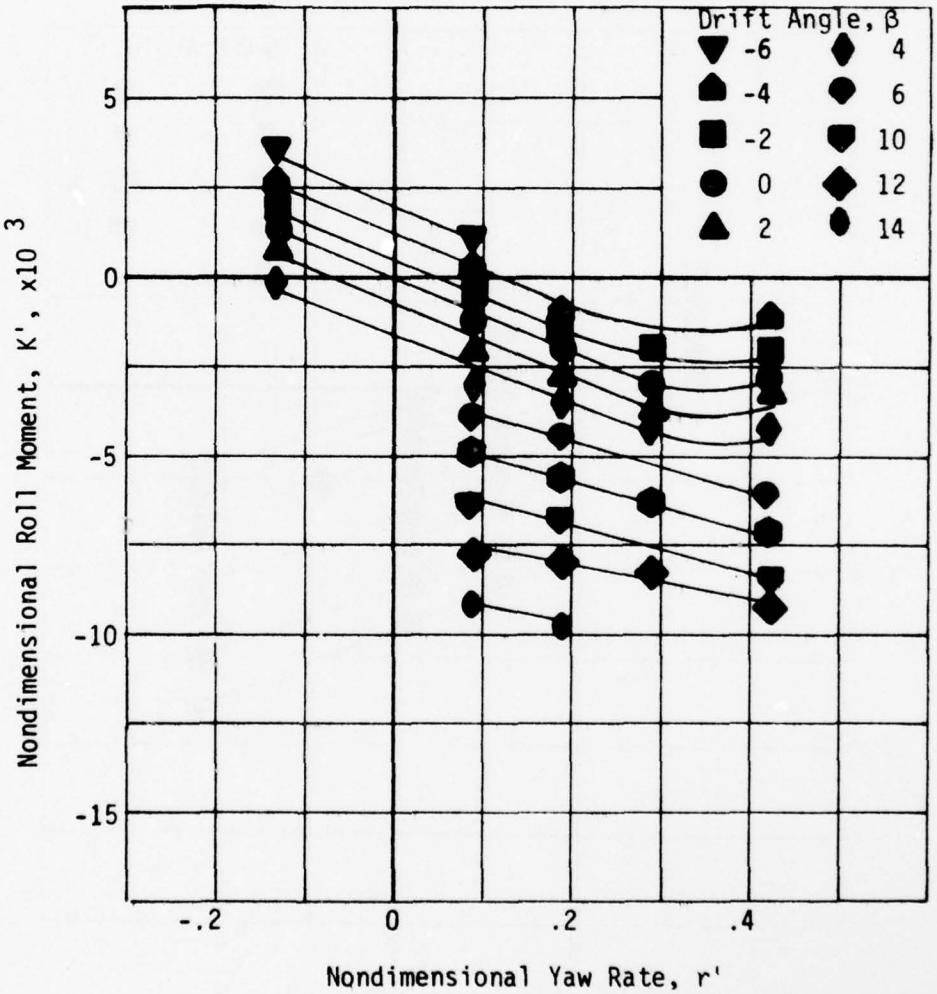

Figure 34 - Variation of Nondimensional Roll Moment with Nondimensional Yaw Rate for a Series of Drift Angles at a Full Scale Speed of 3 Knots at Design Draft

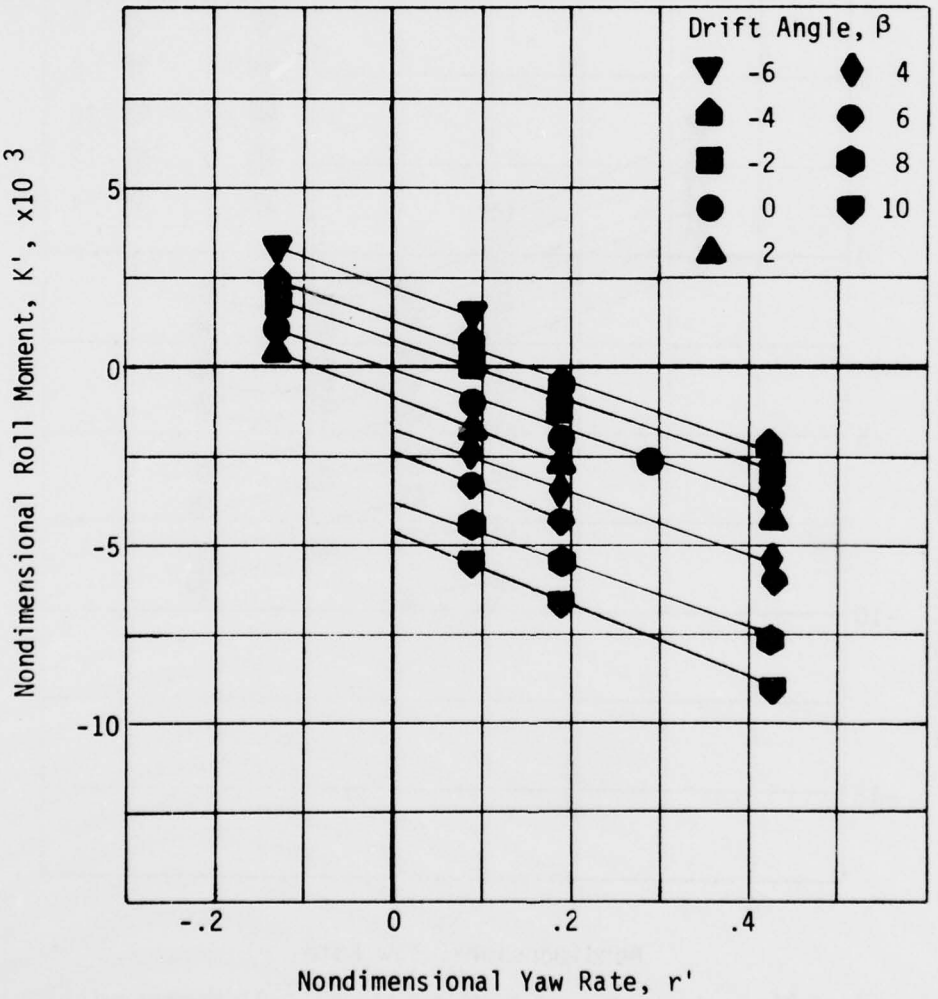

Figure 35 - Variation of Nondimensional Roll Moment with Nondimensional Yaw Rate for a Series of Drift Angles at a Full Scale Speed of 6 Knots at Design Draft

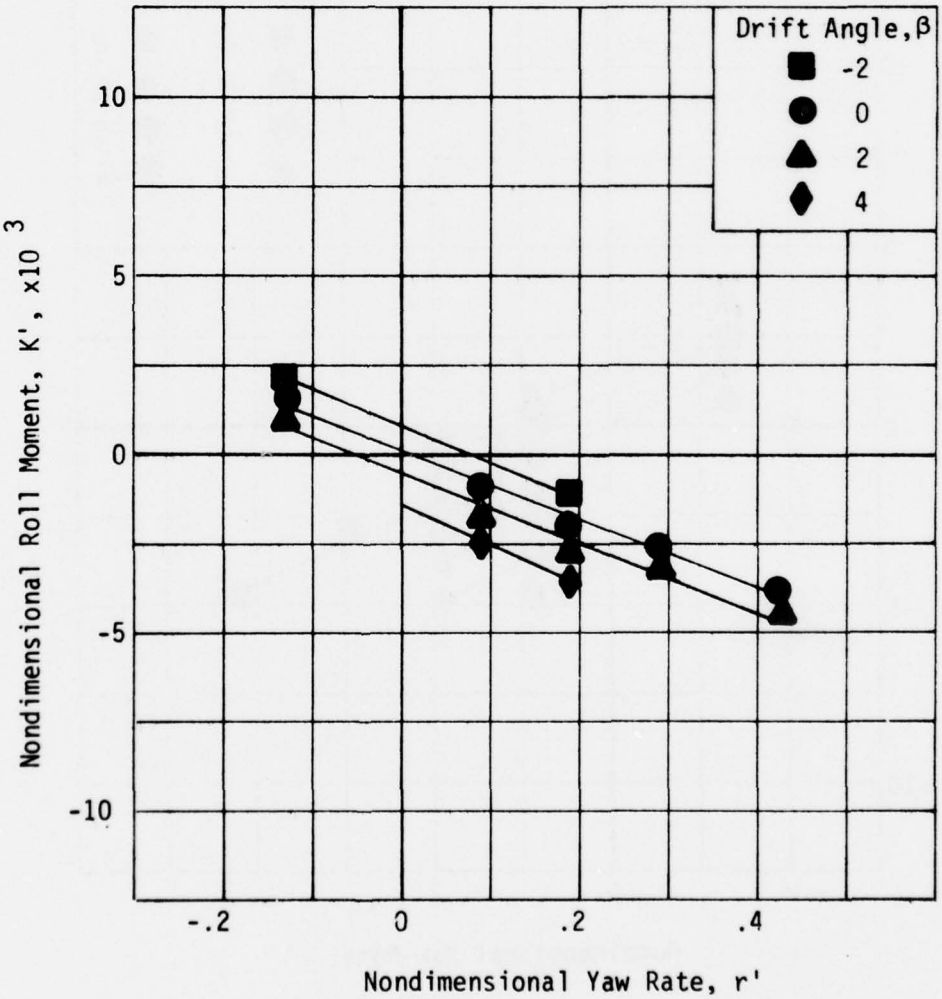

Figure 36 - Variation of Nondimensional Roll Moment with Nondimensional Yaw Rate for a Series of Drift Angles at a Full Scale Speed of 7 Knots at Design Draft

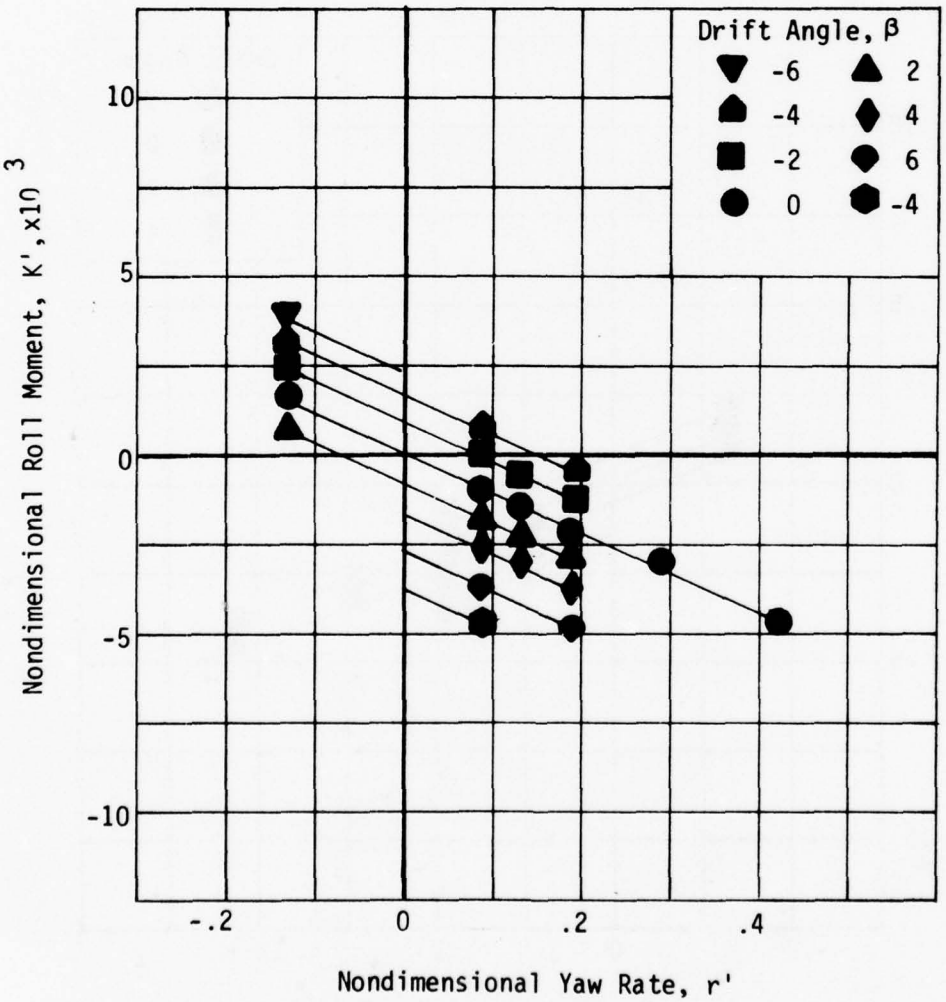

Figure 37 - Variation of Nondimensional Roll Moment with Nondimensional Yaw Rate for a Series of Drift Angles at a Full Scale Speed of 9 Knots at Design Draft

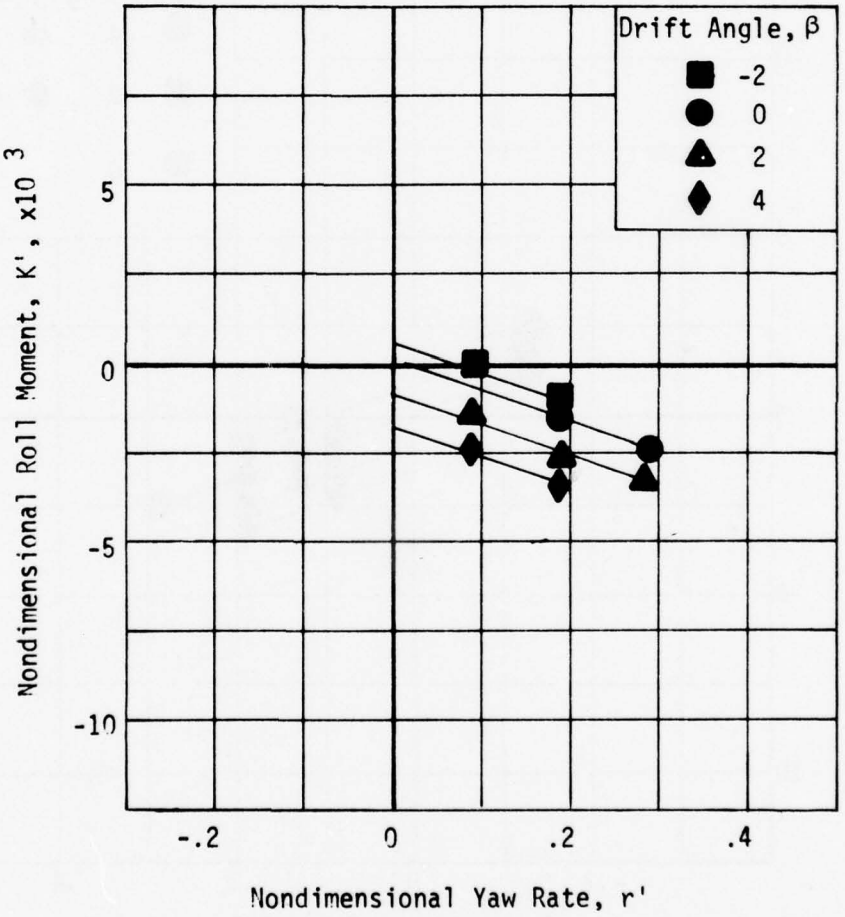

Figure 38 - Variation of Nondimensional Roll Moment with Nondimensional Yaw Rate for a Series of Drift Angles at a Full Scale Speed of 11 Knots at Design Draft

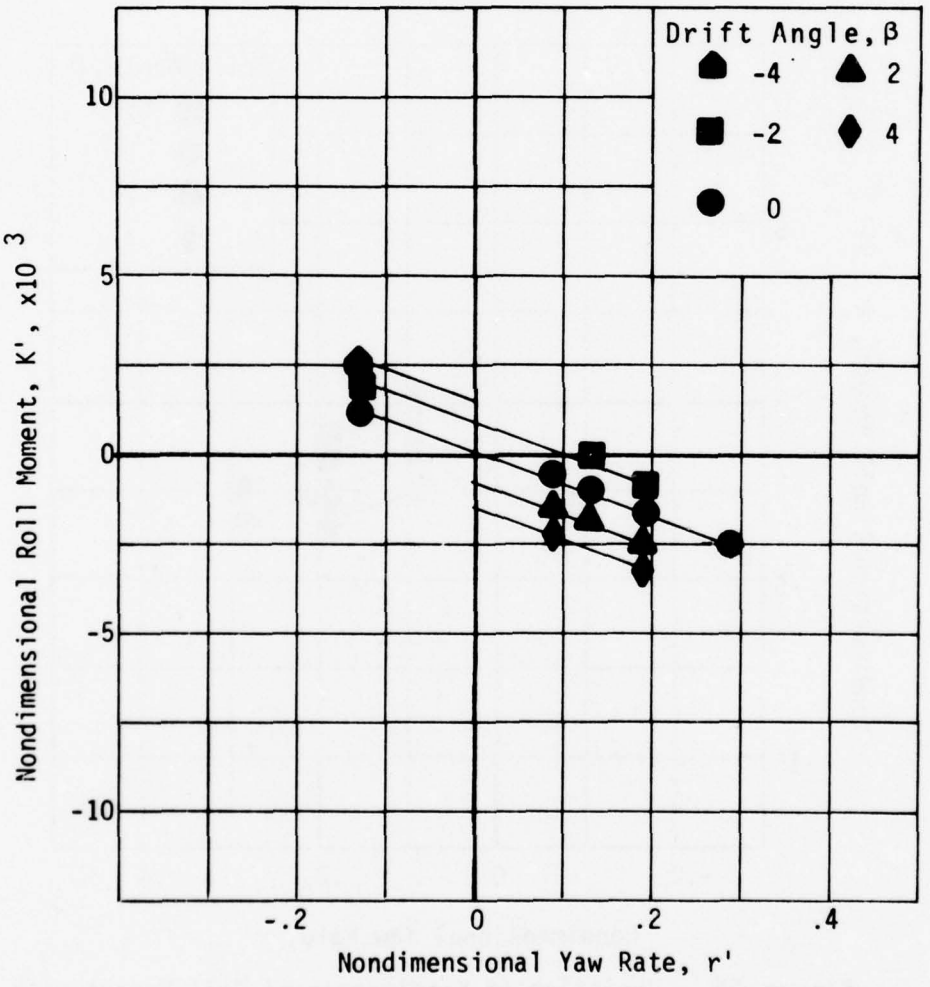

Figure 39 - Variation of Nondimensional Roll Moment with Nondimensional Yaw Rate for a Series of Drift Angles at a Full Scale Speed of 14 Knots at Design Draft

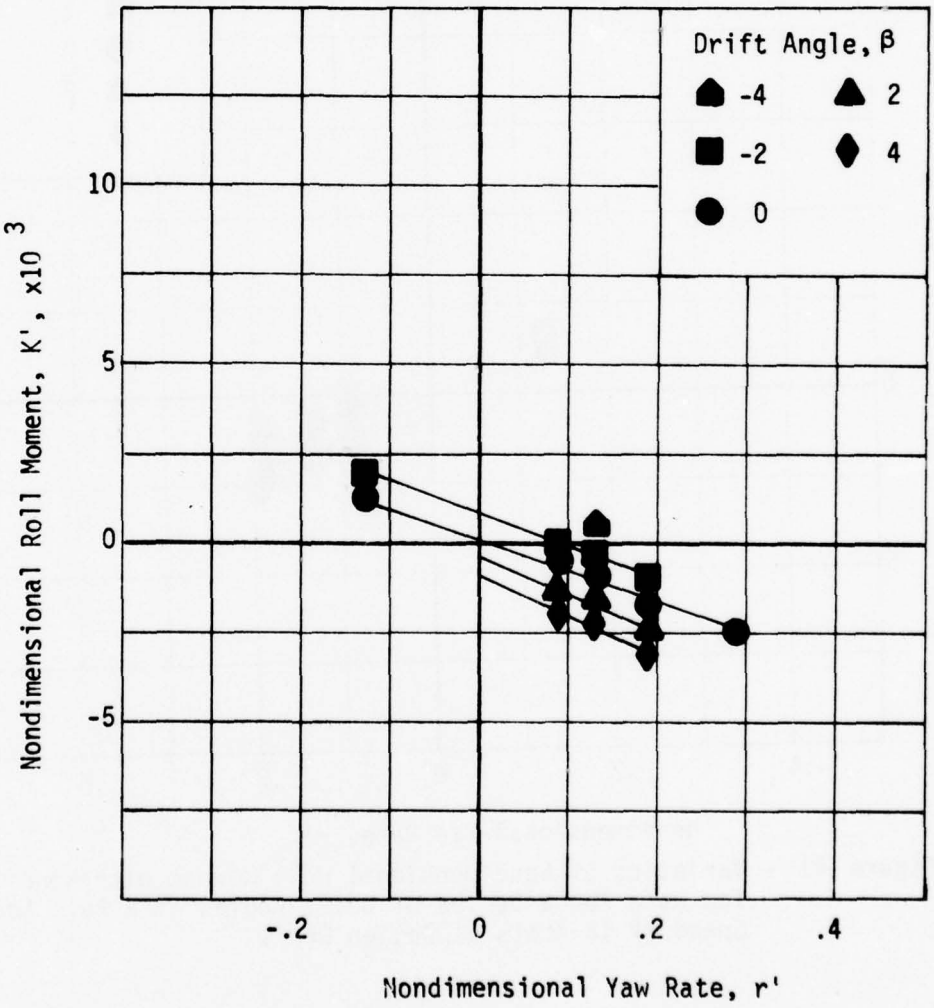

Figure 40 - Variation of Nondimensional Roll Moment with Nondimensional Yaw Rate for a Series of Drift Angles at a Full Scale Speed of 15 Knots at Design Draft

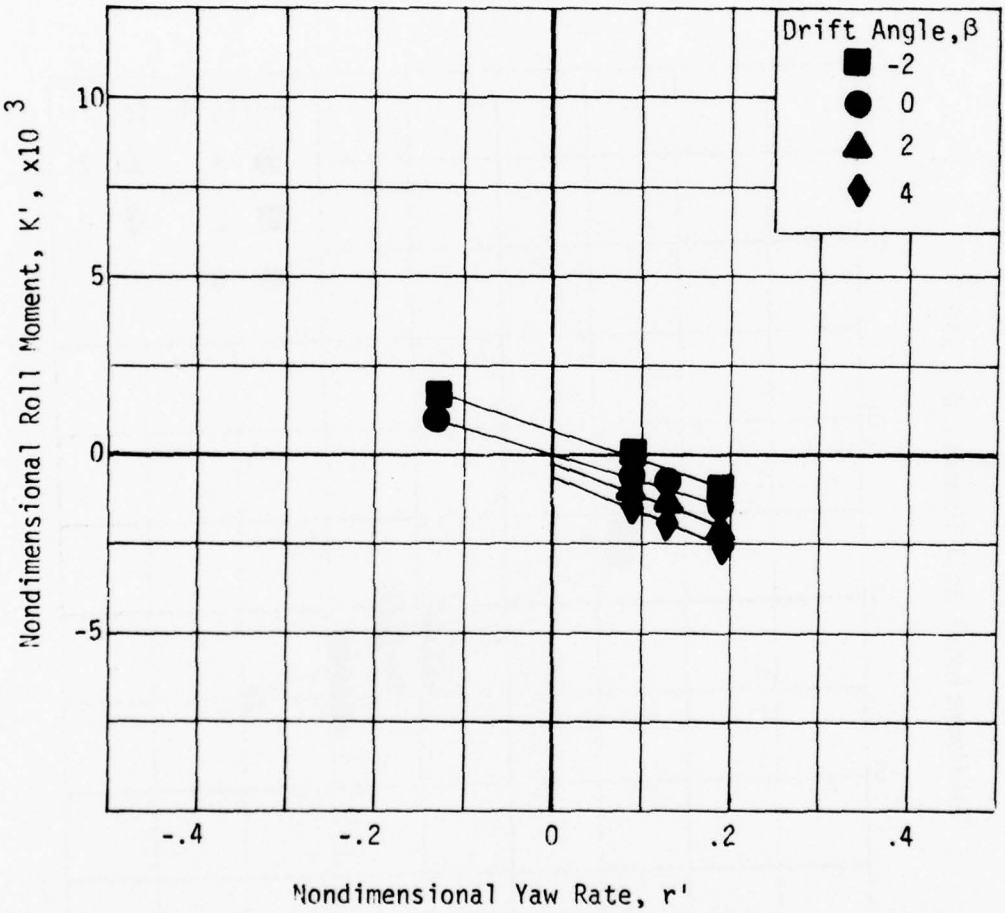

Figure 41 - Variation of Nondimensional Roll Moment with Nondimensional Yaw Rate for a Series of Drift Angles at a Full Scale Speed of 18 Knots at Design Draft

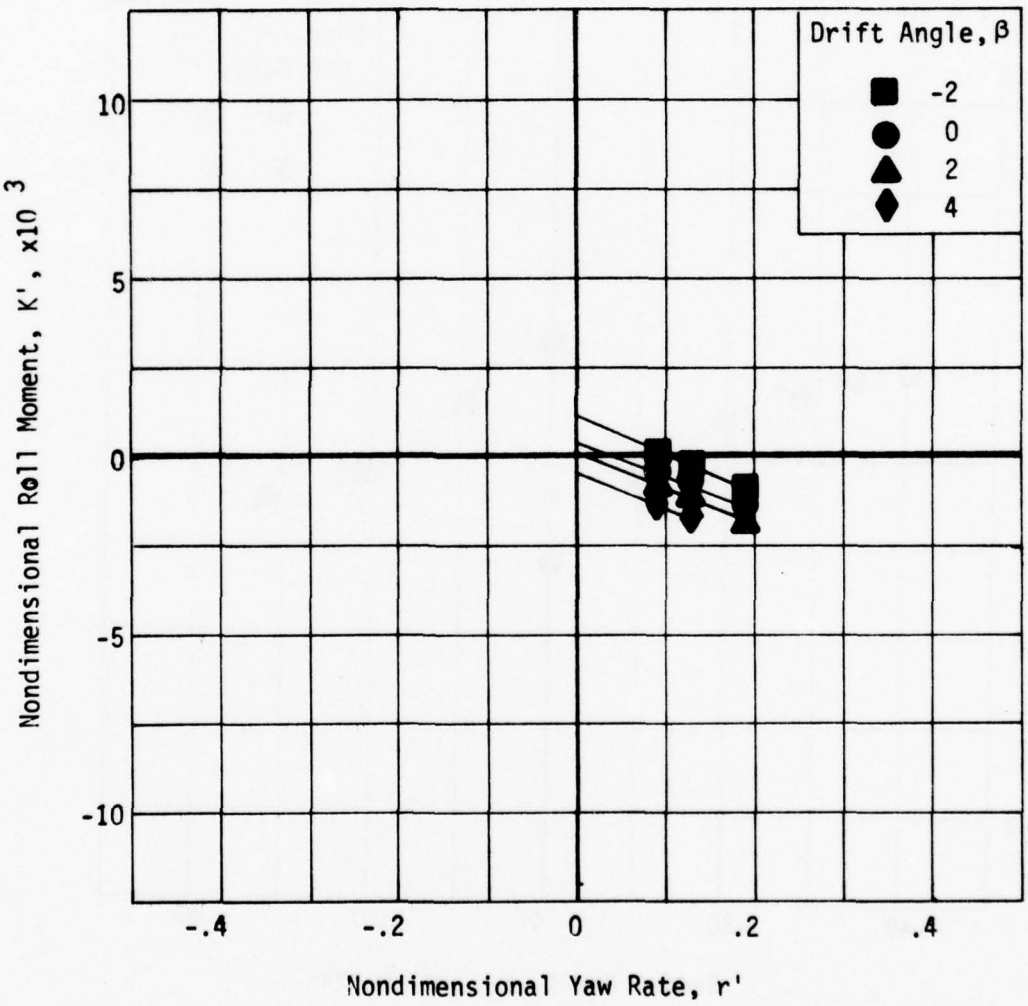

Figure 42 - Variation of Nondimensional Roll Moment with Nondimensional Yaw Rate for a Series of Drift Angles at a Full Scale Speed of 21 Knots at Design Draft

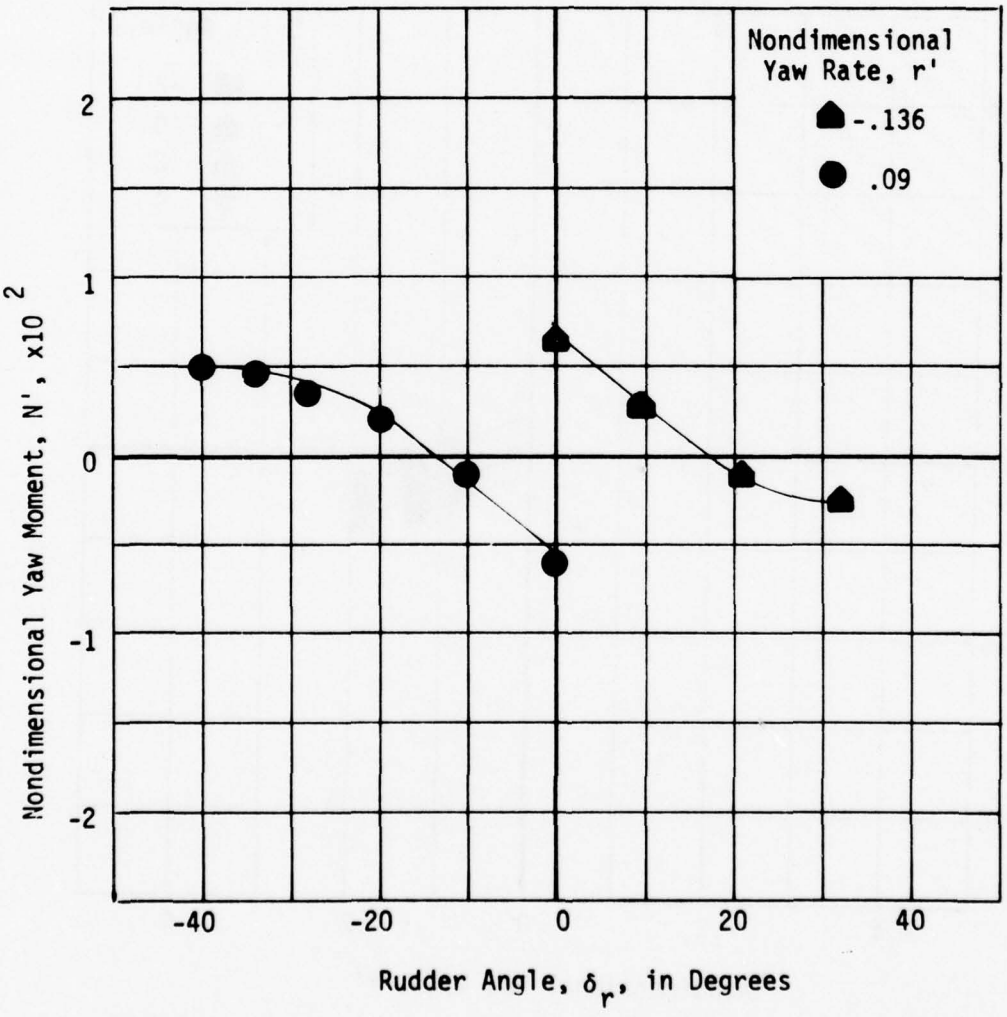

Figure 43 - Variation of Nondimensional Yaw Moment with Rudder Angle for a Series of Nondimensional Yaw Rates at a Full Scale Speed of 3 Knots at Design Draft

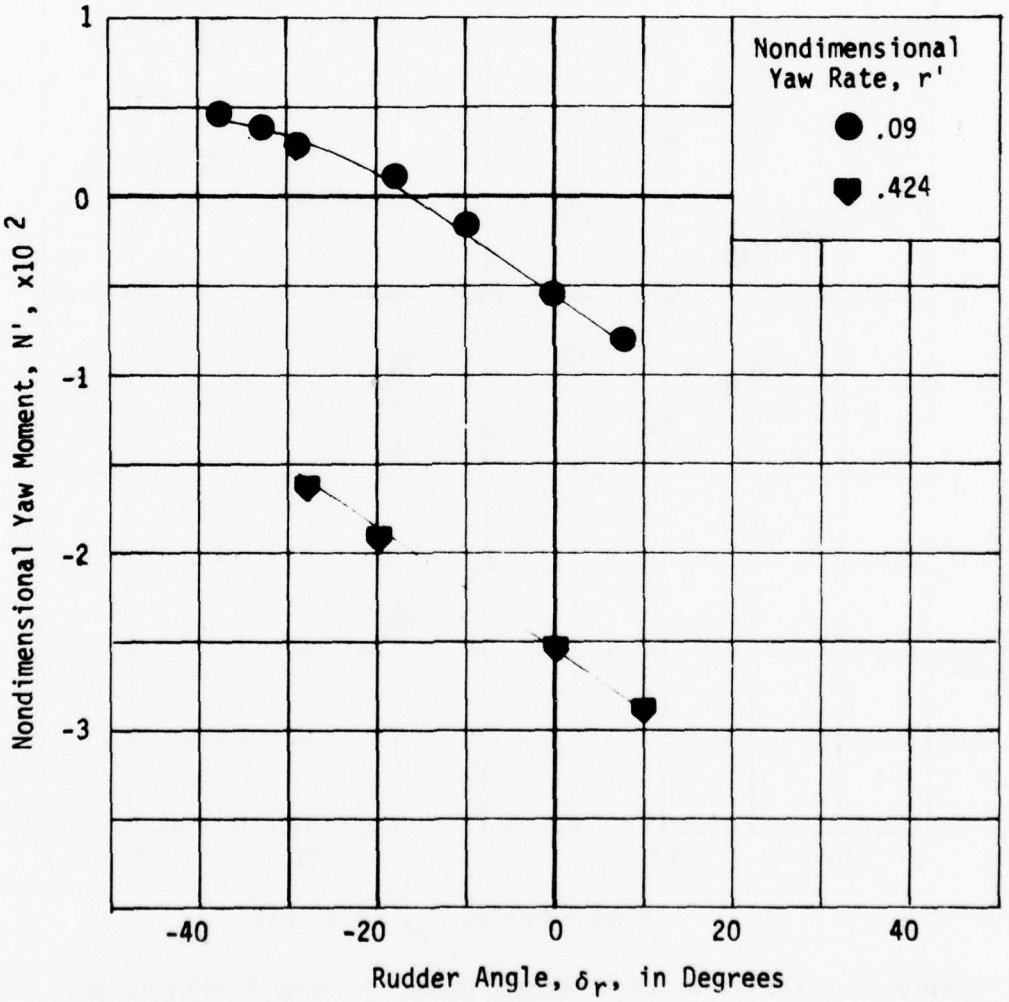

Figure 44 - Variation of Nondimensional Yaw Moment with Rudder Angle for a Series of Nondimensional Yaw Rates at a Full Scale Speed of 6 Knots at Design Draft

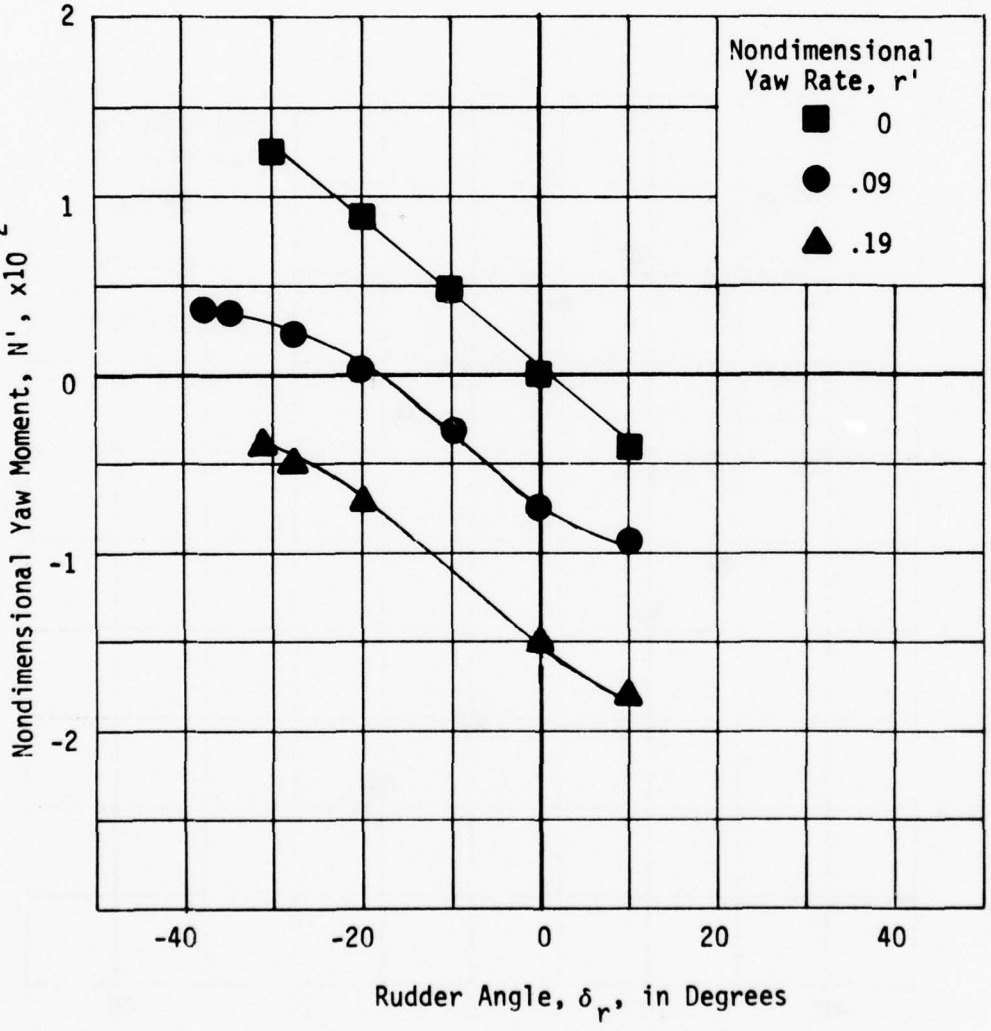

Figure 45 - Variation of Nondimensional Yaw Moment with Rudder Angle for a Series of Nondimensional Yaw Rates at a Full Scale Speed of 7 Knots at Design Draft

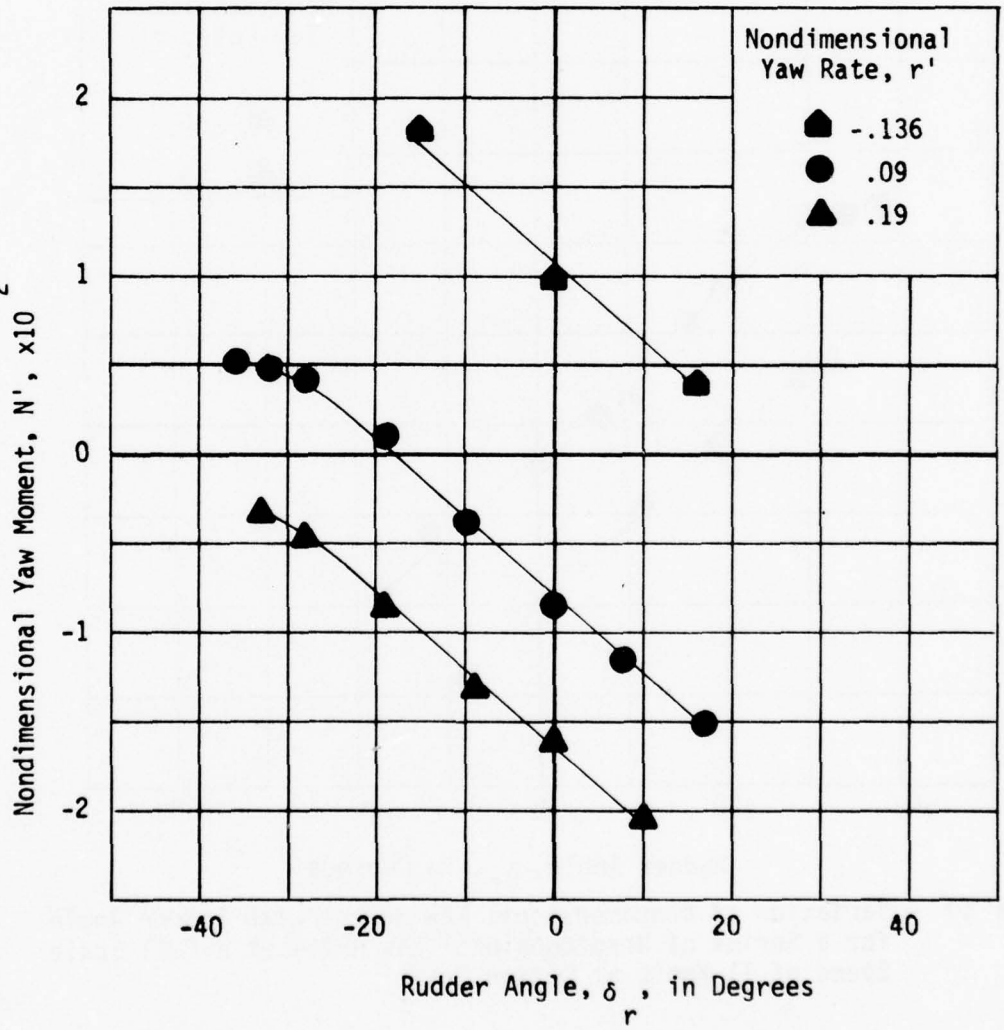

Figure 46 - Variation of Nondimensional Yaw Moment with Rudder Angle for a Series of Nondimensional Yaw Rates at a Full Scale Speed of 9 Knots at Design Draft

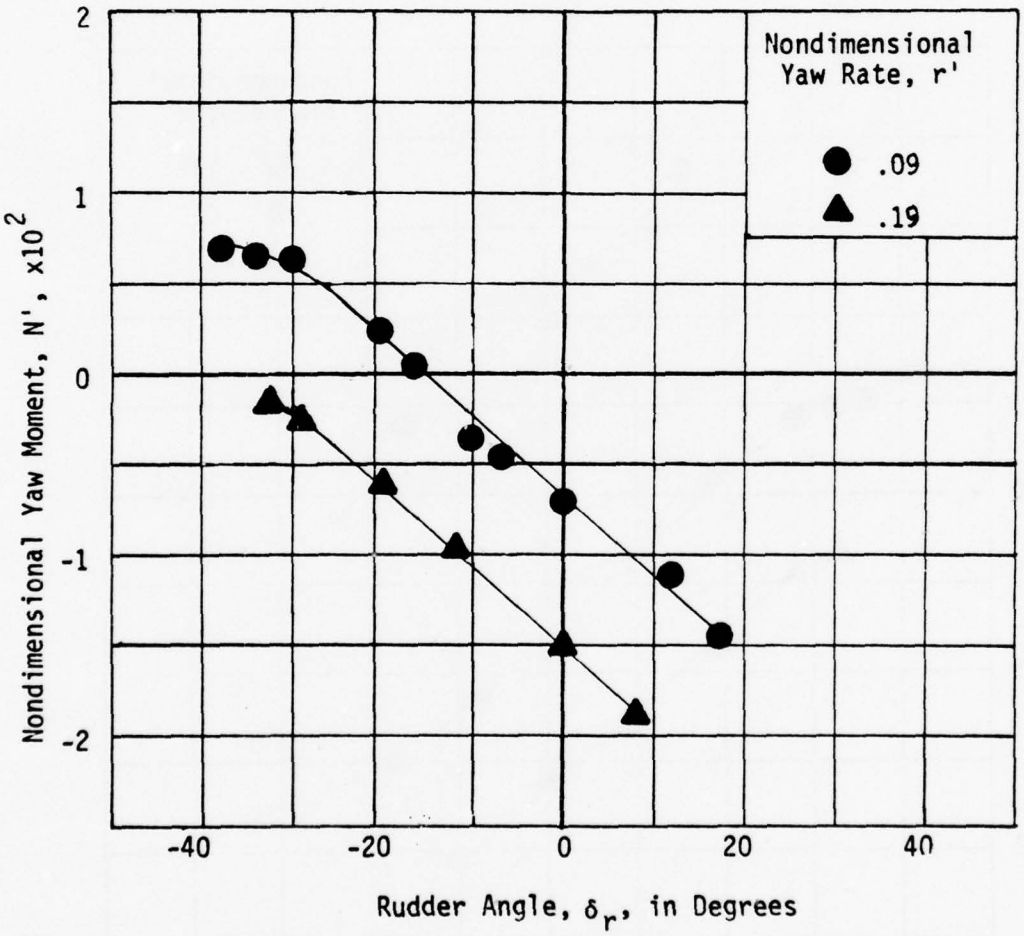

Figure 47 - Variation of Nondimensional Yaw Moment with Rudder Angle for a Series of Nondimensional Yaw Rates at a Full Scale Speed of 11 Knots at Design Draft

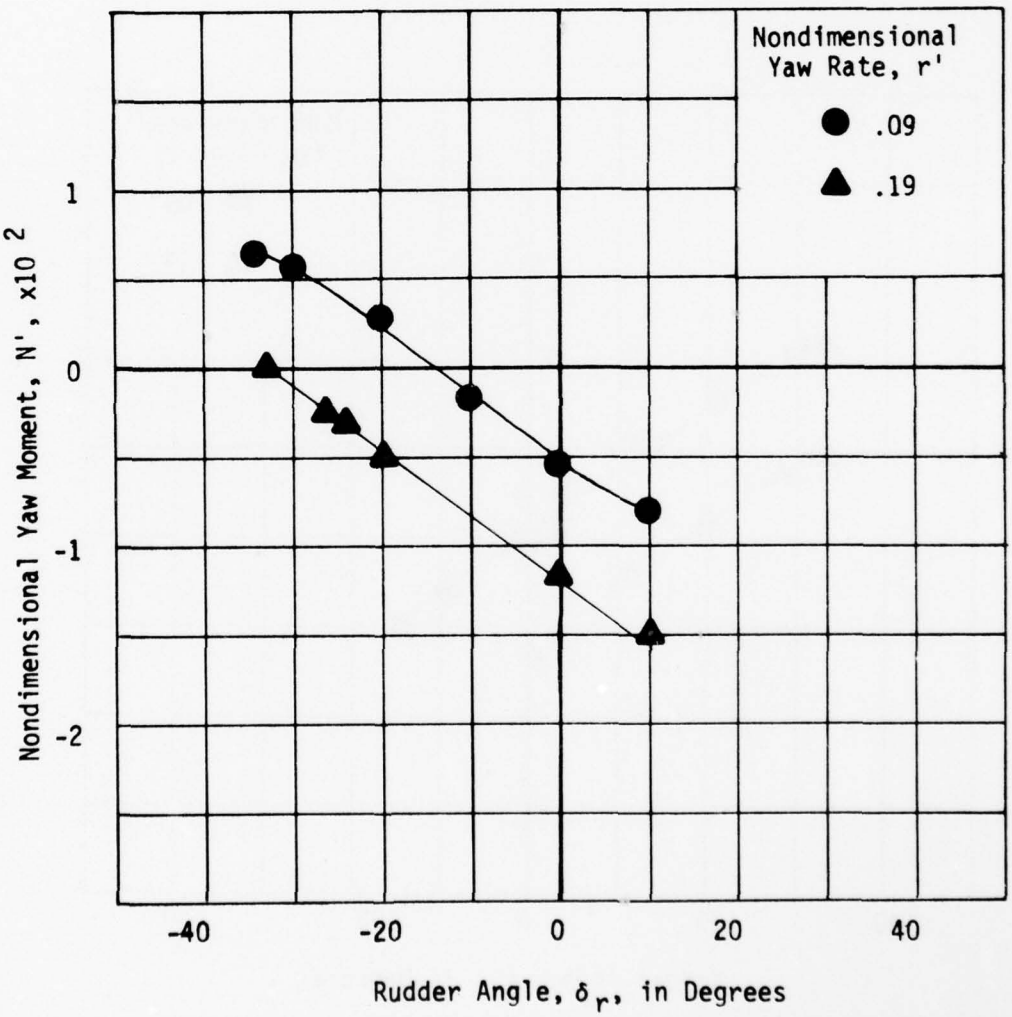

Figure 48 - Variation of Nondimensional Yaw Moment with Rudder Angle for a Series of Nondimensional Yaw Rates at a Full Scale Speed of 14 Knots at Design Draft

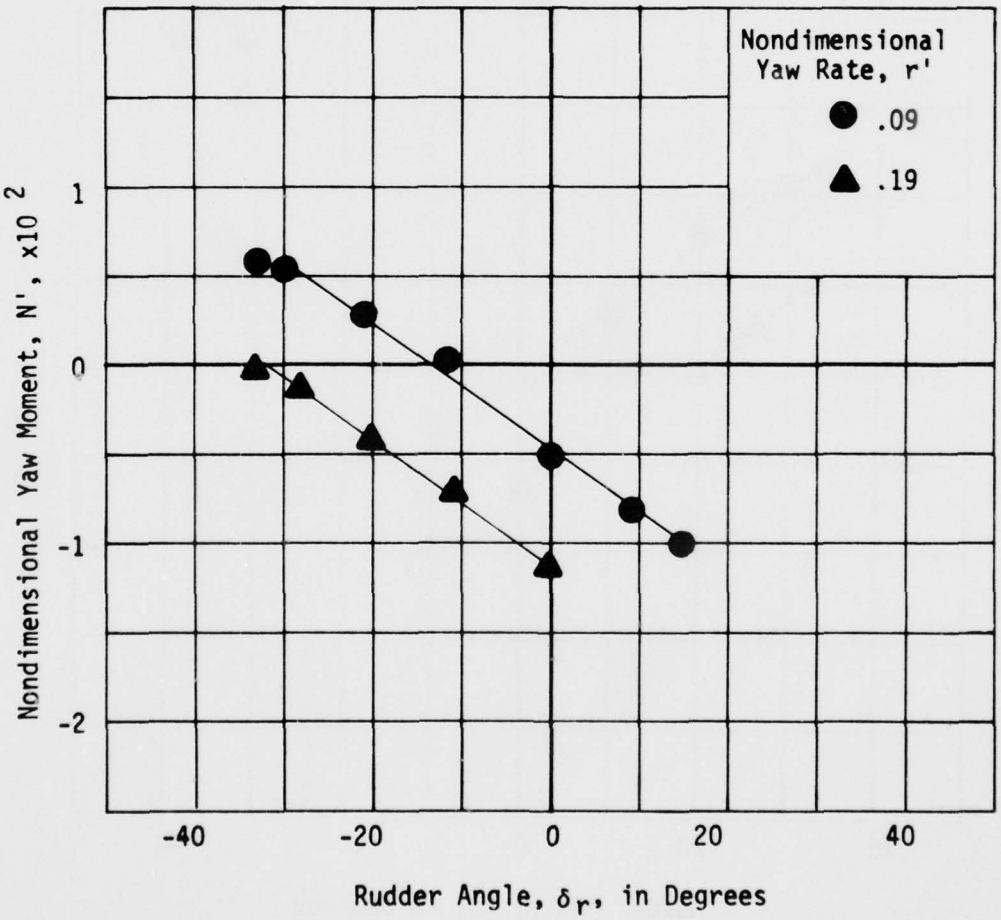

Figure 49 - Variation of Nondimensional Yaw Moment with Rudder Angle for a Series of Nondimensional Yaw Rates at a Full Scale Speed of 15 Knots at Design Draft

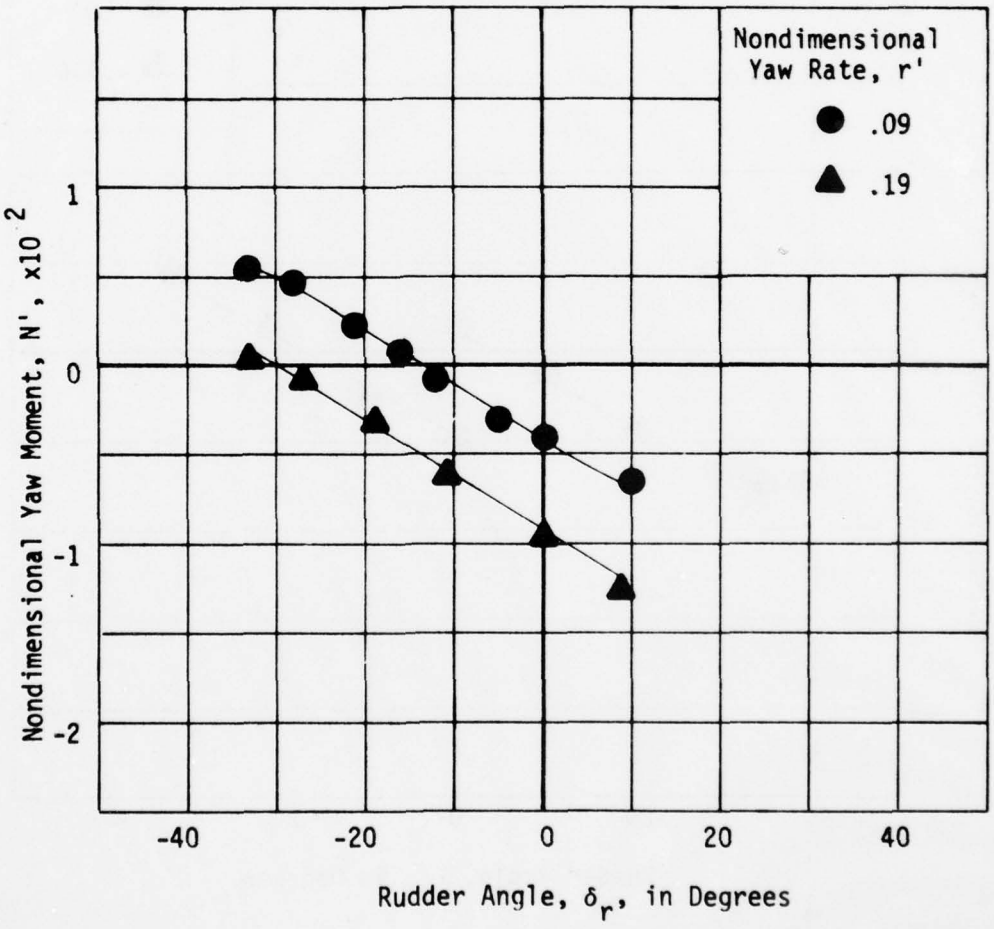

Figure 50- Variation of Nondimensional Yaw Moment with Rudder Angle for a Series of Nondimensional Yaw Rates at a Full Scale Speed of 18 Knots at Design Draft

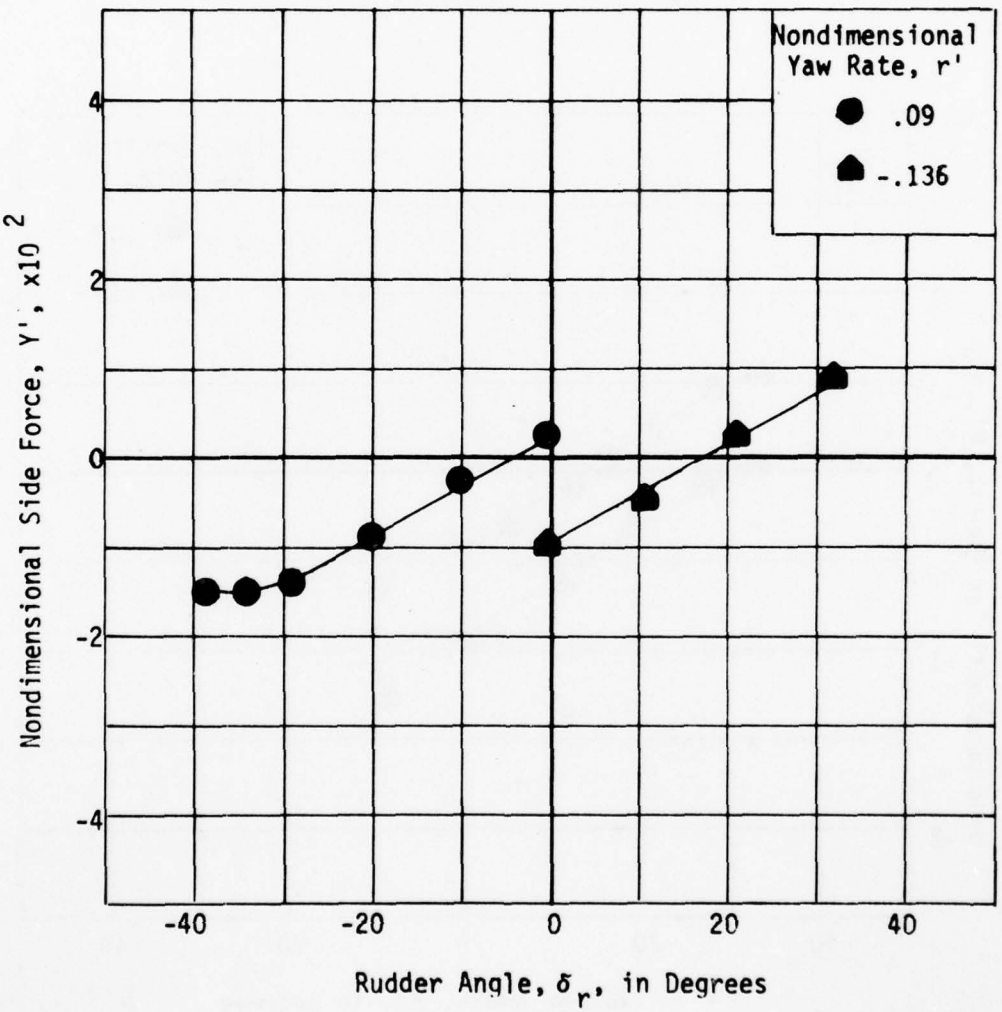

Figure 51 - Variation of Nondimensional Side Force with Rudder Angle for a Series of Nondimensional Yaw Rates at a Full Scale Speed of 3 Knots at Design Draft

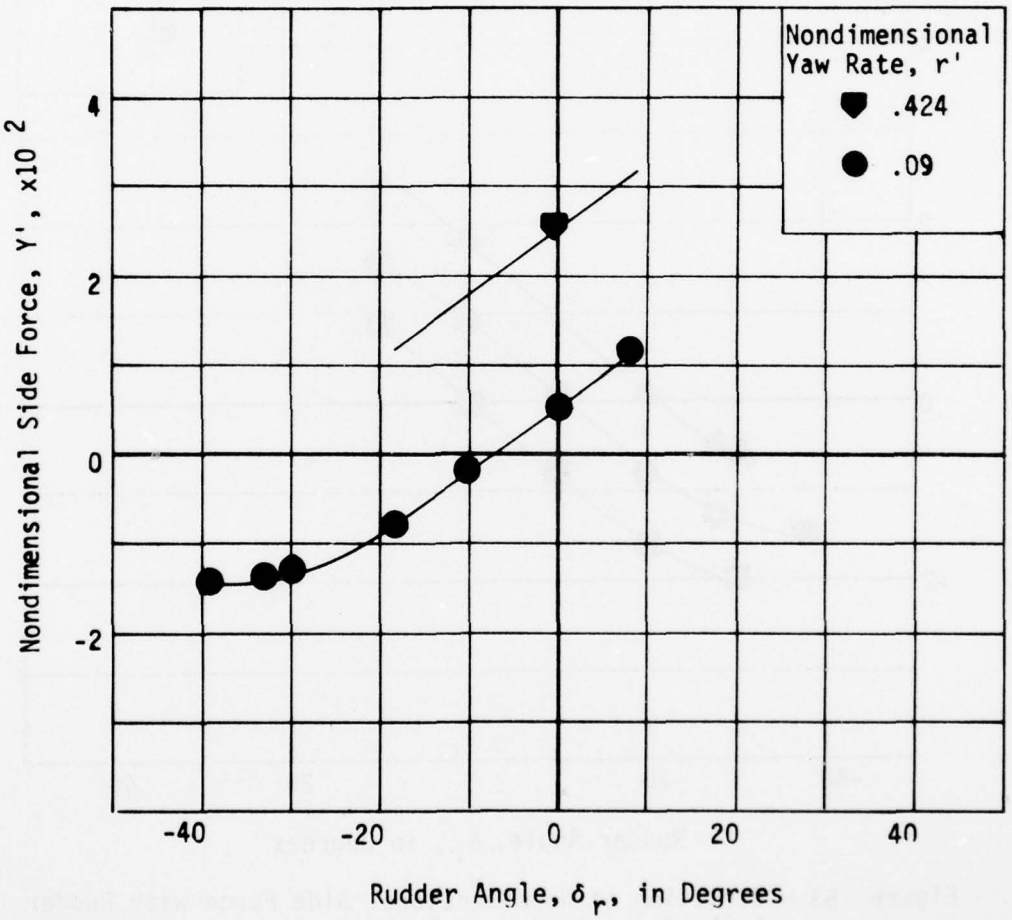

Figure 52 - Variation of Nondimensional Side Force with Rudder Angle for a Series of Nondimensional Yaw Rates at a Full Scale Speed of 6 Knots at Design Draft

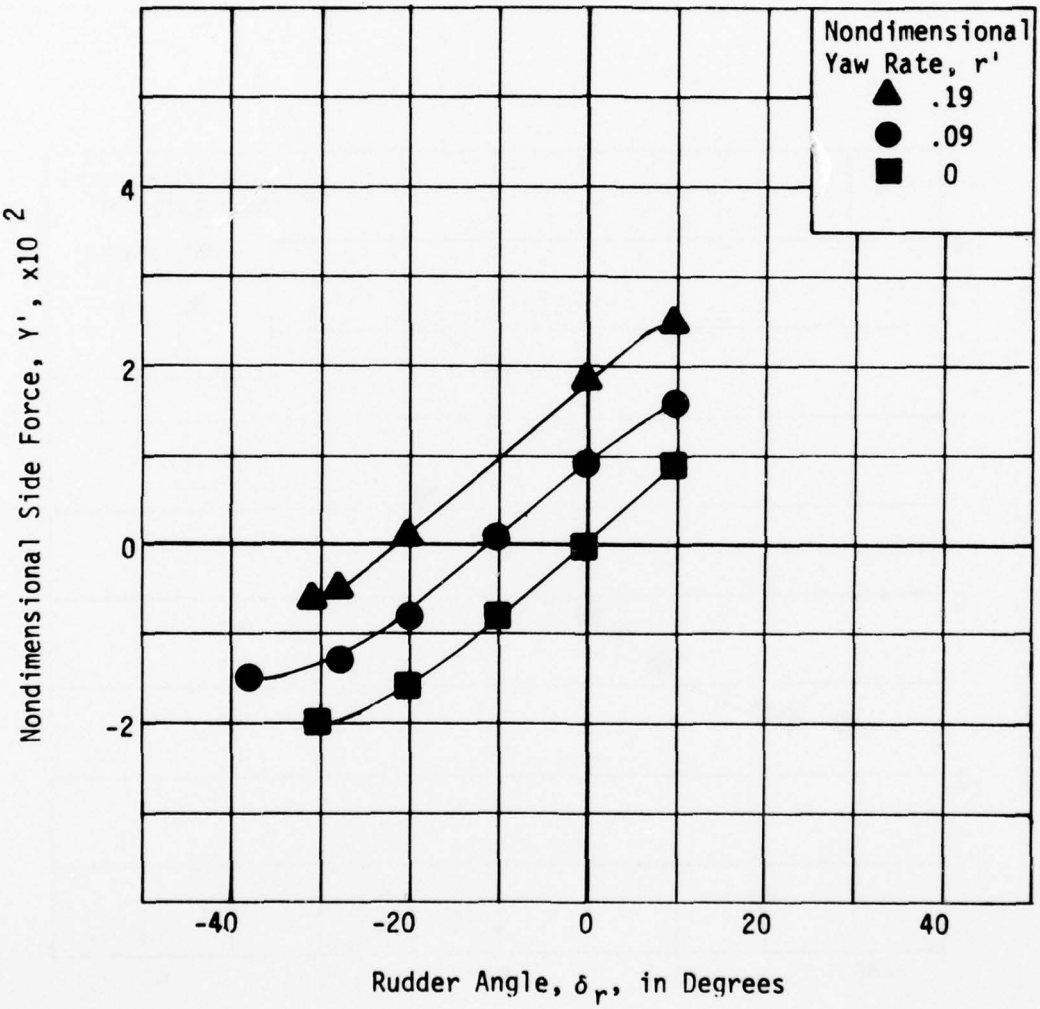

Figure 53 - Variation of Nondimensional Side Force with Rudder Angle for a Series of Nondimensional Yaw Rates at a Full Scale Speed of 7 Knots at Design Draft

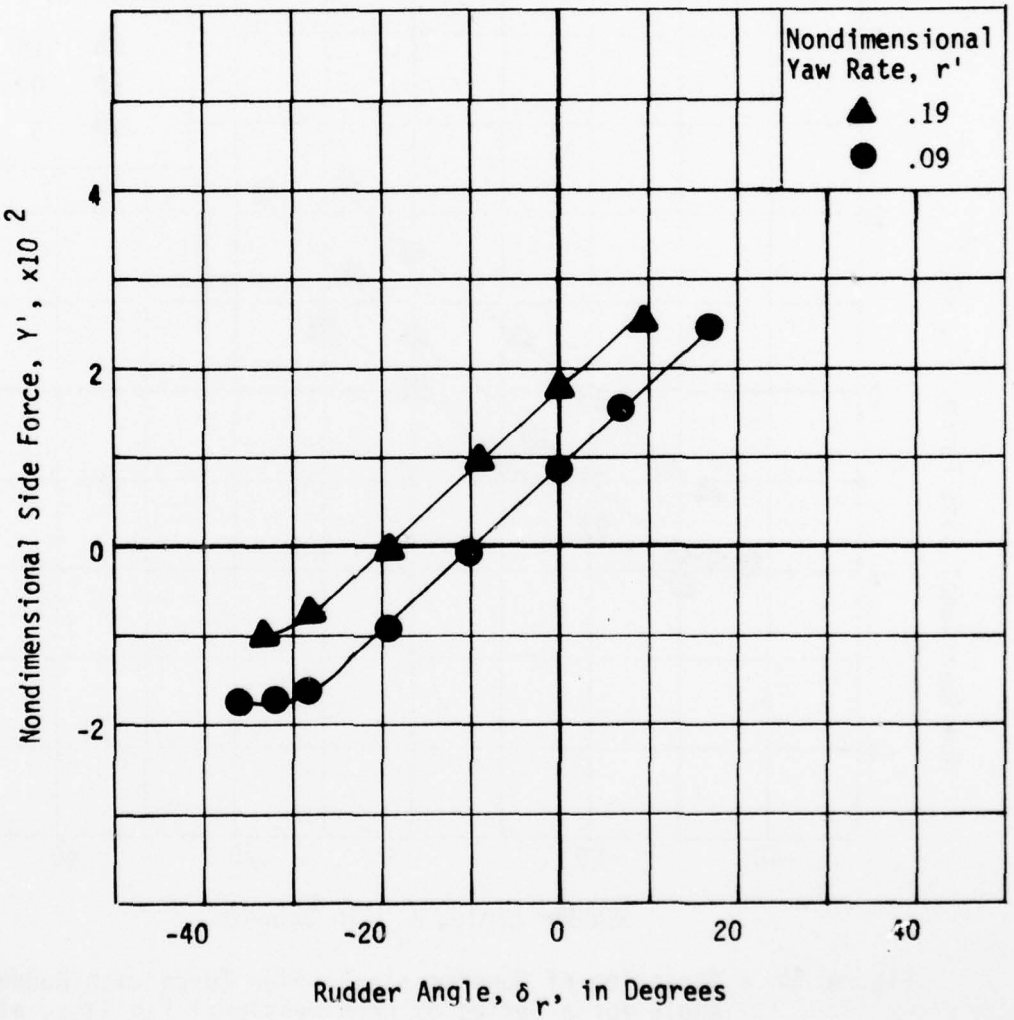

Figure 54 - Variation of Nondimensional Side Force with Rudder Angle for a Series of Nondimensional Yaw Rates at a Full Scale Speed of 9 Knots at Design Draft

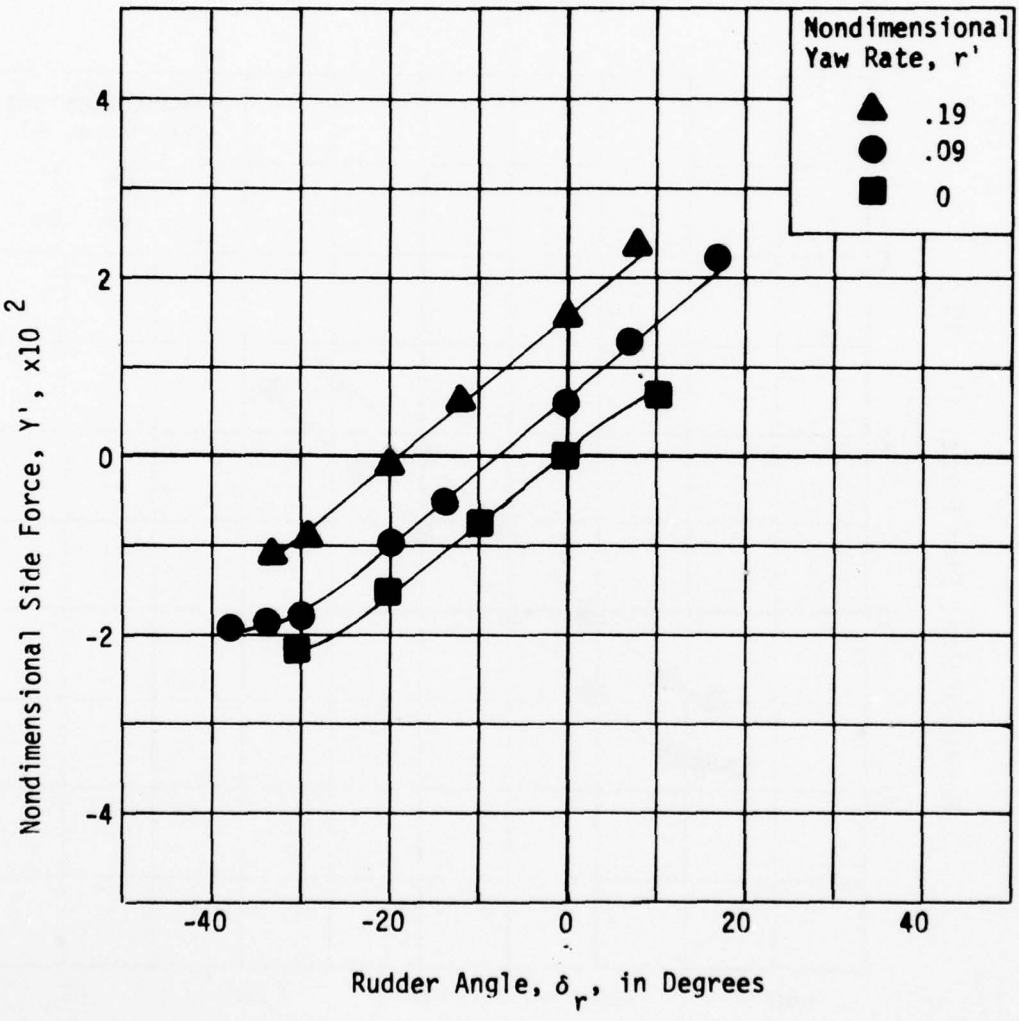

Figure 55 - Variation of Nondimensional Side Force with Rudder Angle for a Series of Nondimensional Yaw Rates at a Full Scale Speed of 11 Knots at Design Draft

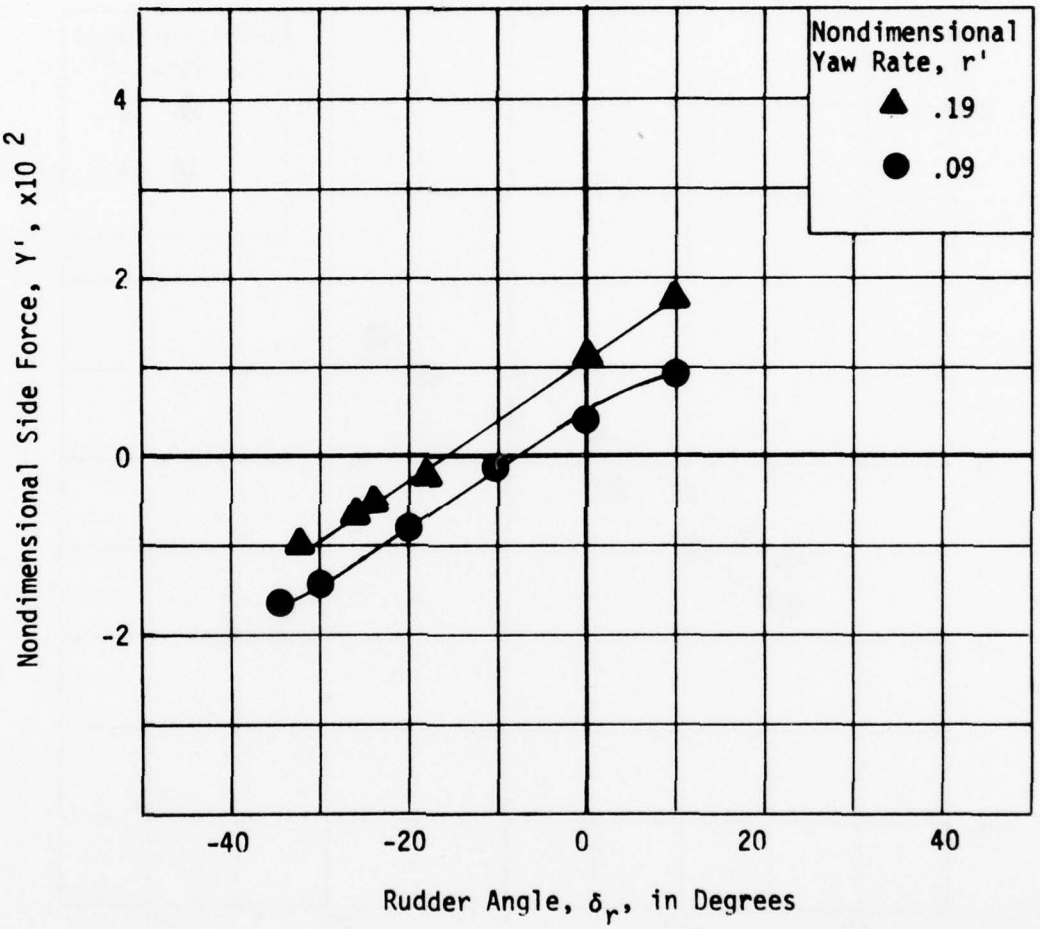

Figure 56 - Variation of Nondimensional Side Force with Rudder Angle for a Series of Nondimensional Yaw Rates at a Full Scale Speed of 14 Knots at Design Draft

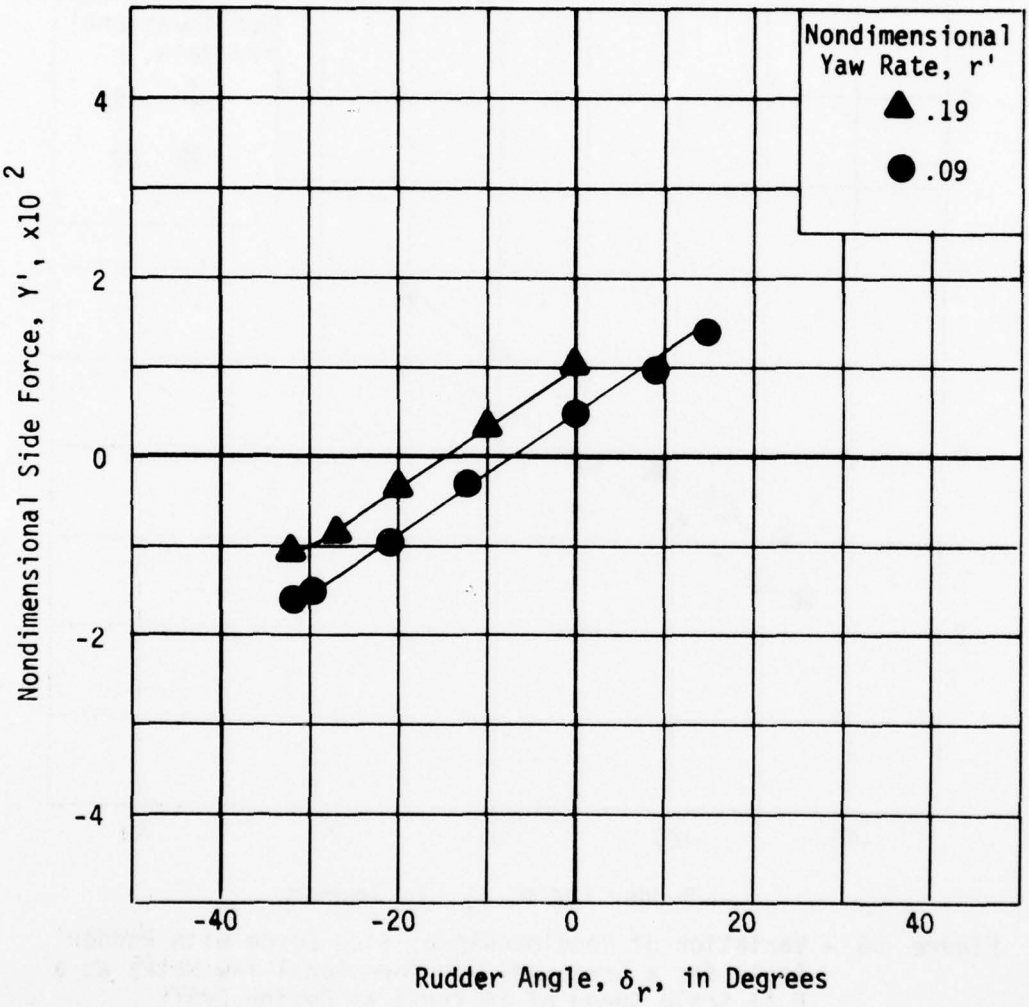

Figure 57 - Variation of Nondimensional Side Force with Rudder Angle for a Series of Nondimensional Yaw Rates at a Full Scale Speed of 15 Knots at Design Draft

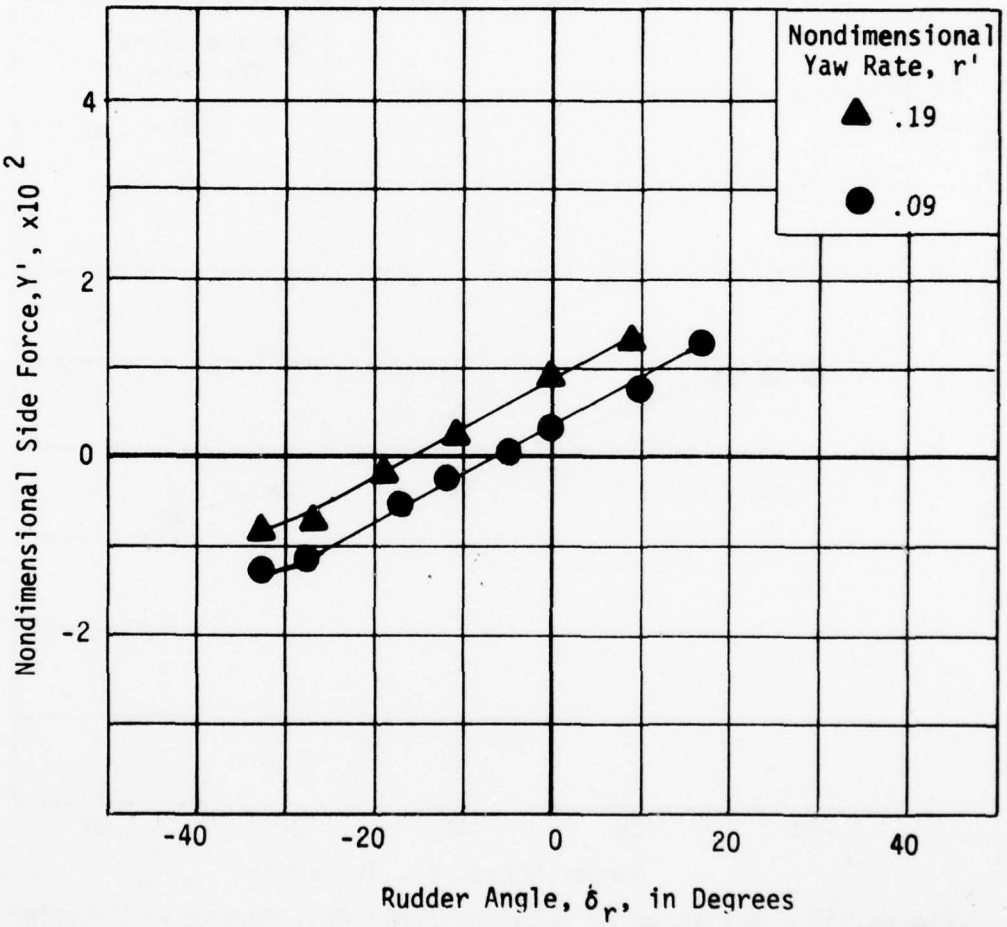

Figure 58 - Variation of Nondimensional Side Force with Rudder Angle for a Series of Nondimensional Yaw Rates at a Full Scale Speed of 18 Knots at Design Draft

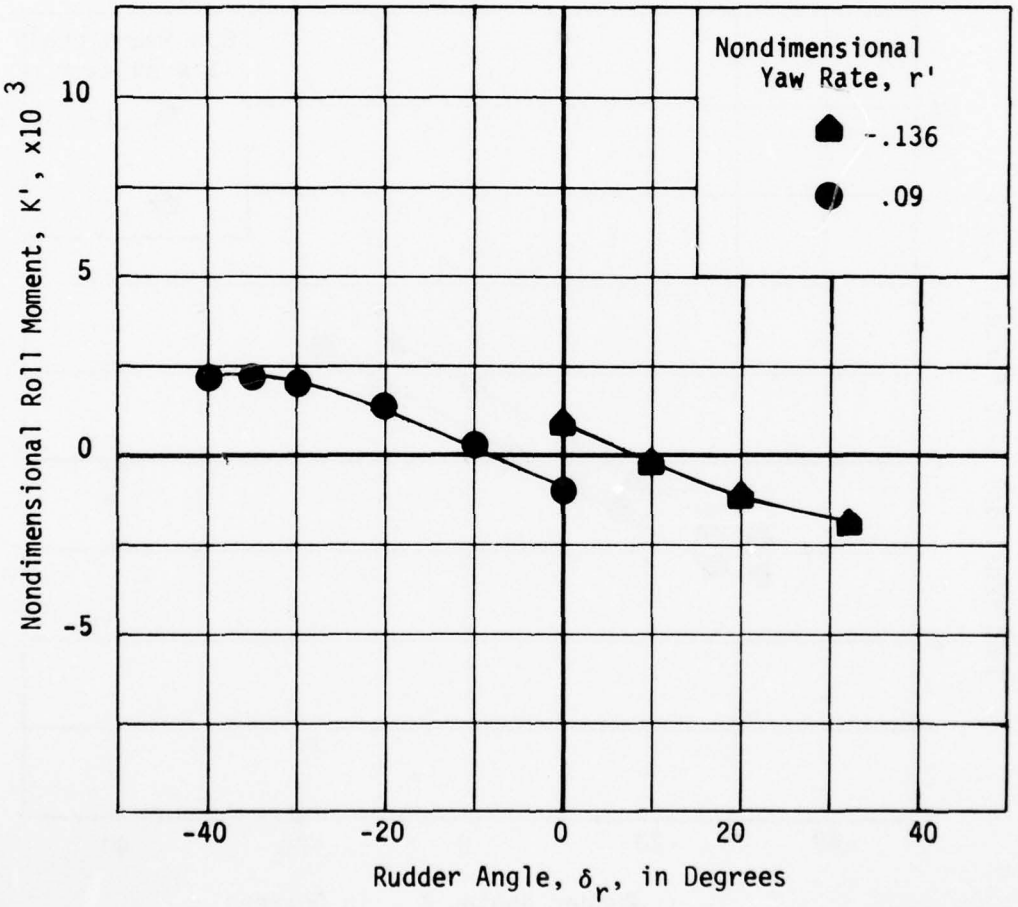

Figure 59 - Variation of Nondimensional Roll Moment with Rudder Angle for a Series of Nondimensional Yaw Rates at a Full Scale Speed of 3 Knots at Design Draft

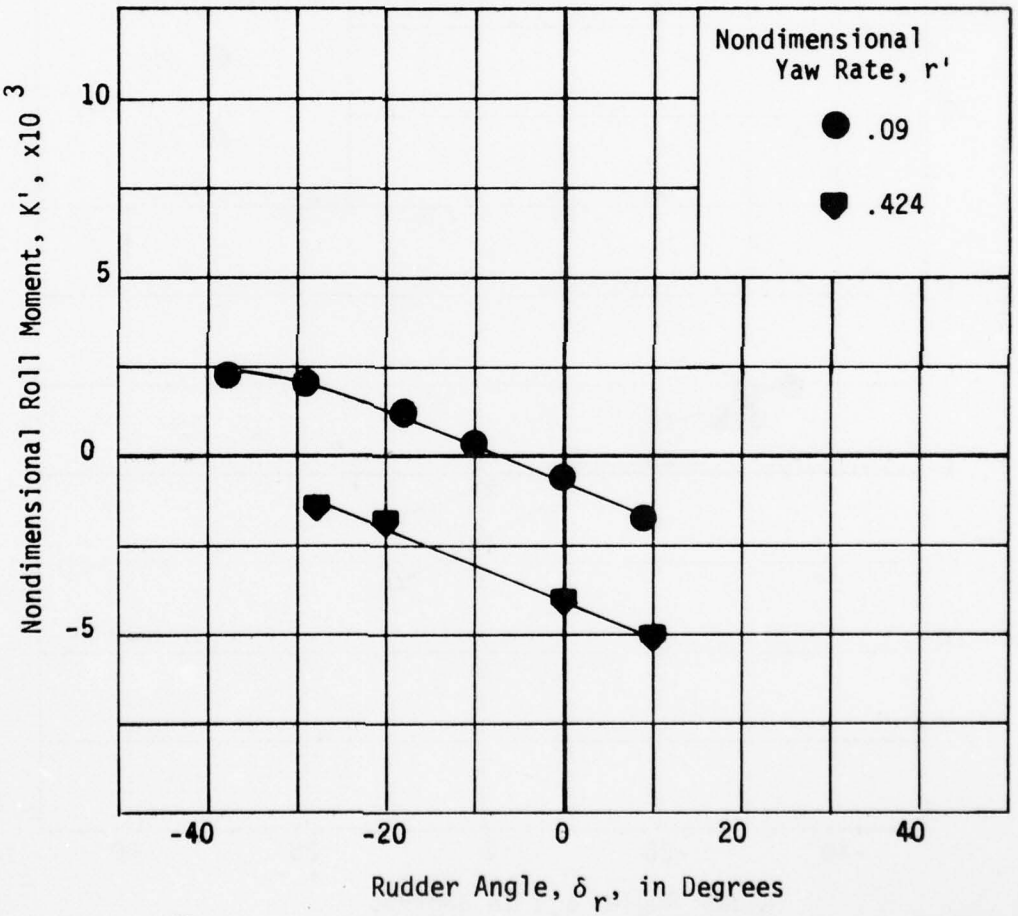

Figure 60 - Variation of Nondimensional Roll Moment with Rudder Angle for a Series of Nondimensional Yaw Rates at a Full Scale Speed of 6 Knots at Design Draft

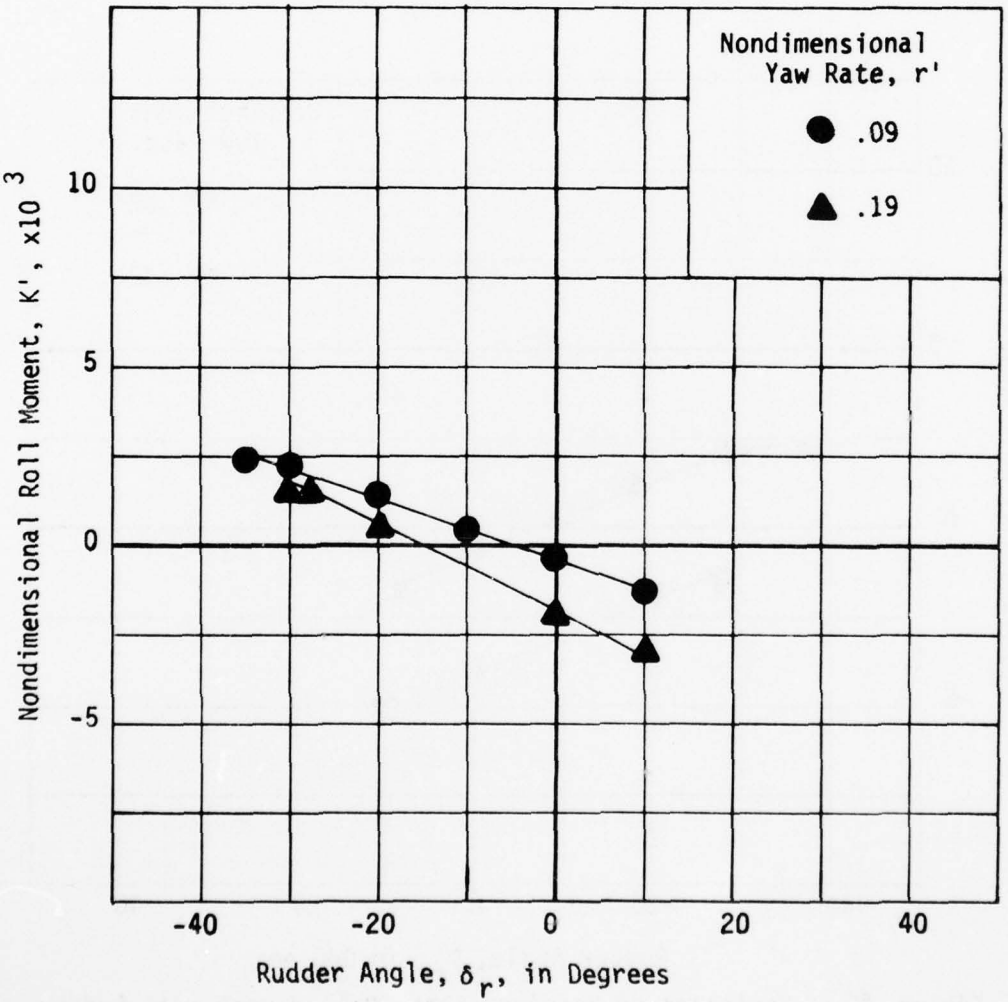

Figure 61 - Variation of Nondimensional Roll Moment with Rudder Angle for a Series of Nondimensional Yaw Rates at a Full Scale Speed of 7 Knots at Design Draft

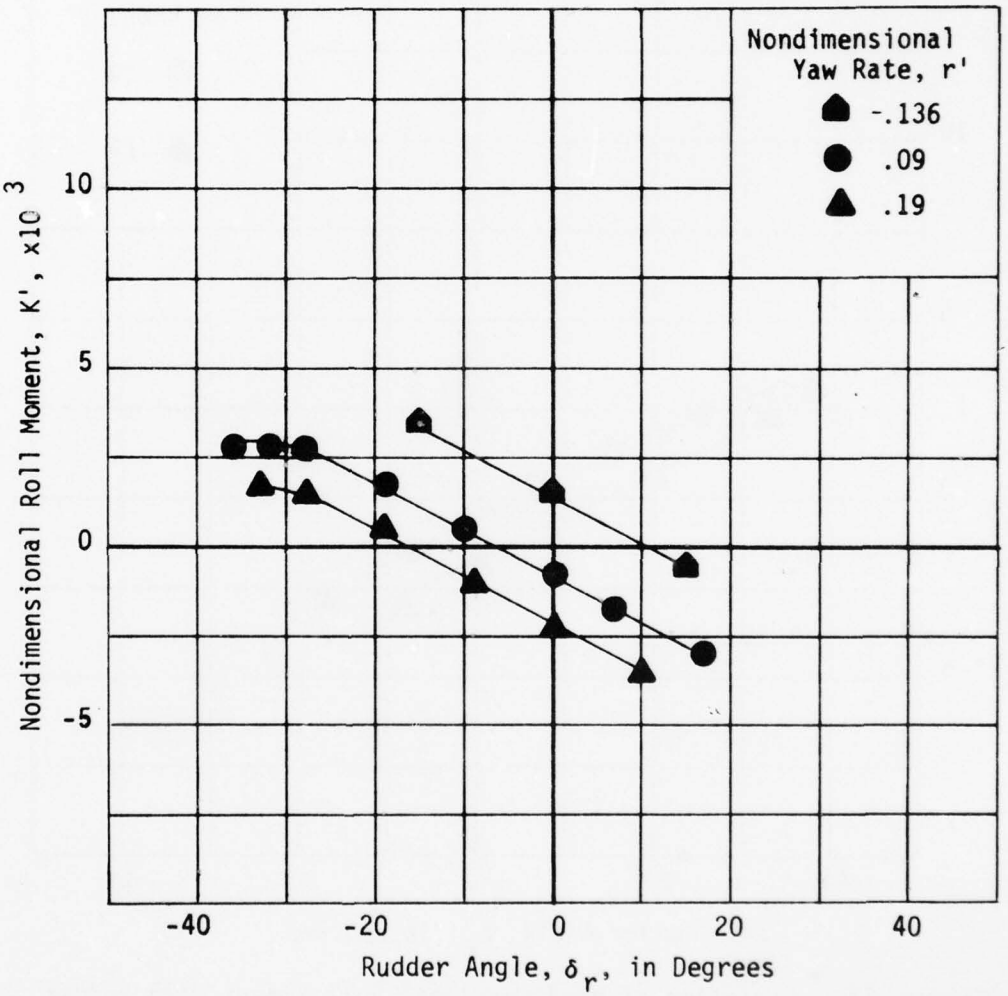

Figure 62 - Variation of Nondimensional Roll Moment with Rudder Angle for a Series of Nondimensional Yaw Rates at a Full Scale Speed of 9 Knots at Design Draft

AD-A055 721 DAVID W TAYLOR NAVAL SHIP RESEARCH AND DEVELOPMENT CE--ETC F/G 14/2
ROTATING ARM EXPERIMENTS FOR THE STABLE SEMI-SUBMERGED PLATFORM--ETC(U)
SEP 77 J A FEIN

UNCLASSIFIED DTNSRDC/SPD-698-02

NL

2 OF 2
AD
A055721

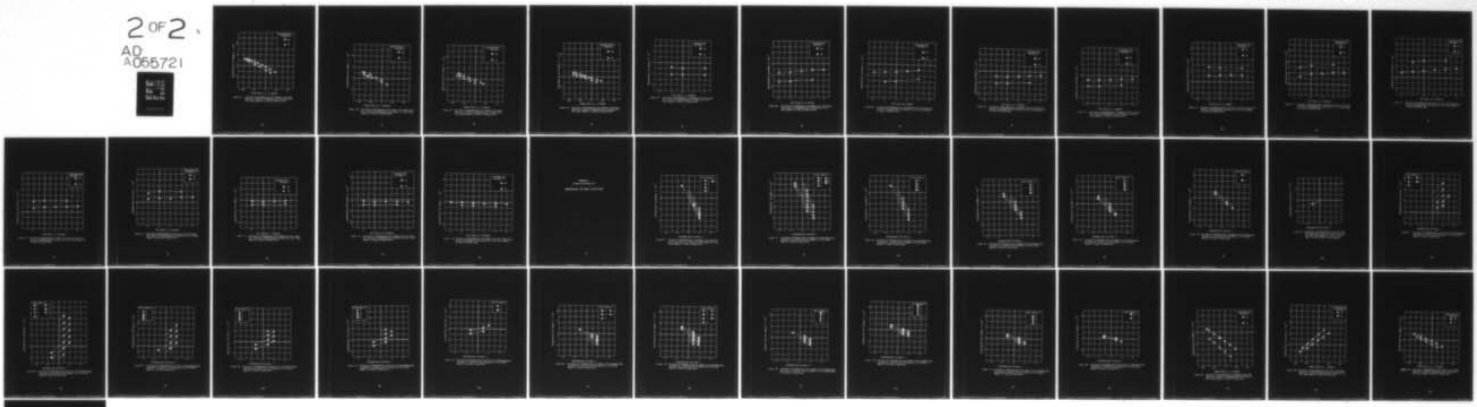

END
DATE
FILMED
8 -78
DDC

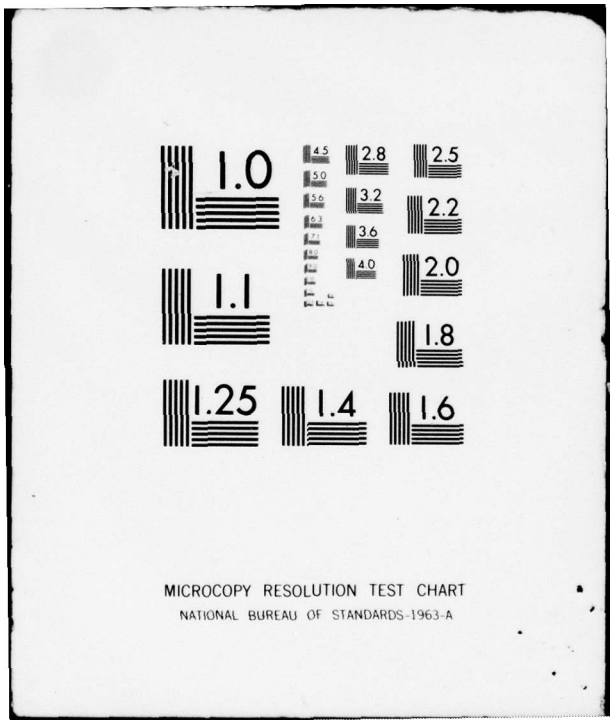
1.0
4.5
5.0
5.6
6.3
7.1
2.8
3.2
3.6
4.0
2.5
2.2
2.0
1.8
1.1
1.25
1.4
1.6
MICROCOPY RESOLUTION TEST CHART
NATIONAL BUREAU OF STANDARDS-1963-A

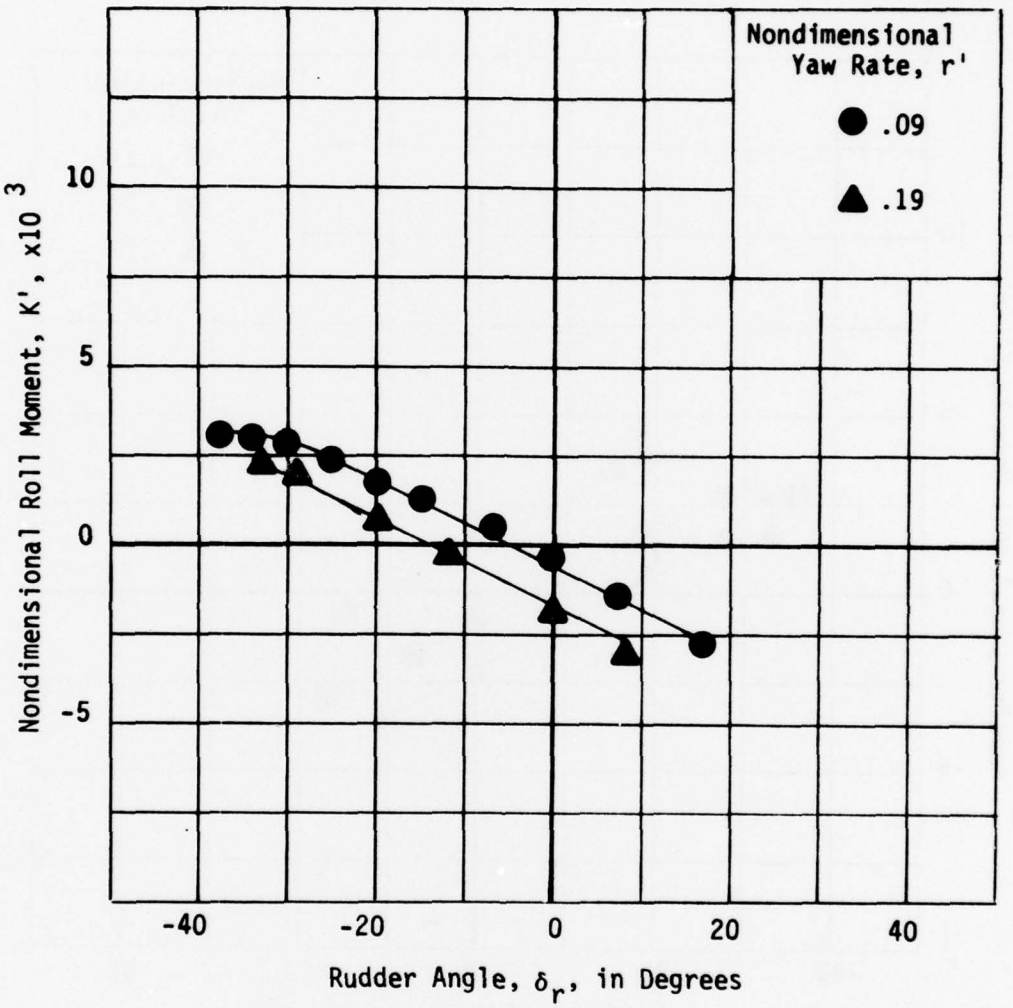

Figure 63 - Variation of Nondimensional Roll Moment with Rudder Angle for a Series of Nondimensional Yaw Rates at a Full Scale Speed of 11 Knots at Design Draft

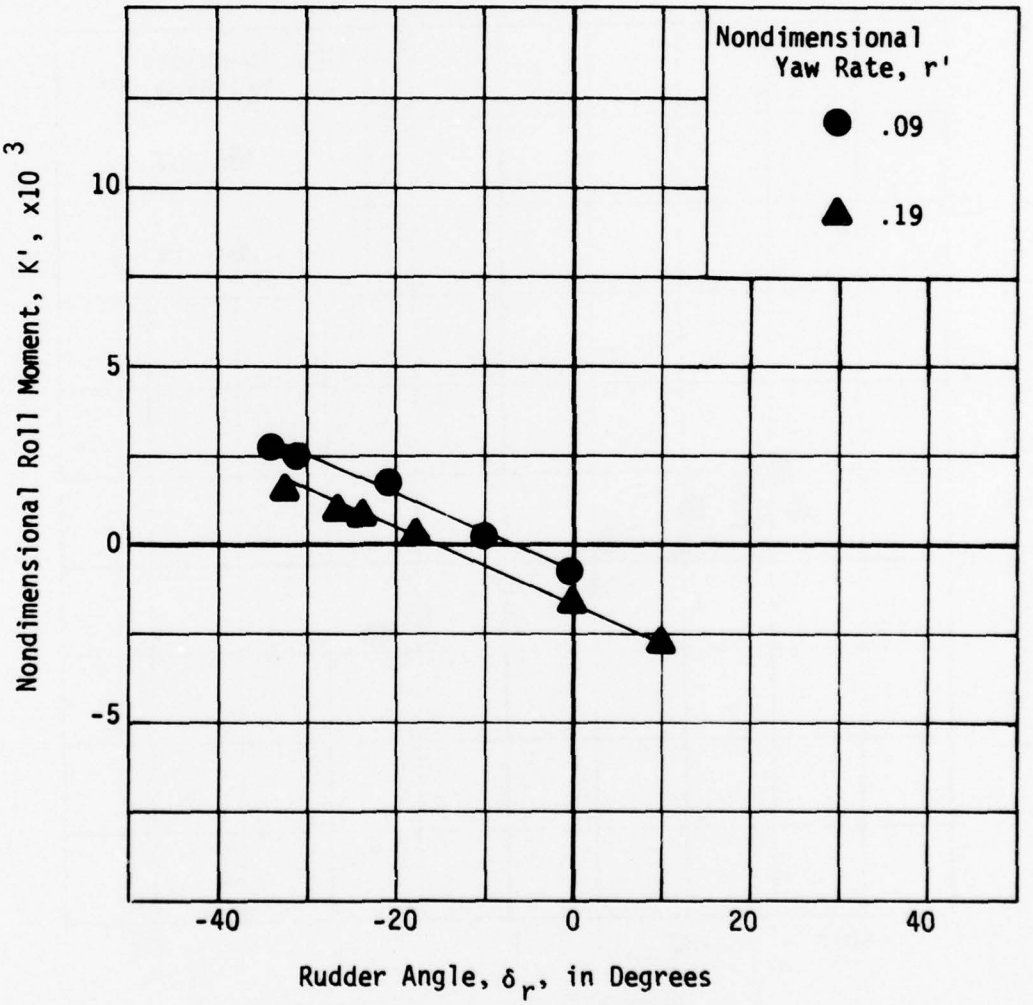

Figure 64 - Variation of Nondimensional Roll Moment with Rudder Angle for a Series of Nondimensional Yaw Rates at a Full Scale Speed of 14 Knots at Design Draft

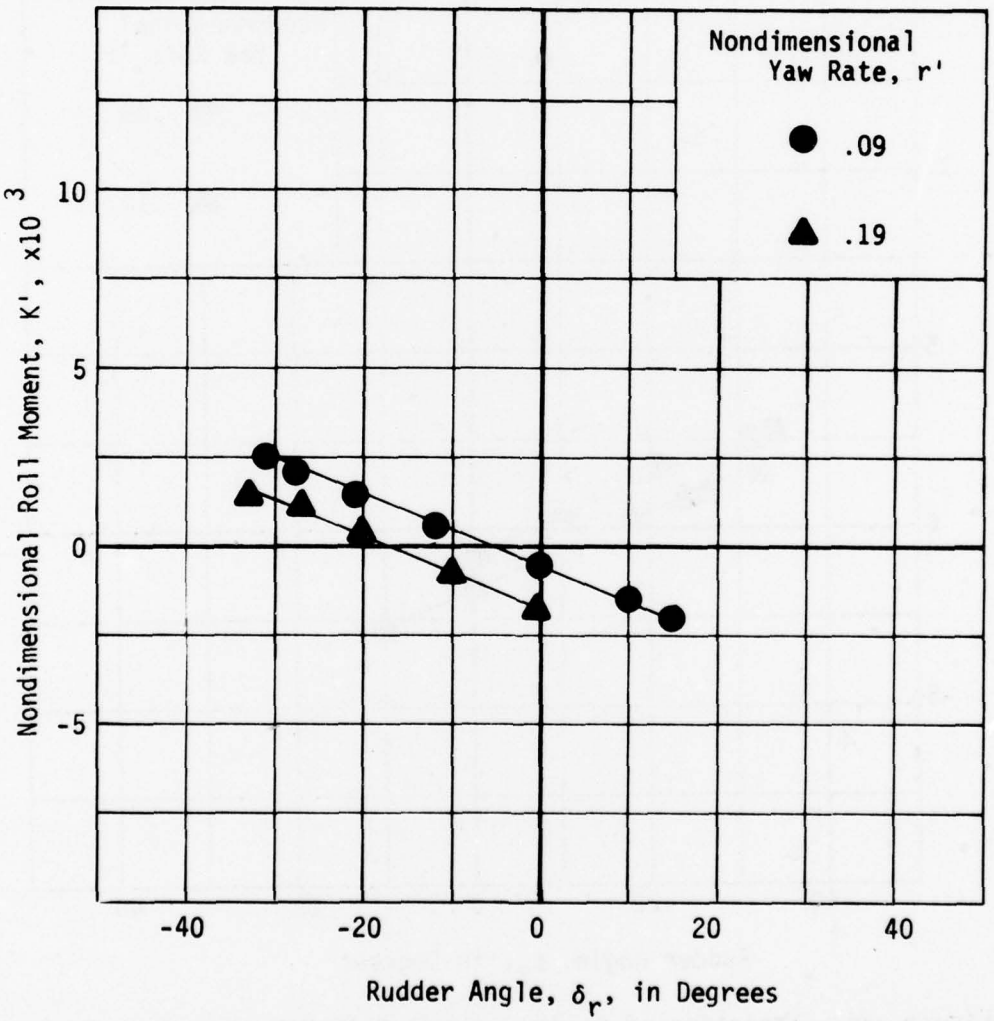

Figure 65 - Variation of Nondimensional Roll Moment with Rudder Angle for a Series of Nondimensional Yaw Rates at a Full Scale Speed of 15 Knots at Design Draft

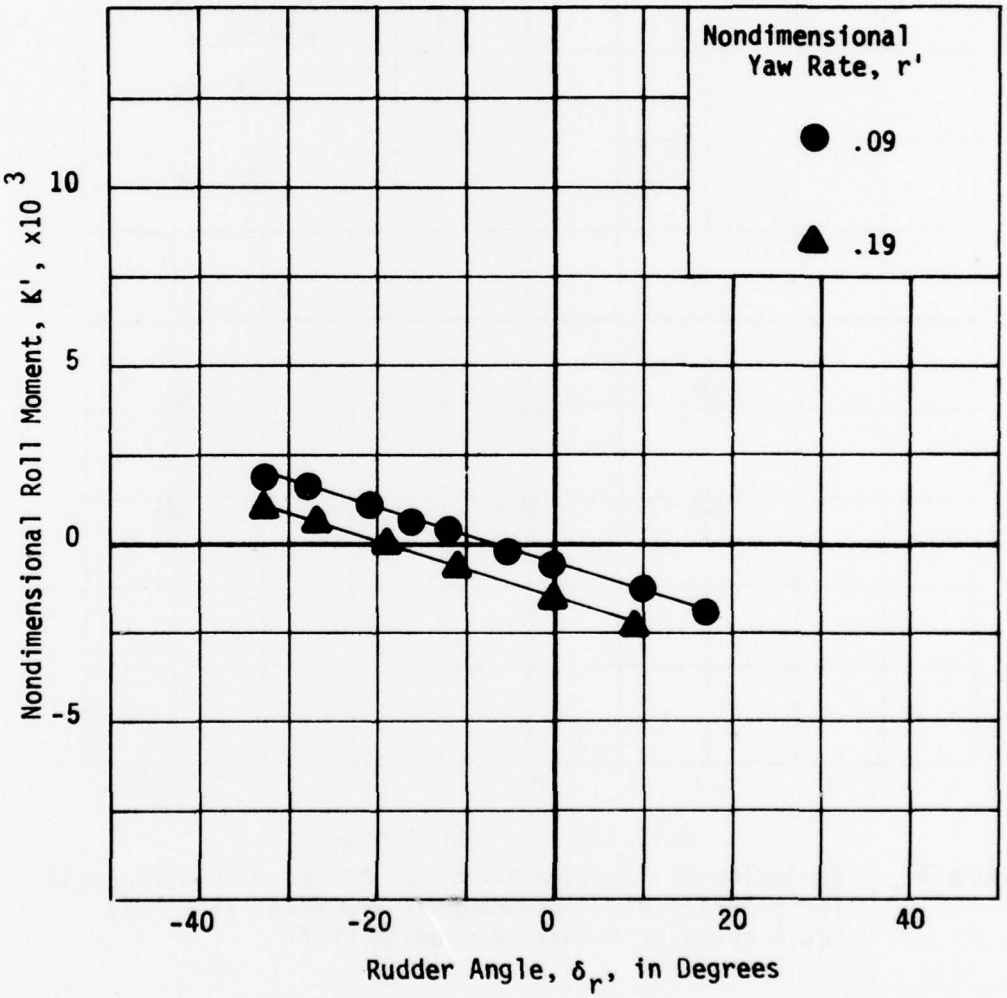

Figure 66 - Variation of Nondimensional Roll Moment with Rudder Angle for a Series of Nondimensional Yaw Rates at a Full Scale Speed of 18 Knots at Design Draft

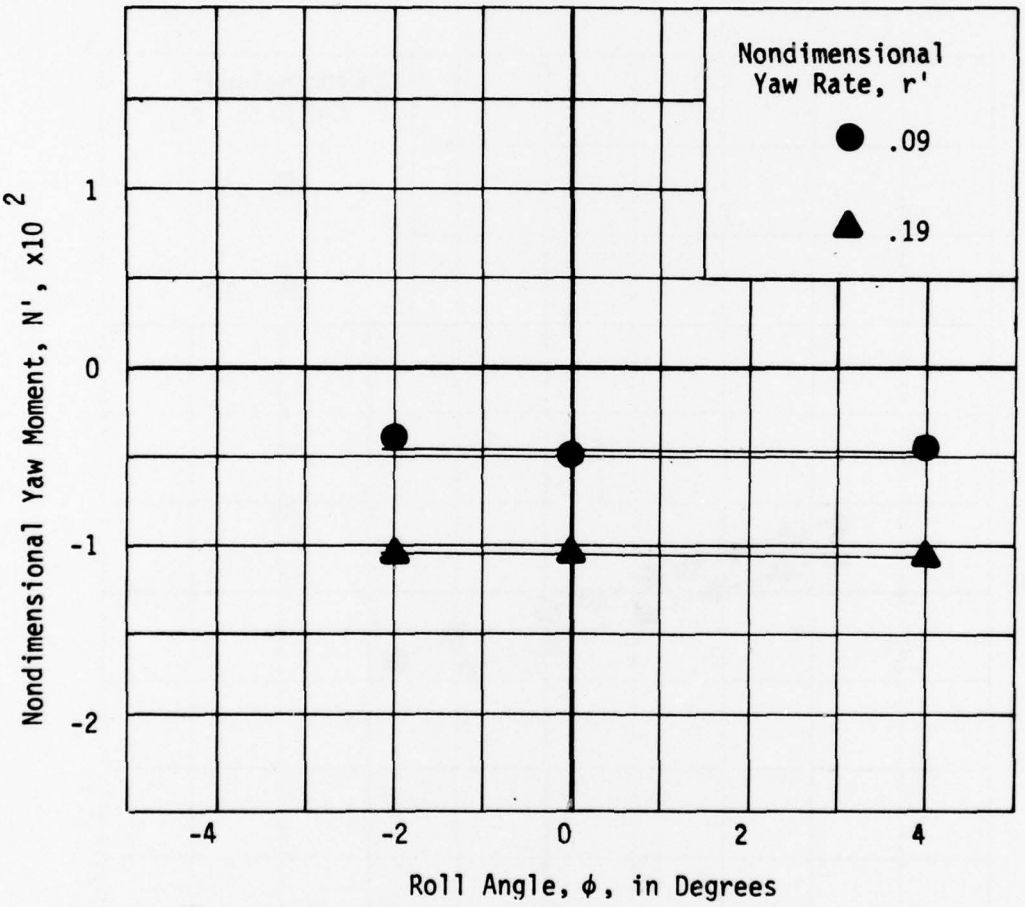

Figure 67 - Variation of Nondimensional Yaw Moment with Roll Angle for a Series of Nondimensional Yaw Rates at a Full Scale Speed of 6 Knots at Design Draft

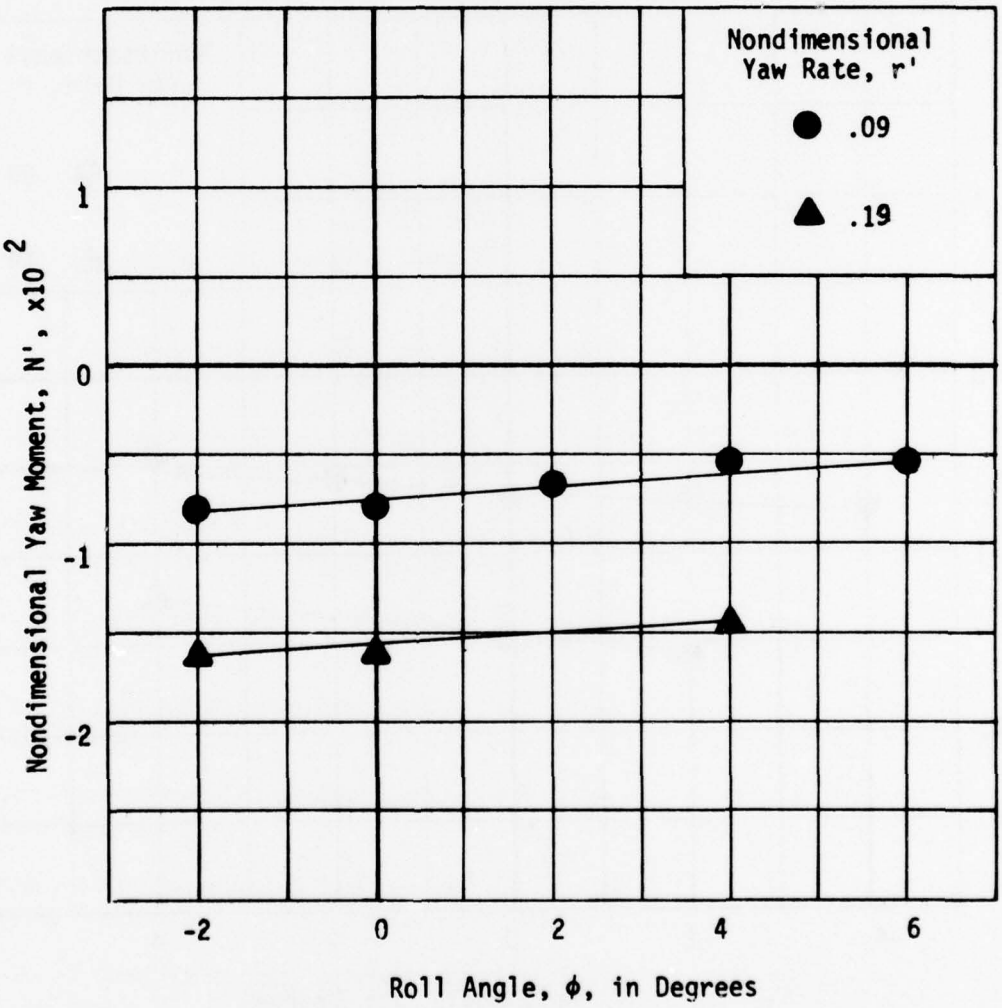

Figure 68 - Variation of Nondimensional Yaw Moment with Roll Angle for a Series of Nondimensional Yaw Rates at a Full Scale Speed of 9 Knots at Design Draft

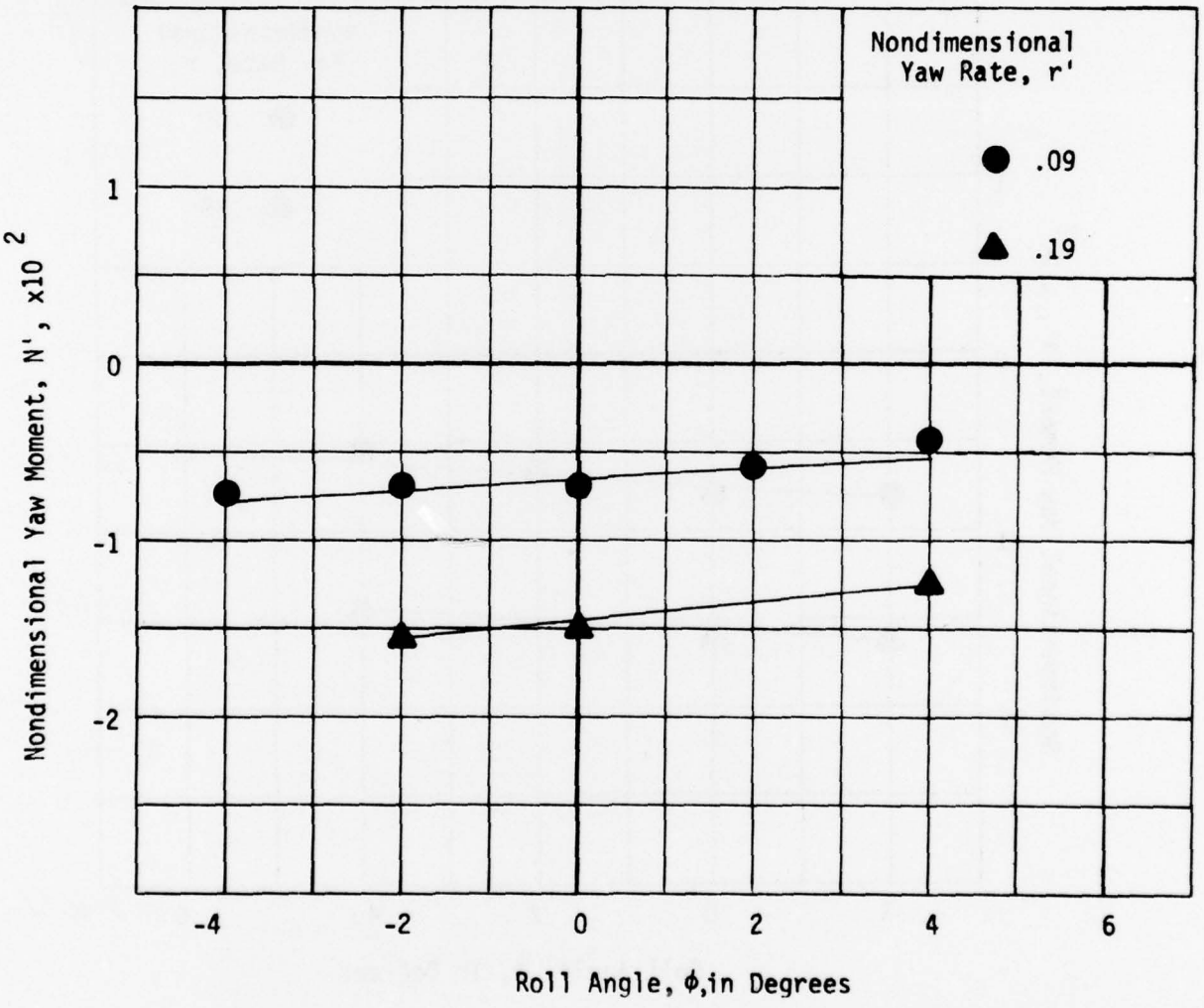

Figure 69 - Variation of Nondimensional Yaw Moment with Roll Angle for a Series of Nondimensional Yaw Rates at a Full Scale Speed of 11 Knots at Design Draft

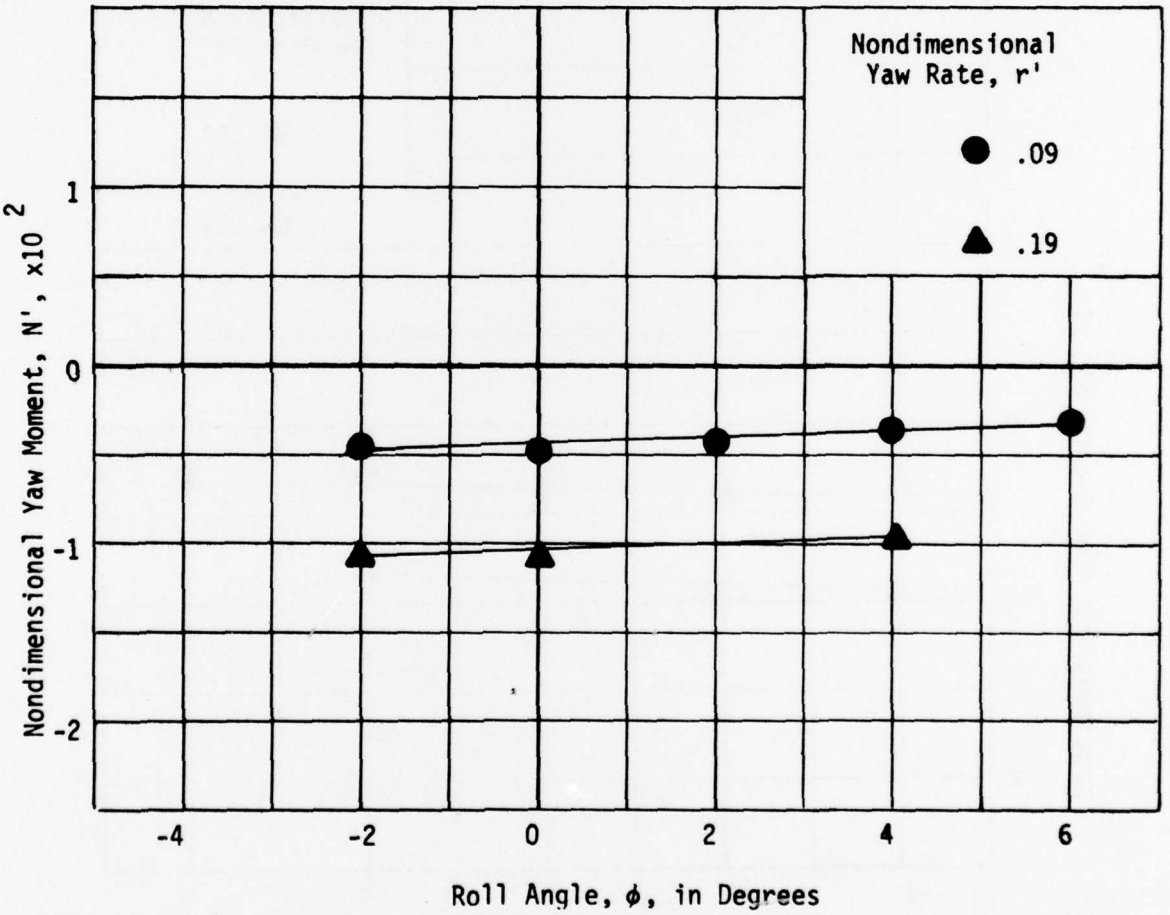

Figure 70 - Variation of Nondimensional Yaw Moment with Roll Angle for a Series of Nondimensional Yaw Rates at a Full Scale Speed of 15 Knots at Design Draft

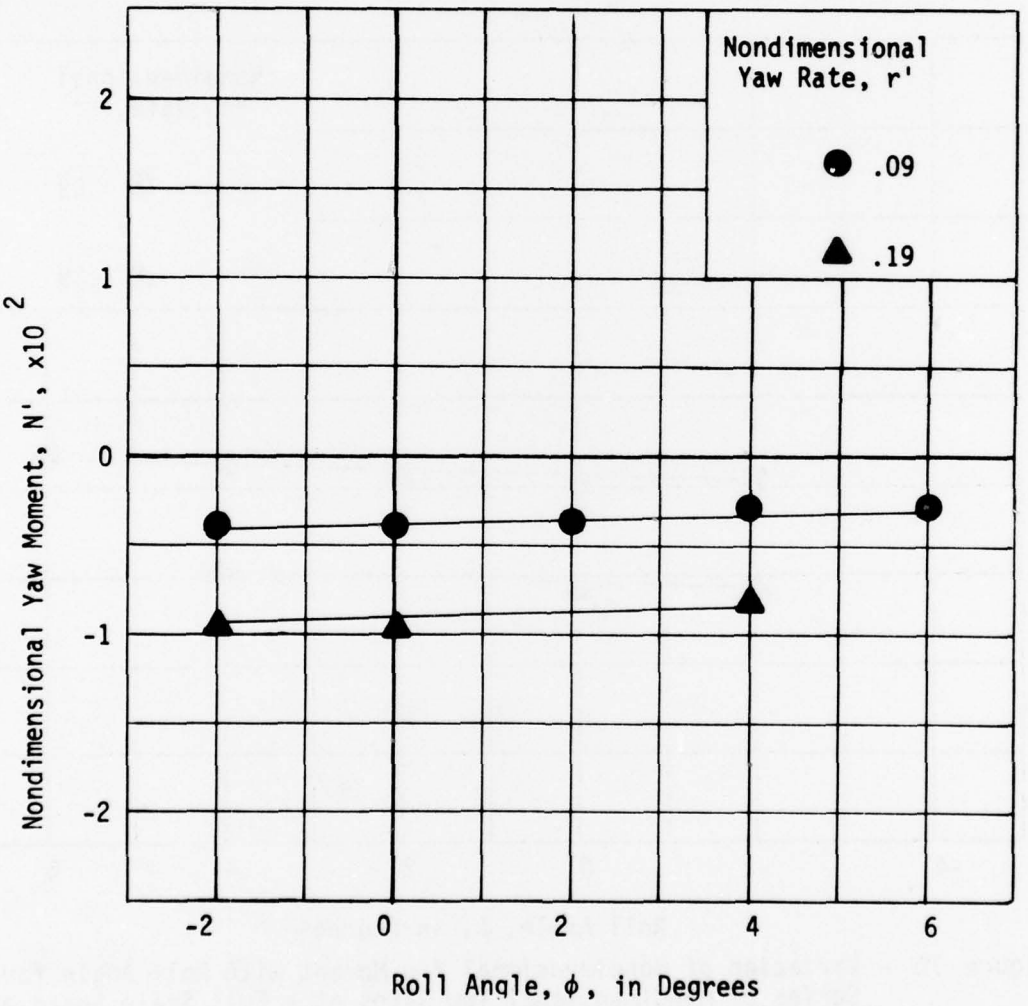

Figure 71 - Variation of Nondimensional Yaw Moment with Roll Angle for a Series of Nondimensional Yaw Rates at a Full Scale Speed of 18 Knots at Design Draft

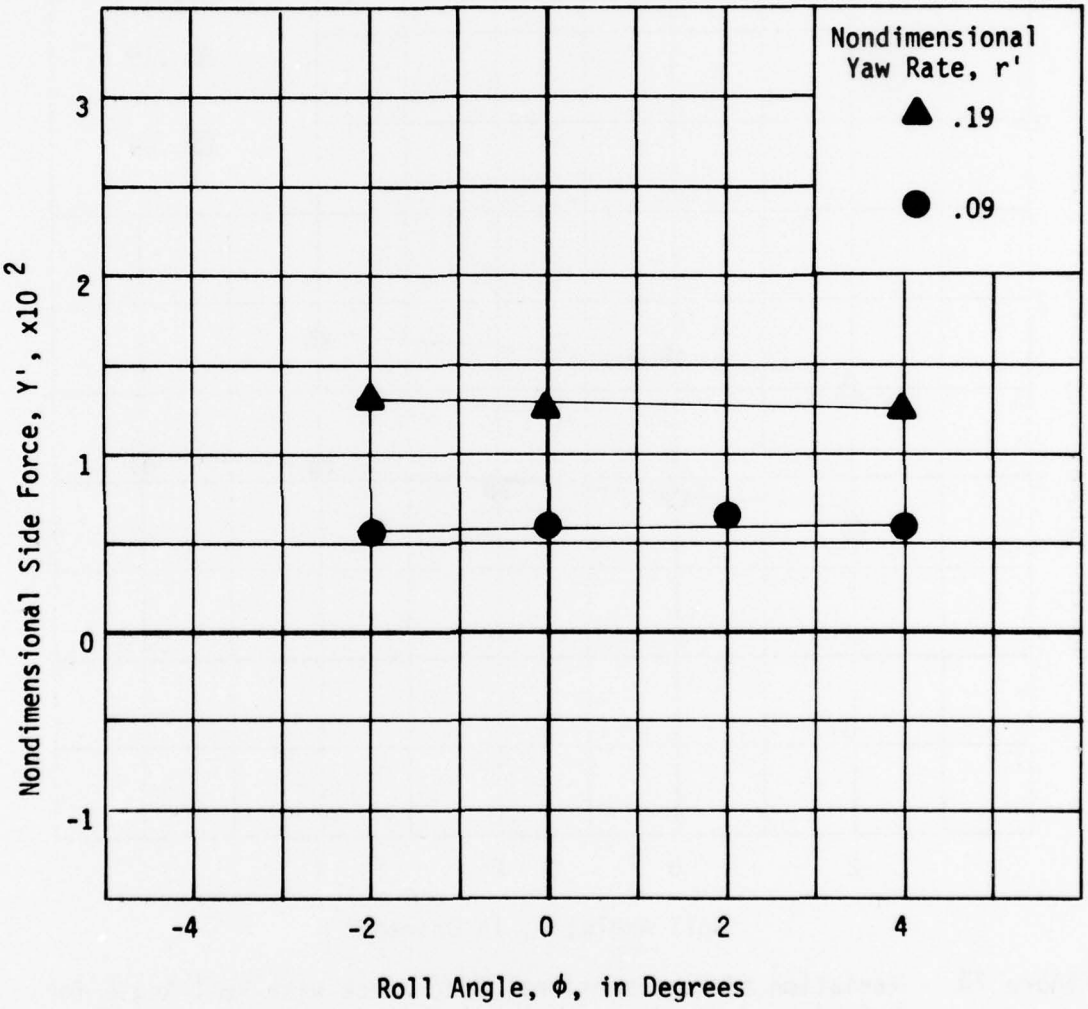

Figure 72 - Variation of Nondimensional Side Force with Roll Angle for a Series of Nondimensional Yaw Rates at a Full Scale Speed of 6 Knots at Design Draft

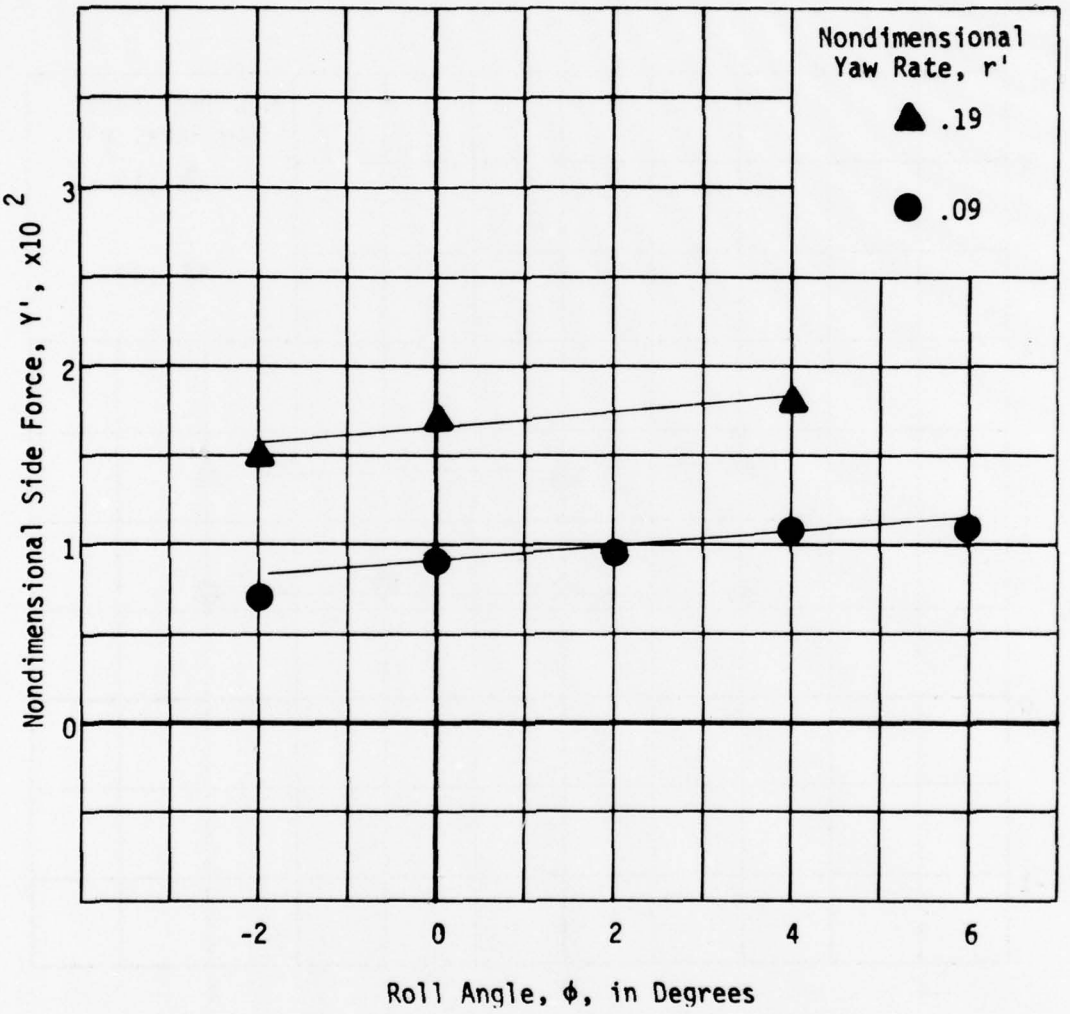

Figure 73 - Variation of Nondimensional Side Force with Roll Angle for a Series of Nondimensional Yaw Rates at a Full Scale Speed of 9 Knots at Design Draft

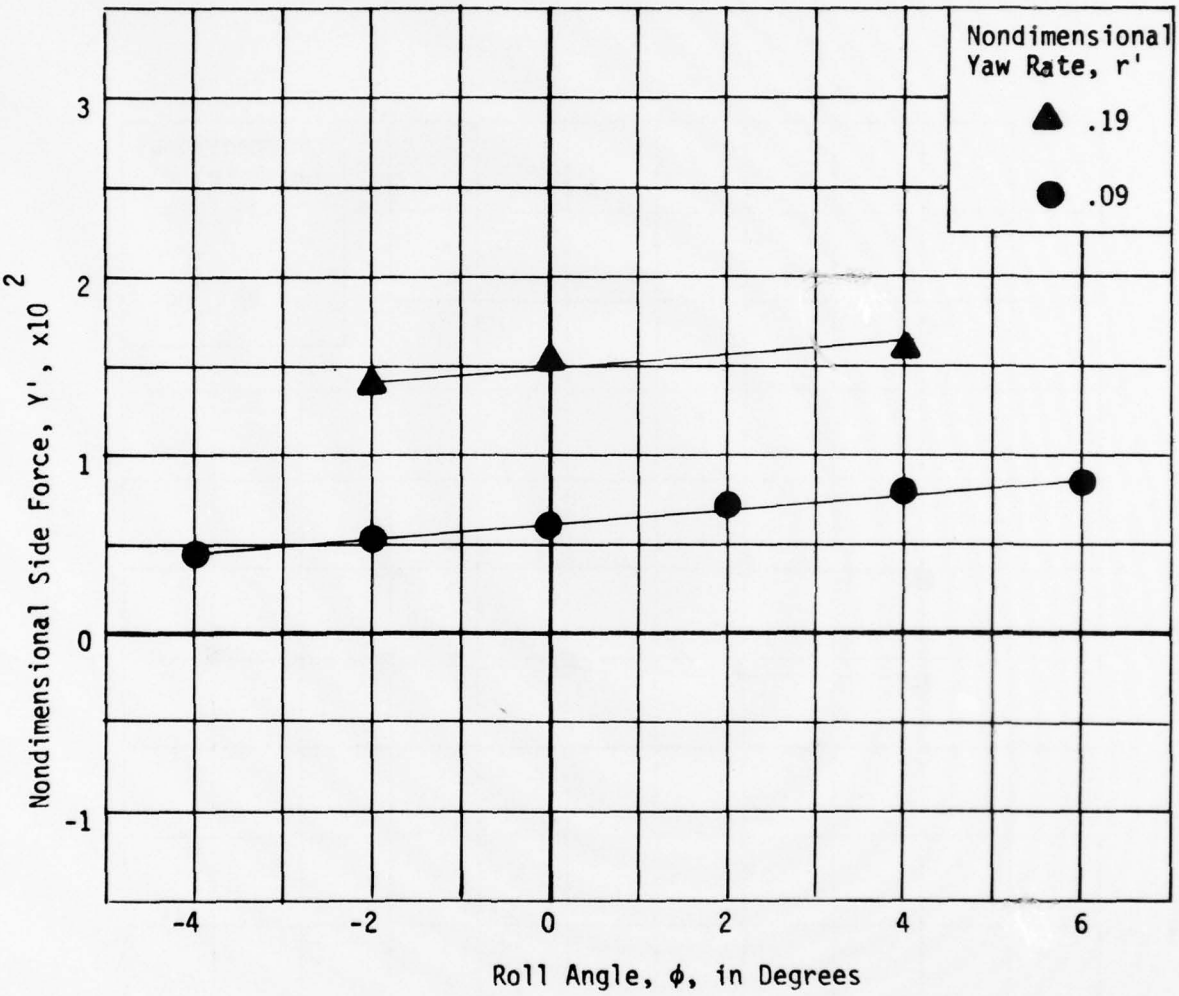

Figure 74 - Variation of Nondimensional Side Force with Roll Angle for a Series of Nondimensional Yaw Rates at a Full Scale Speed of 11 Knots at Design Draft

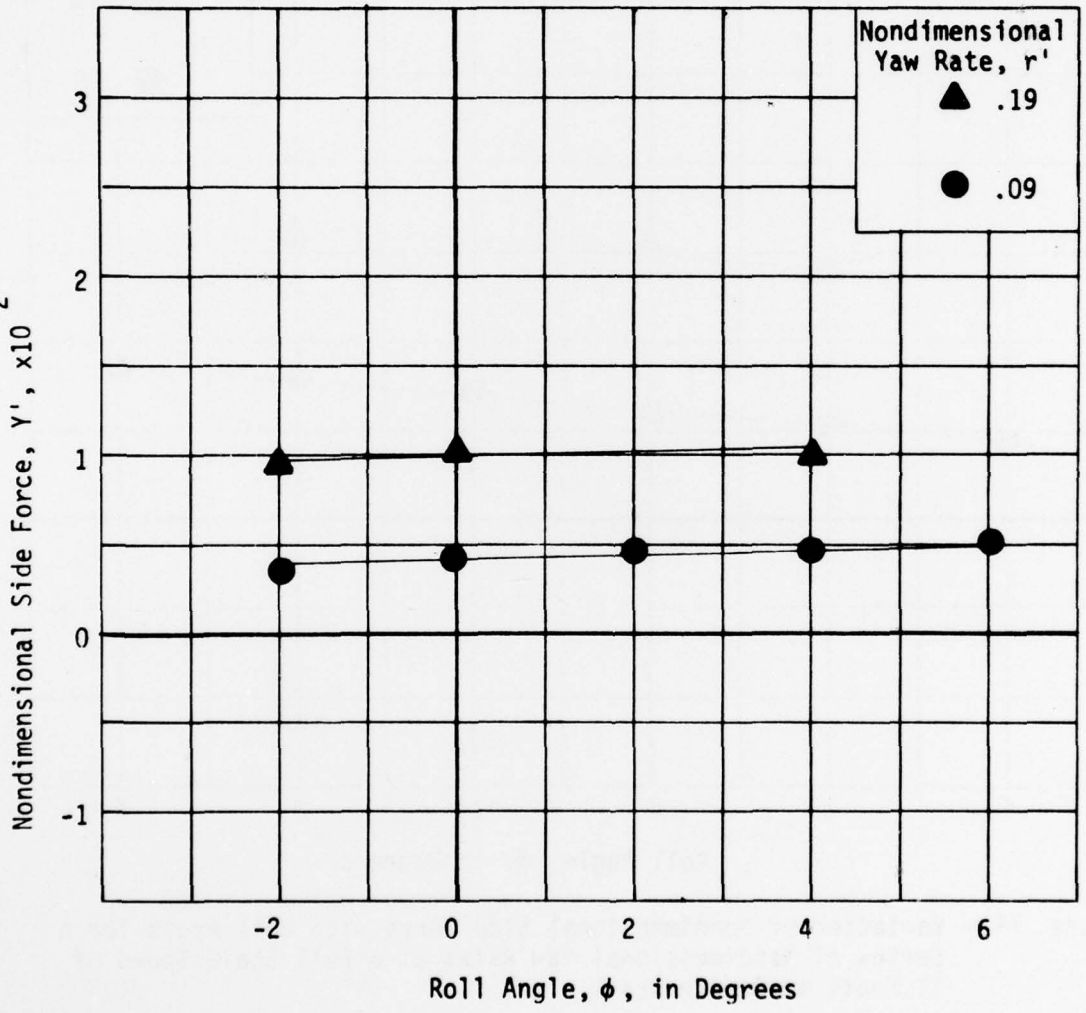

Figure 75 - Variation of Nondimensional Side Force with Roll Angle for a Series of Nondimensional Yaw Rates at a Full Scale Speed of 15 Knots at Design Draft

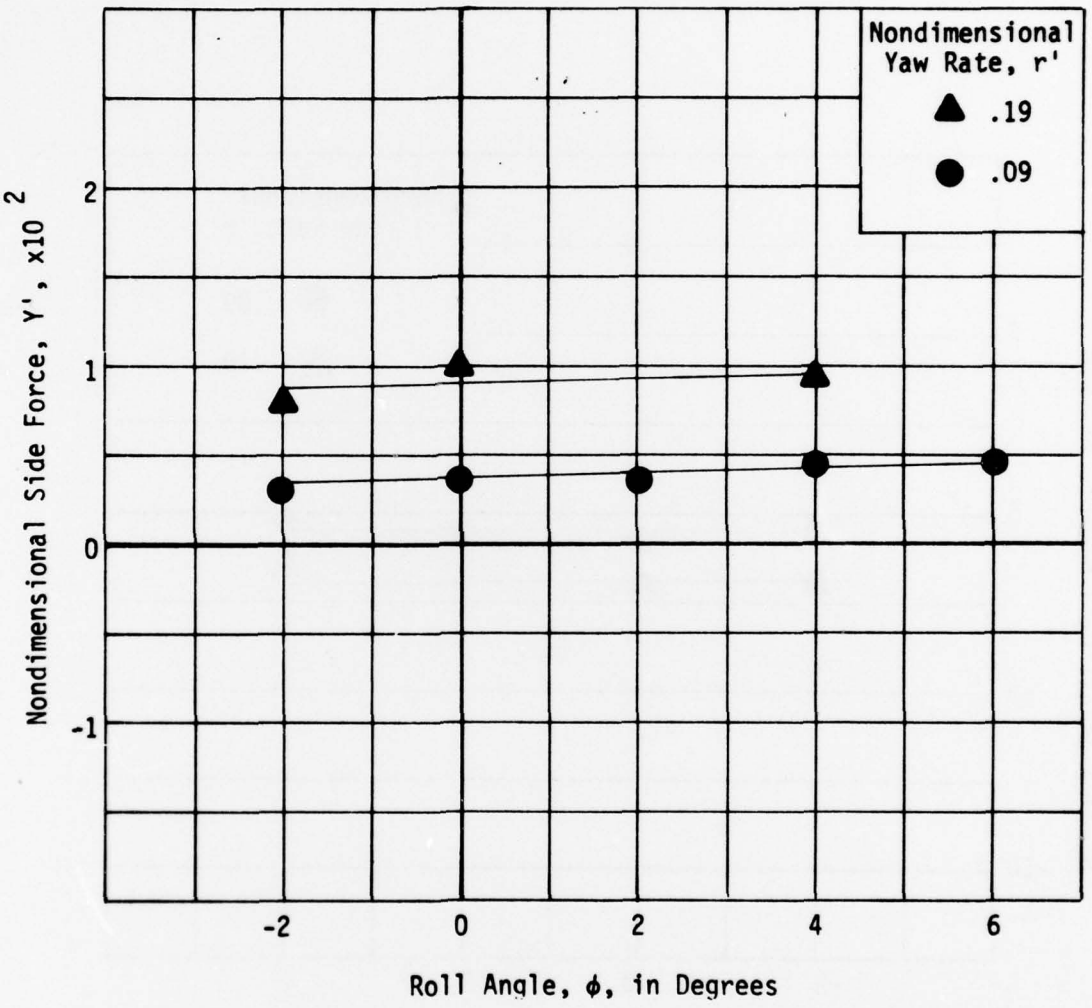

Figure 76 - Variation of Nondimensional Side Force with Roll Angle for a Series of Nondimensional Yaw Rates at a Full Scale Speed of 18 Knots at Design Draft

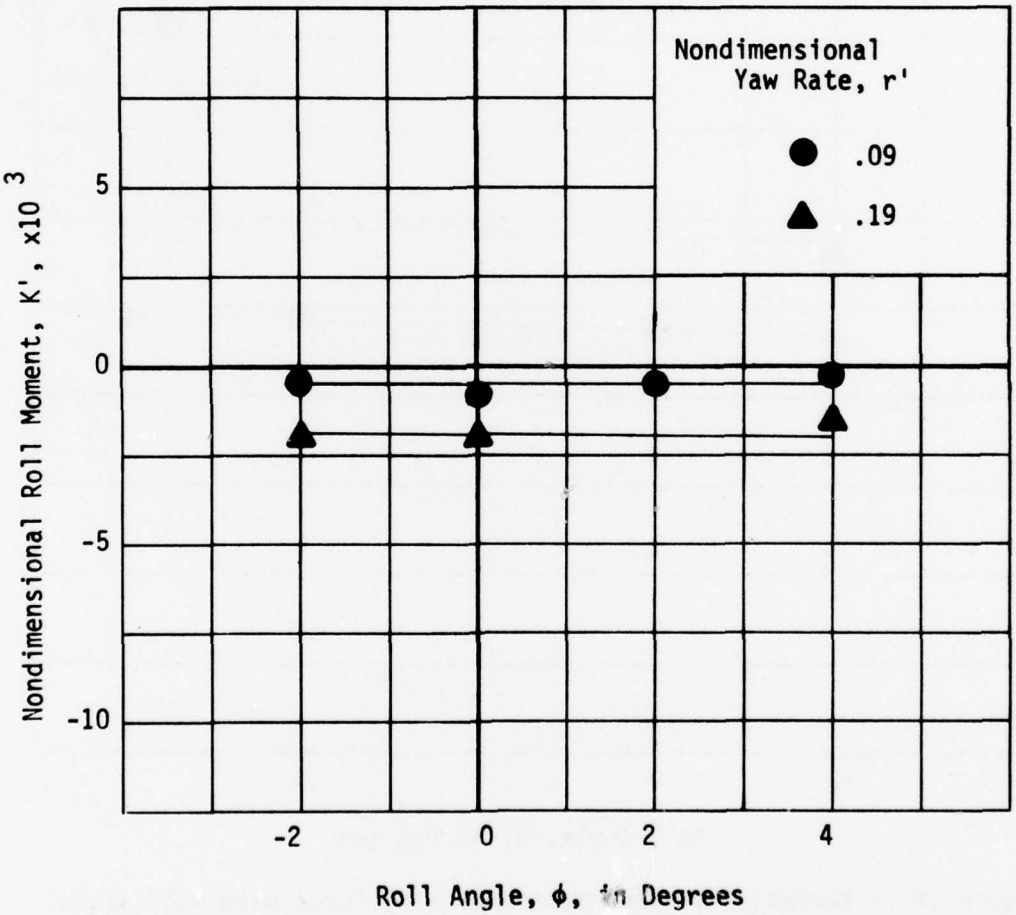

Figure 77 - Variation of Nondimensional Roll Moment with Roll Angle for a Series of Nondimensional Yaw Rates at a Full Scale Speed of 6 Knots at Design Draft

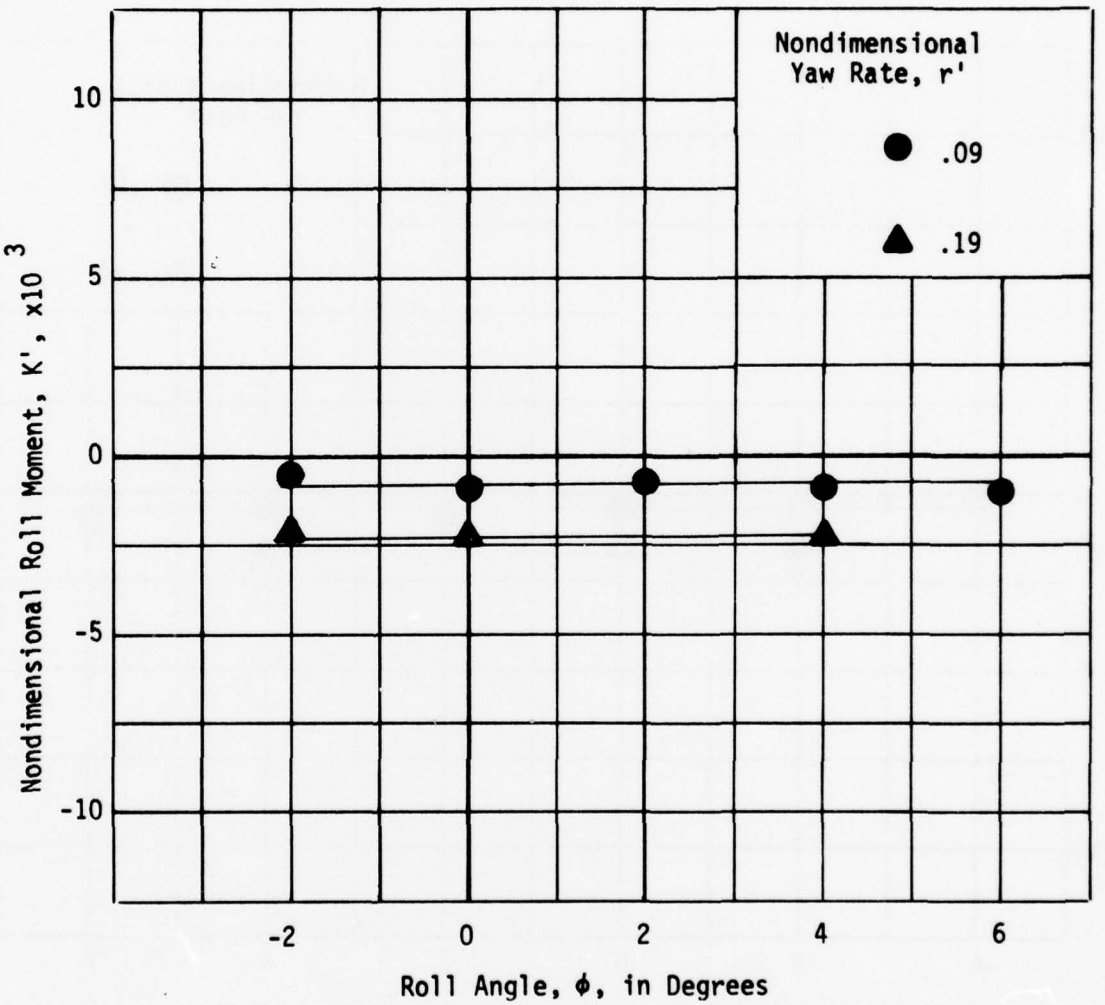

Figure 78 - Variation of Nondimensional Roll Moment with Roll Angle for a Series of Nondimensional Yaw Rates at a Full Scale Speed of 9 Knots at Design Draft

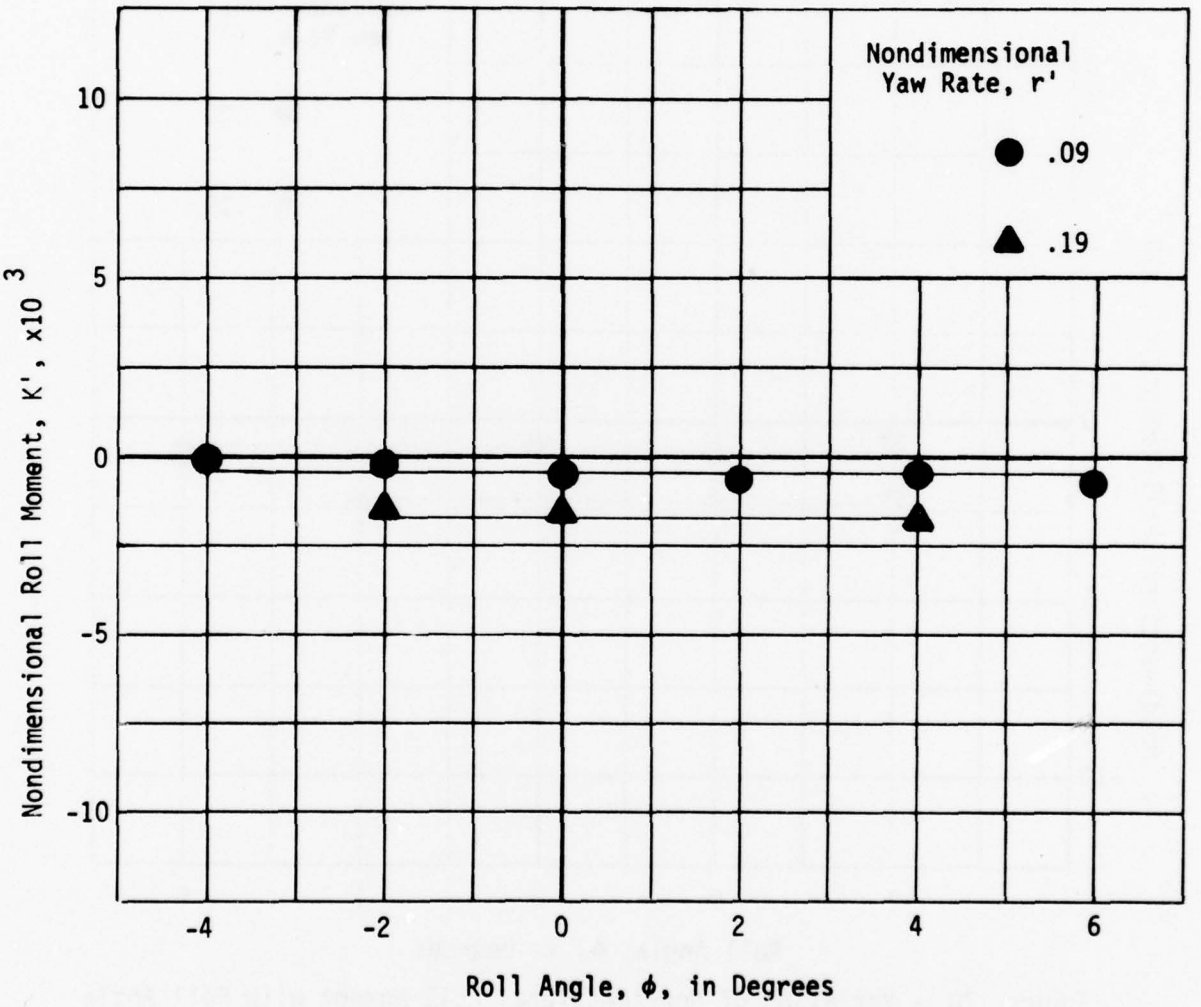

Figure 79 - Variation of Nondimensional Roll Moment with Roll Angle for a Series of Nondimensional Yaw Rates at a Full Scale Speed of 11 Knots at Design Draft

APPENDIX B

(Figures 80 through 101)

NONDIMENSIONAL DATA CURVES FOR DEEP DRAFT

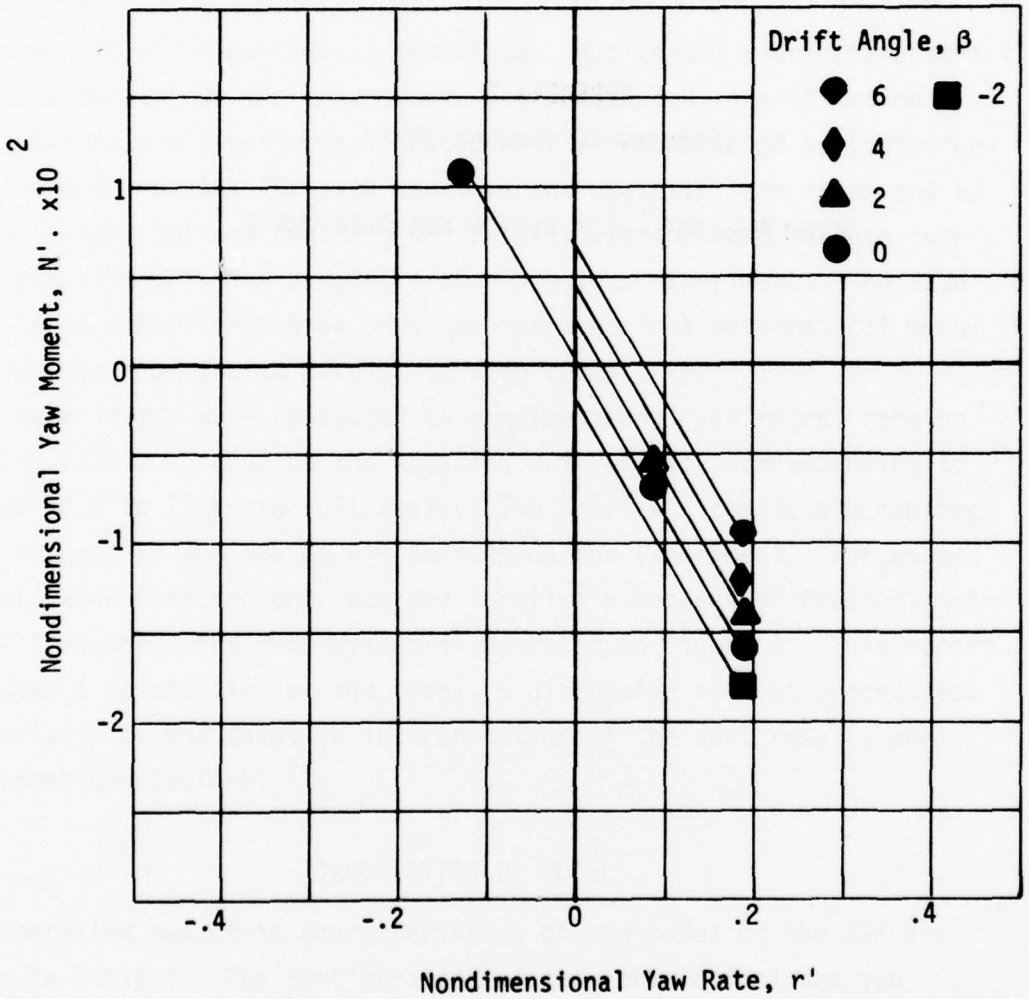

Figure 80 - Variation of Nondimensional Yaw Moment with Nondimensional Yaw Rate for a Series of Drift Angles at a Full Scale Speed of 7 Knots at Deep Draft

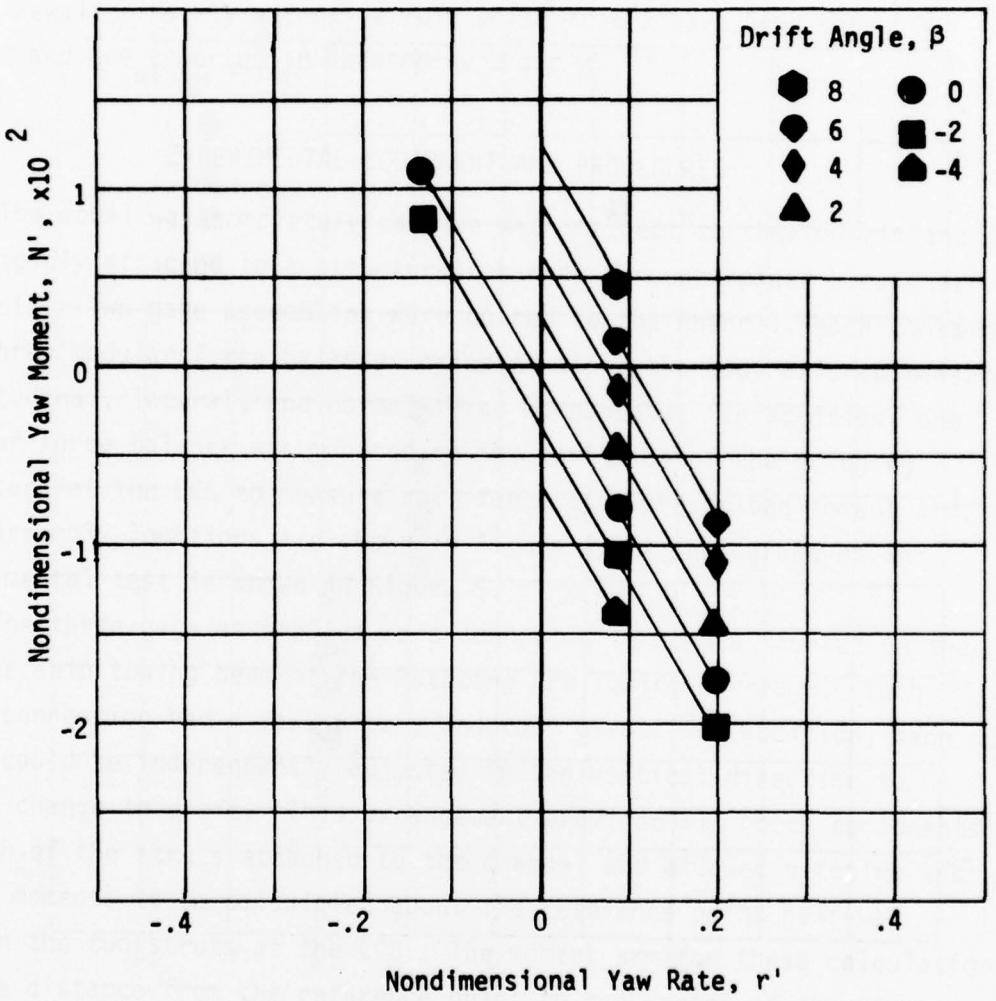

Figure 81 - Variation of Nondimensional Yaw Moment with Nondimensional Yaw Rate for a Series of Drift Angles at a Full Scale Speed of 9 Knots at Deep Draft

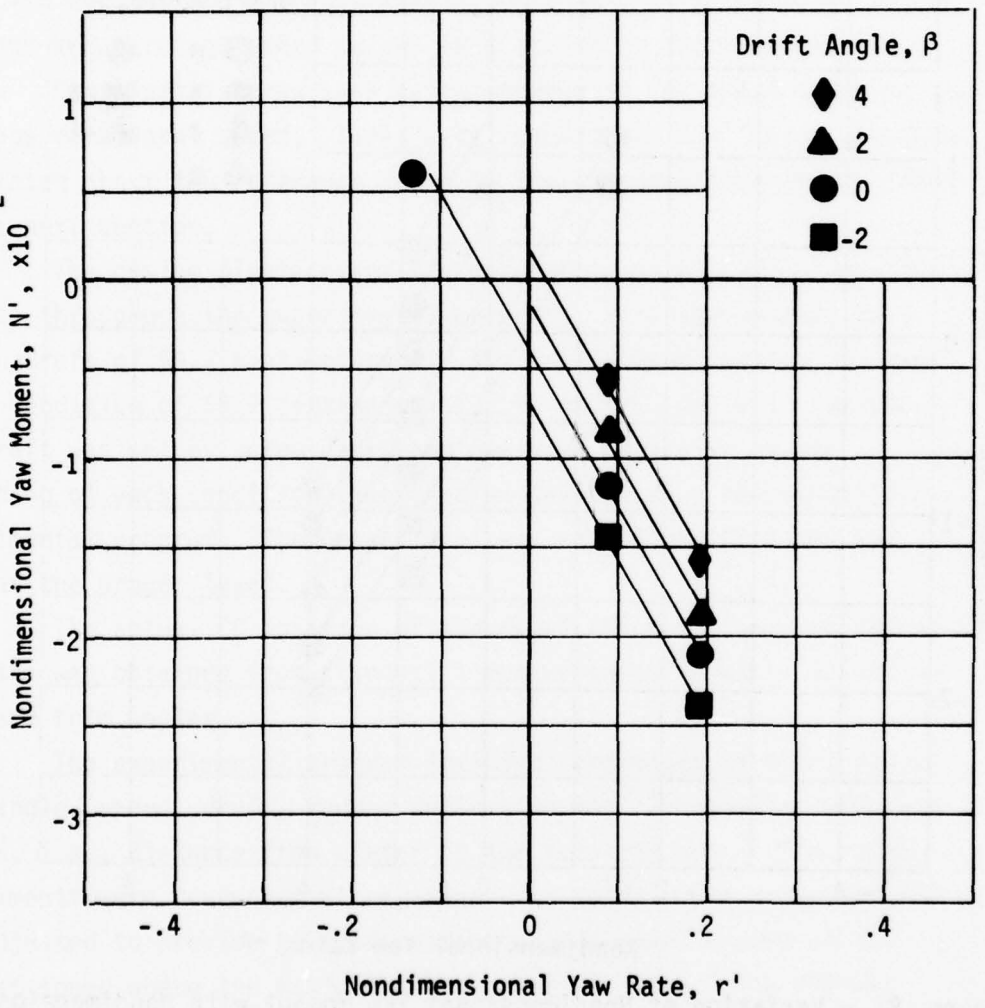

Figure 82 - Variation of Nondimensional Yaw Moment with Nondimensional Yaw Rate for a Series of Drift Angles at a Full Scale Speed of 11 Knots at Deep Draft

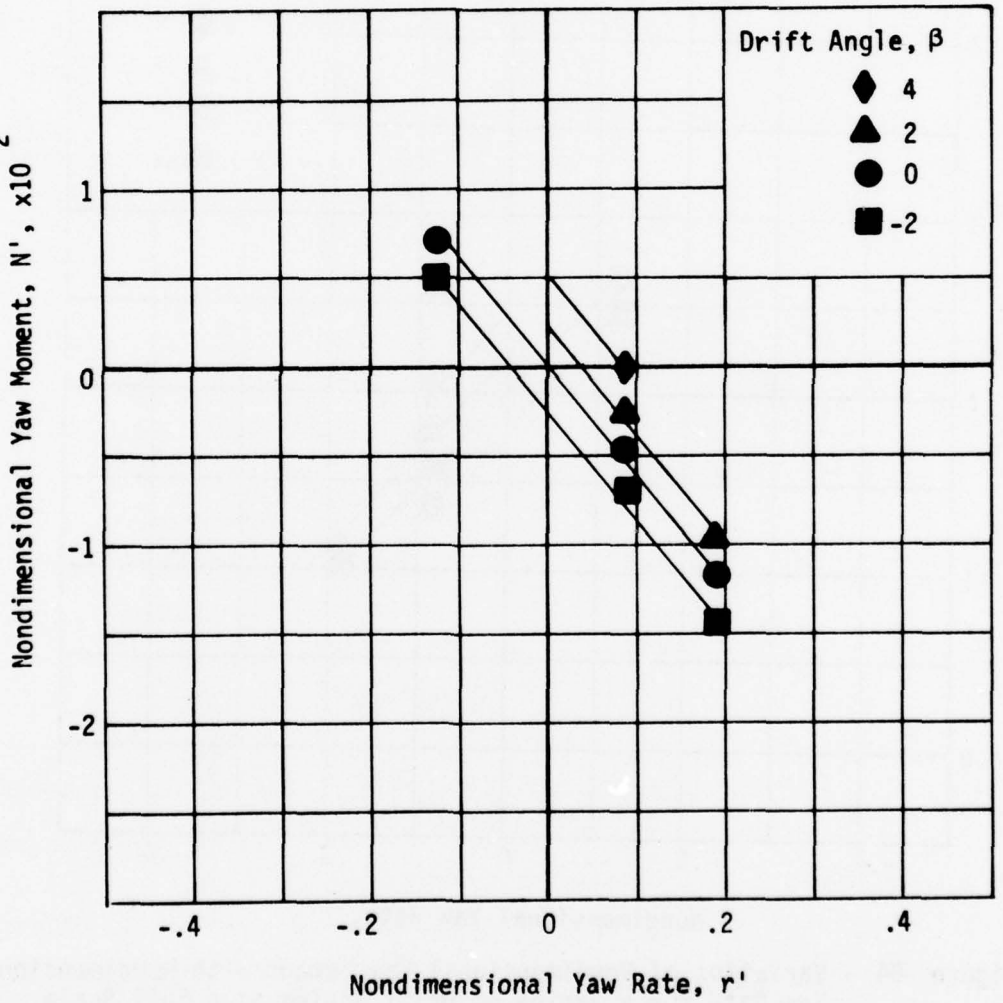

Figure 83 - Variation of Nondimensional Yaw Moment with Nondimensional Yaw Rate for a Series of Drift Angles at a Full Scale Speed of 15 Knots at Deep Draft

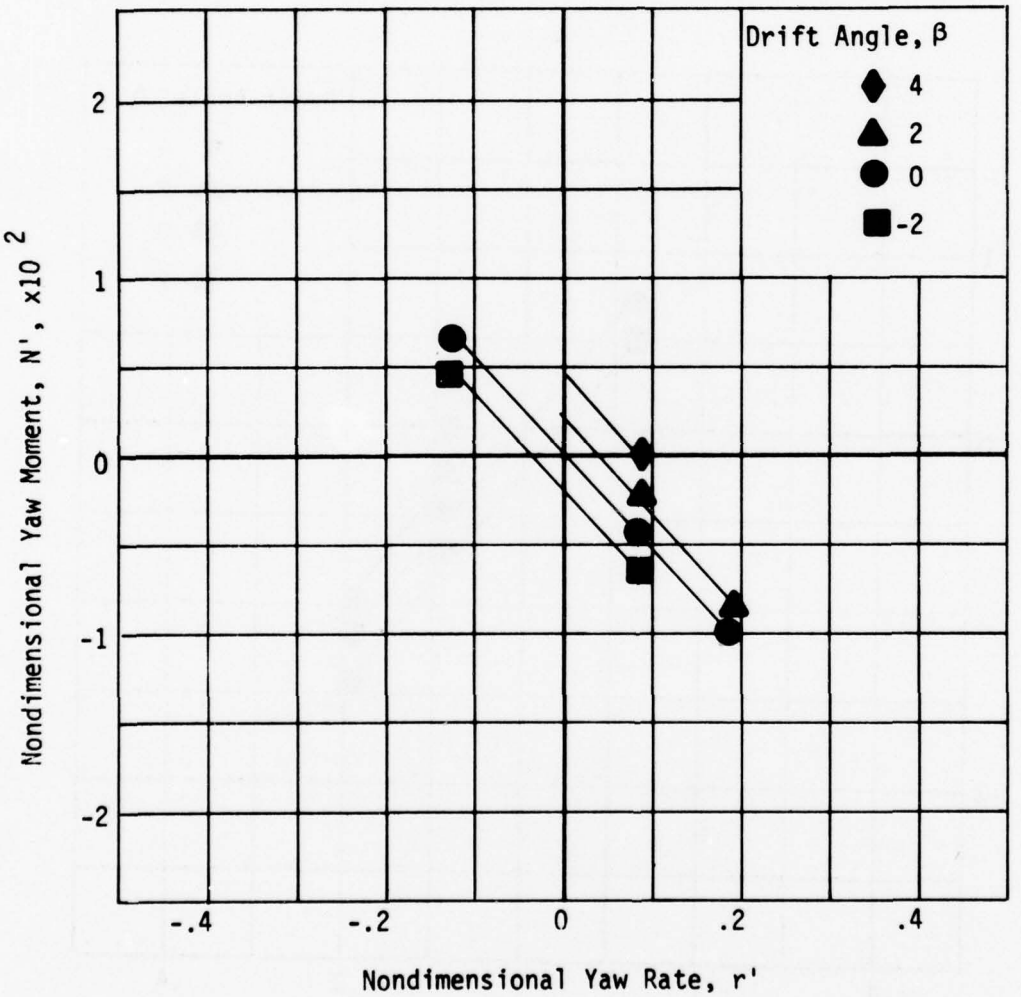

Figure 84 - Variation of Nondimensional Yaw Moment with Nondimensional Yaw Rate for a Series of Drift Angles at a Full Scale Speed of 18 Knots at Deep Draft

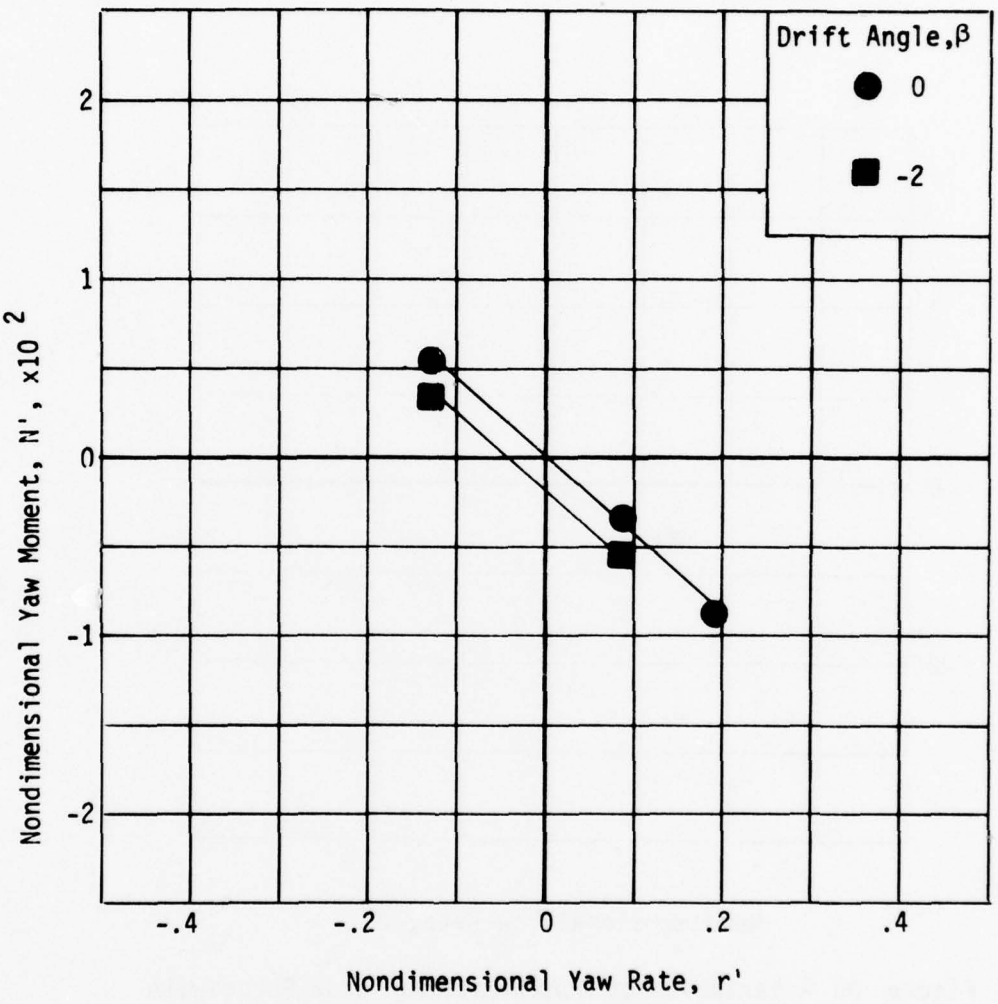

Figure 85 - Variation of Nondimensional Yaw Moment with Nondimensional Yaw Rate for a Series of Drift Angles at a Full Scale Speed of 21 Knots at Deep Draft

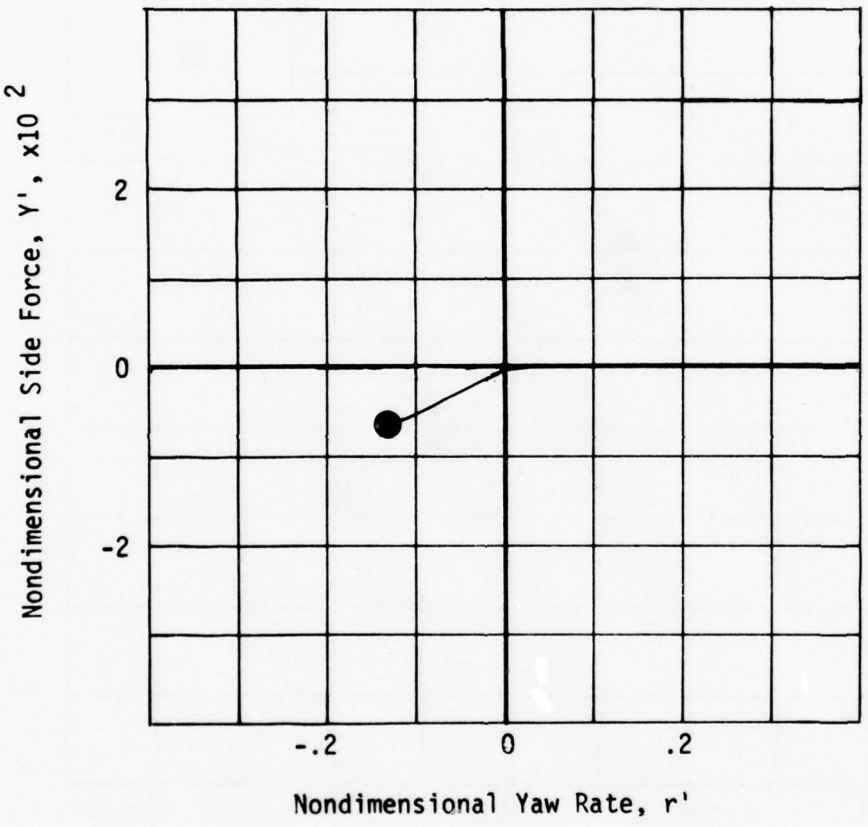

Figure 86 - Variation of Nondimensional Side Force with Nondimensional Yaw Rate for Zero Drift Angle at a Full Scale Speed of 3 Knots at Deep Draft for Drift Angle of Zero Degrees

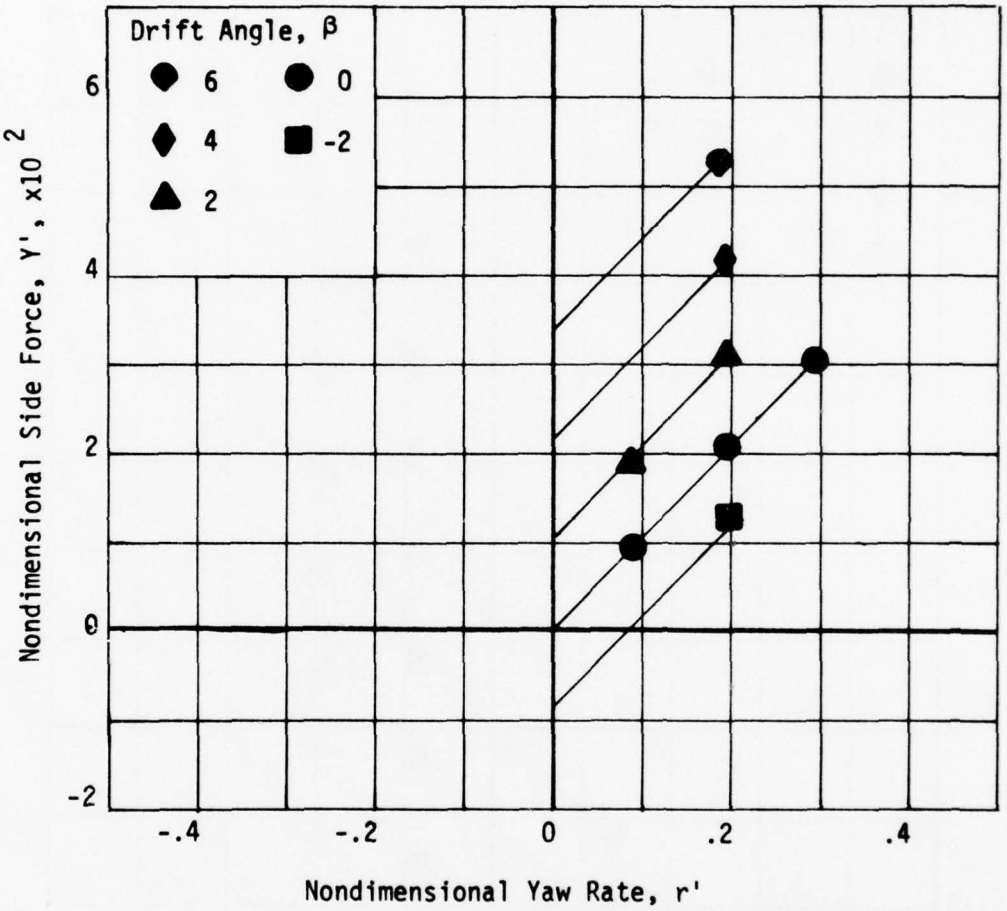

Figure 87 - Variation of Nondimensional Side Force with Nondimensional Yaw Rate for a Series of Drift Angles at a Full Scale Speed of 7 Knots at Deep Draft

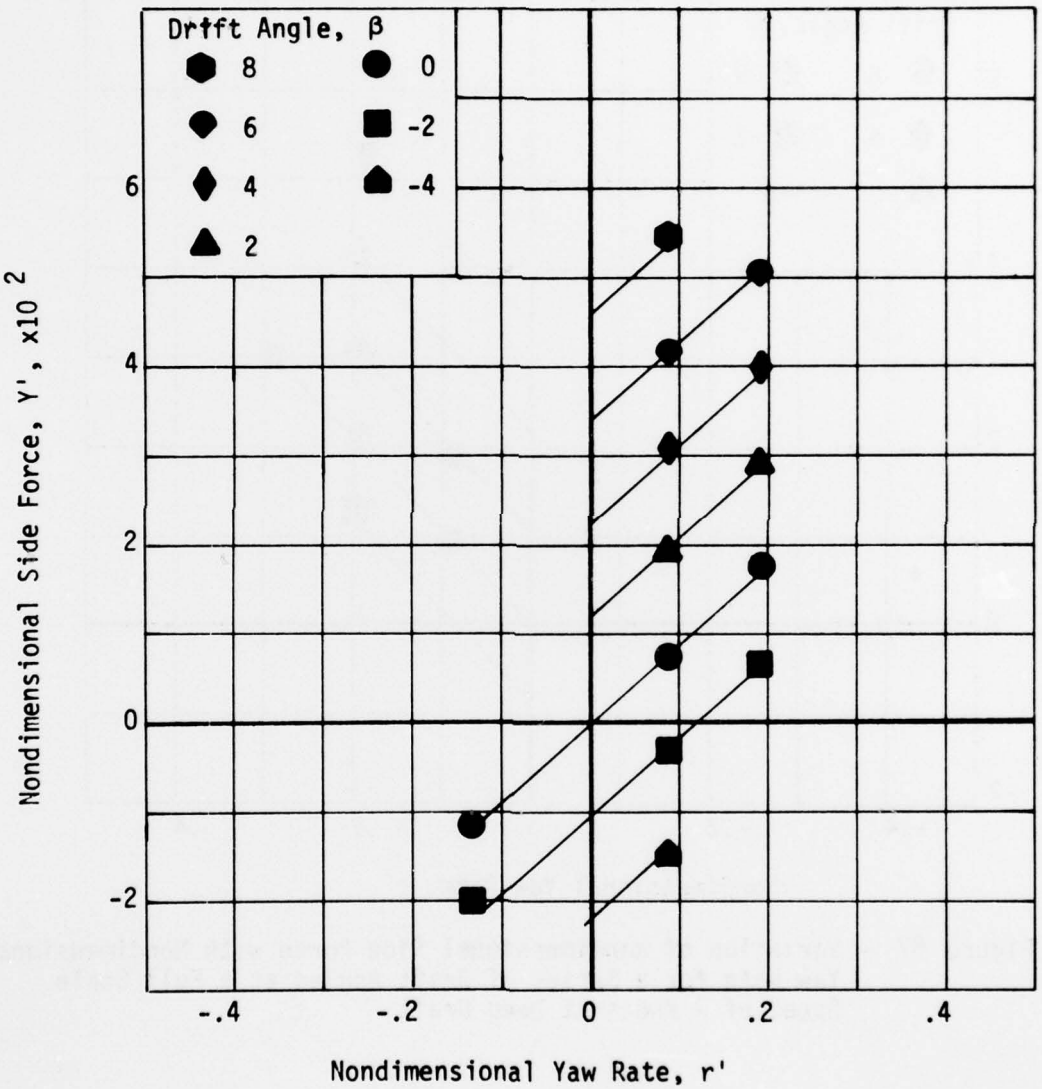

Figure 88 - Variation of Nondimensional Side Force with Nondimensional Yaw Rate for a Series of Drift Angles at a Full Scale Speed of 9 Knots at Deep Draft

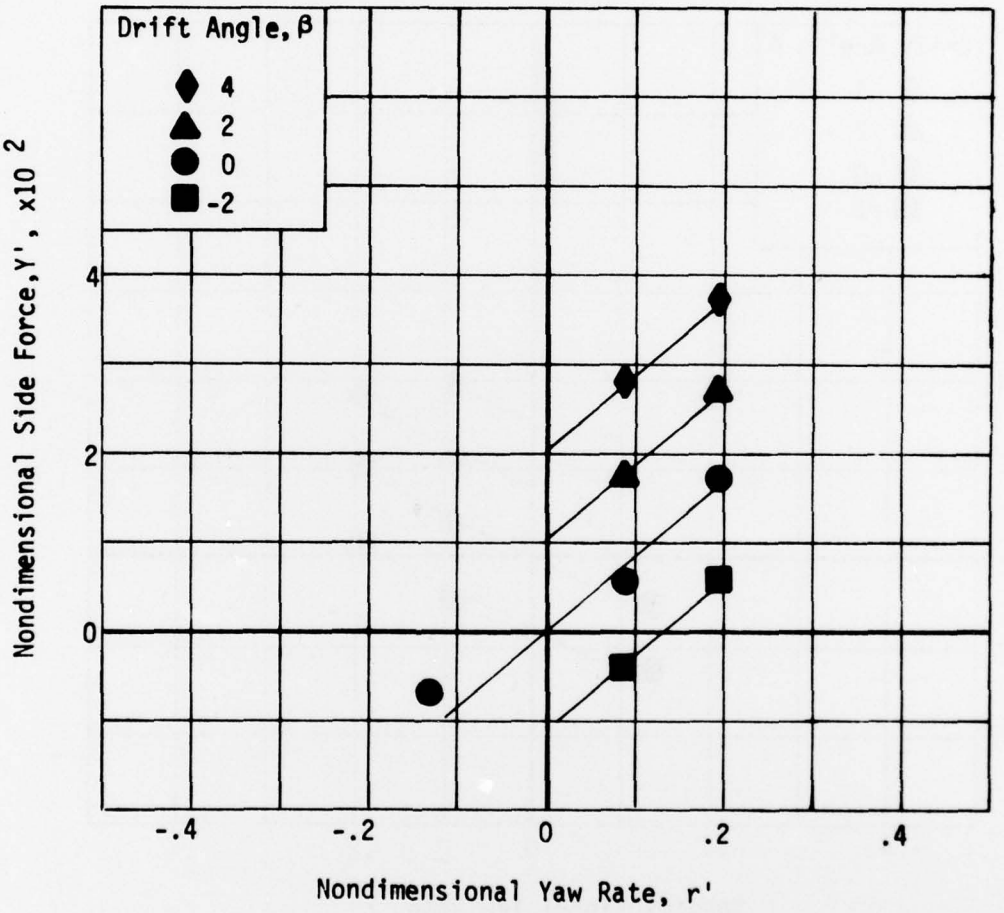

Figure 89 - Variation of Nondimensional Side Force with Nondimensional Yaw Rate for a Series of Drift Angles at a Full Scale Speed of 11 Knots at Deep Draft

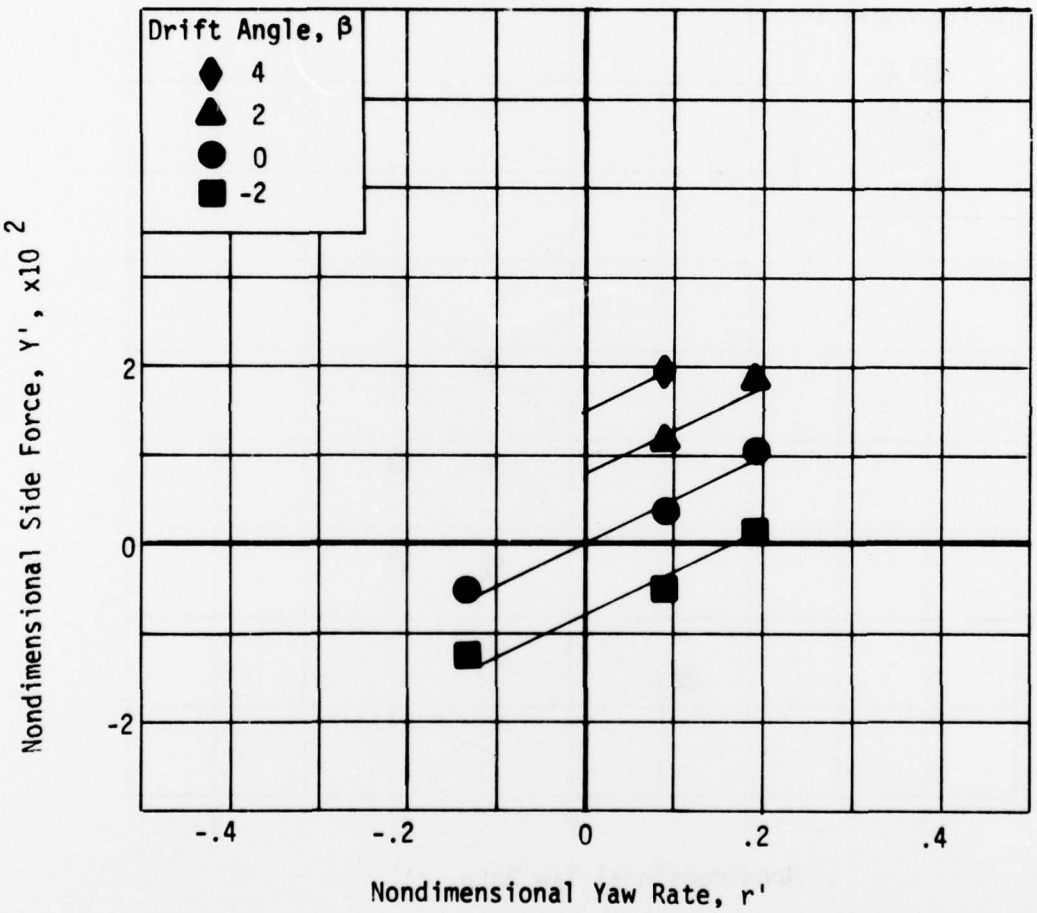

Figure 90 - Variation of Nondimensional Side Force with Nondimensional Yaw Rate for a Series of Drift Angles at a Full Scale Speed of 15 Knots at Deep Draft

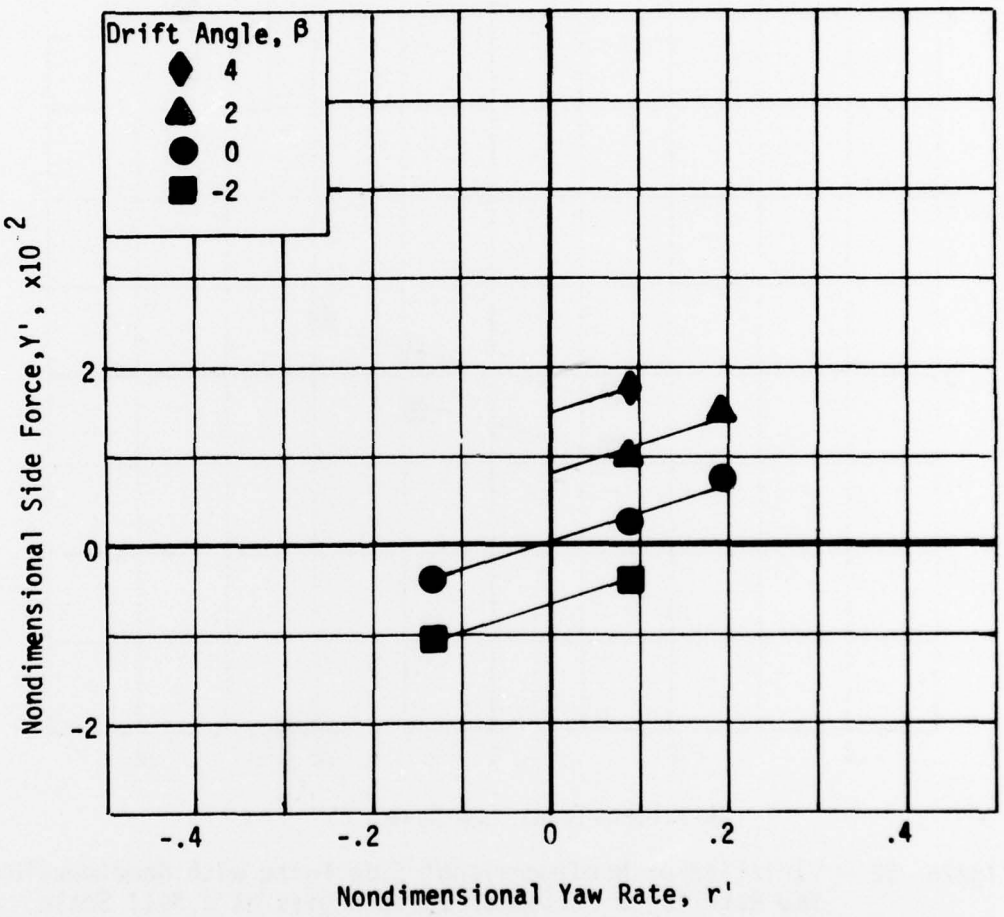

Figure 91 - Variation of Nondimensional Side Force with Nondimensional Yaw Rate for a Series of Drift Angles at a Full Scale Speed of 18 Knots at Deep Draft

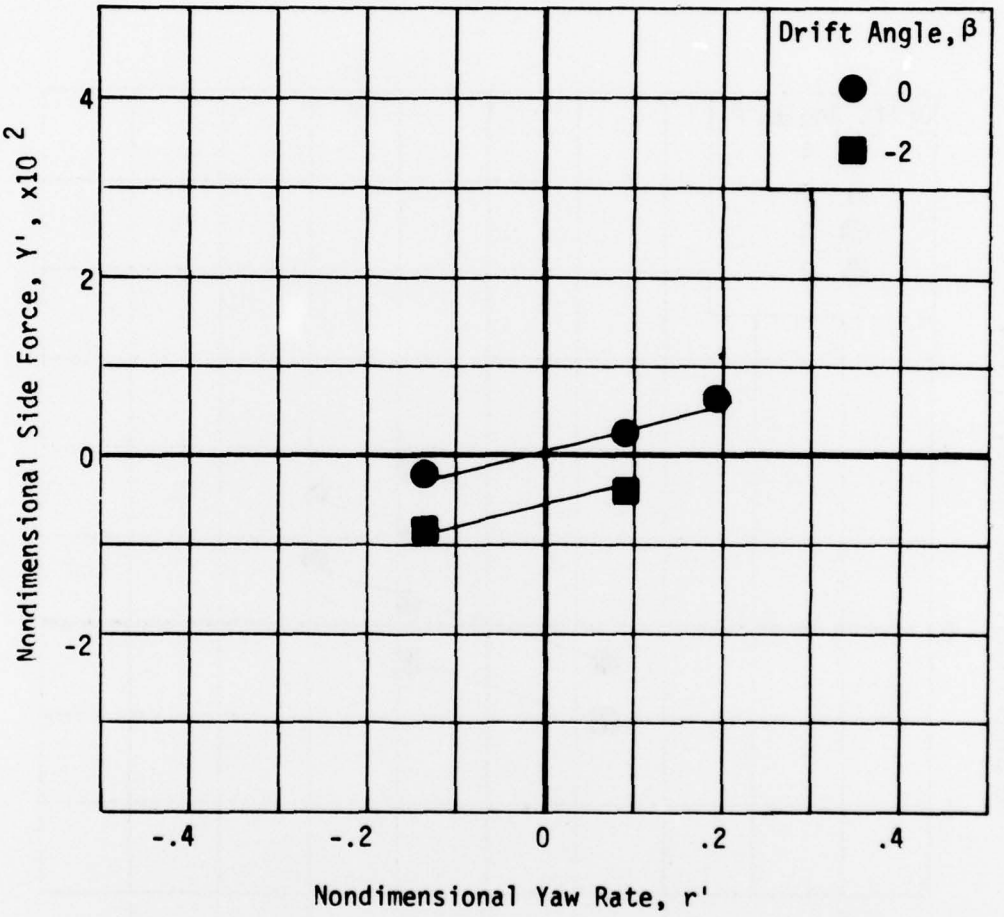

Figure 92 - Variation of Nondimensional Side Force with Nondimensional Yaw Rate for a Series of Drift Angles at a Full Scale Speed of 21 Knots at Deep Draft

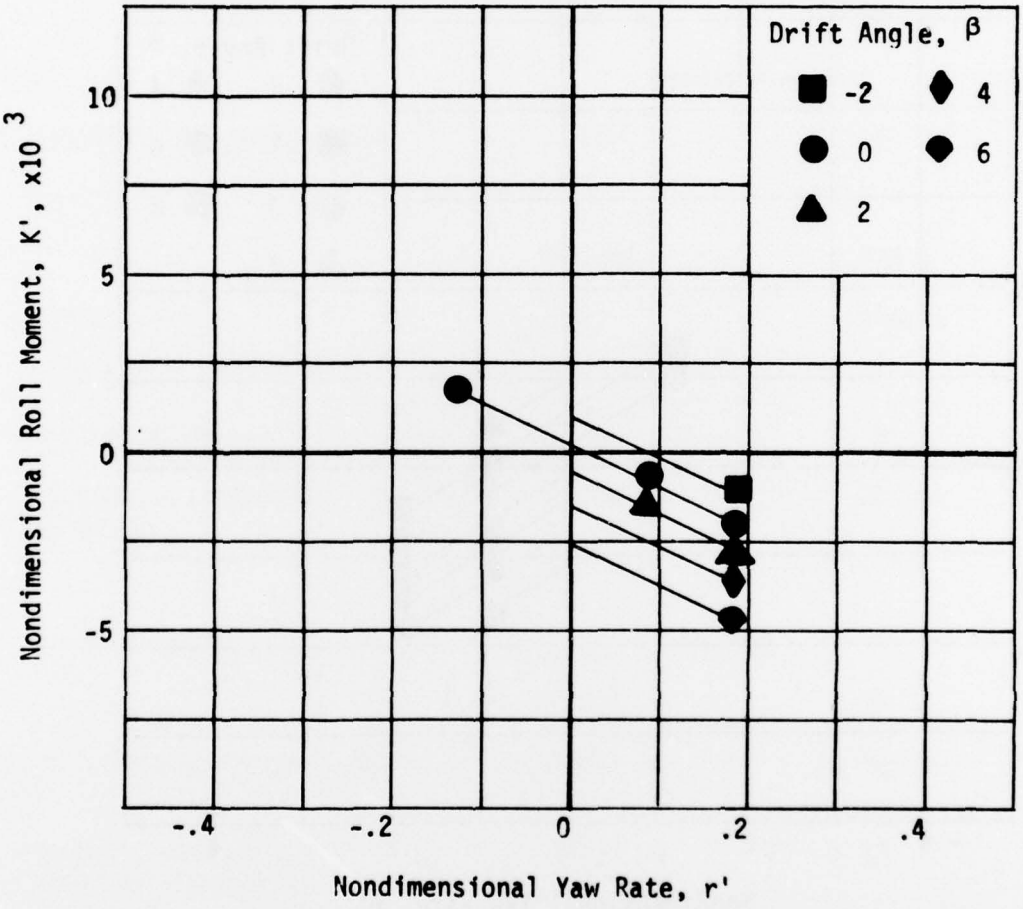

Figure 93 - Variation of Nondimensional Roll Moment with Nondimensional Yaw Rate for a Series of Drift Angles at a Full Scale Speed of 7 Knots at Deep Draft

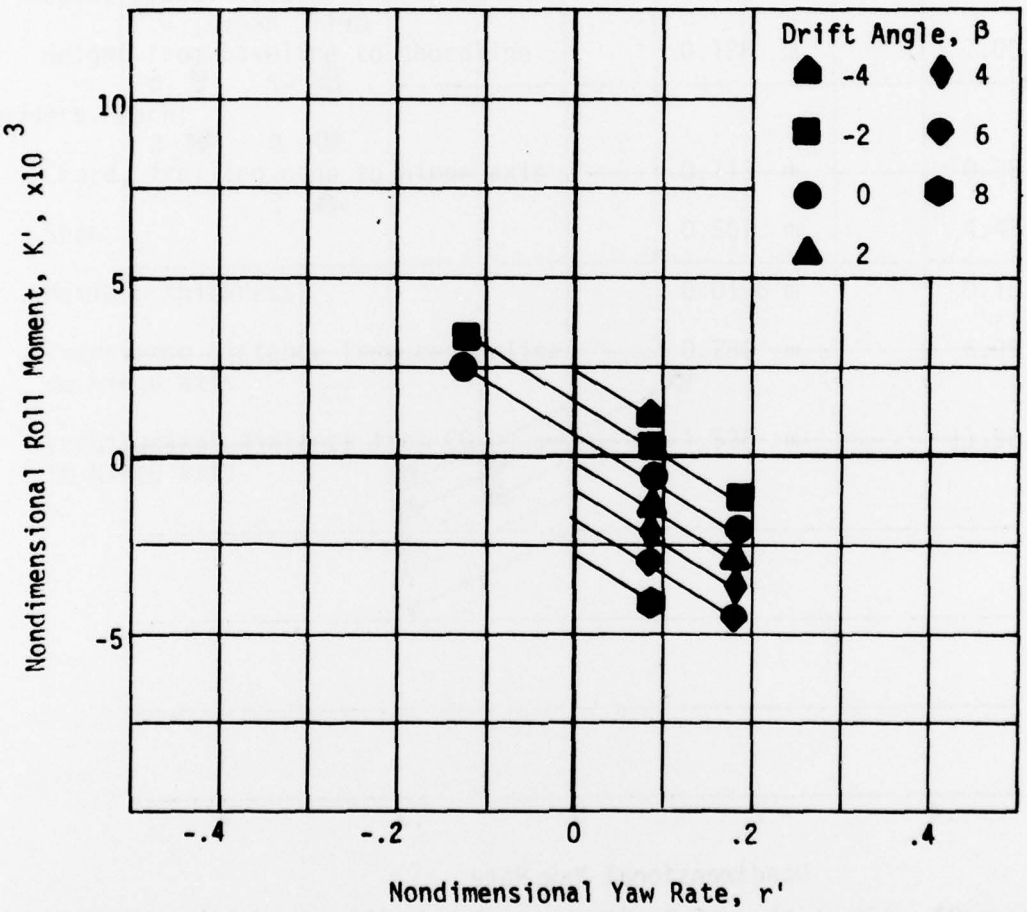

Figure 94 - Variation of Nondimensional Roll Moment with Nondimensional Yaw Rate for a Series of Drift Angles at a Full Scale Speed of 9 Knots at Deep Draft

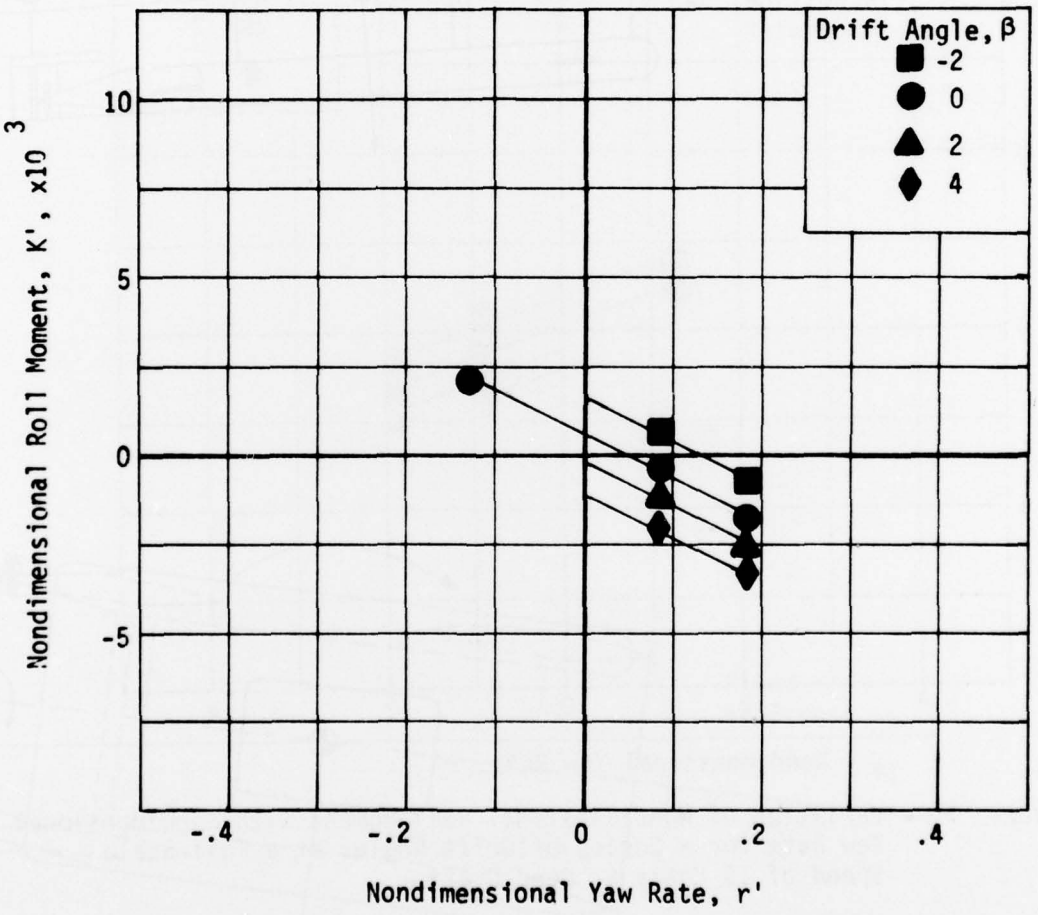

Figure 95 - Variation of Nondimensional Roll Moment with Nondimensional Yaw Rate for a Series of Drift Angles at a Full Scale Speed of 11 Knots at Deep Draft

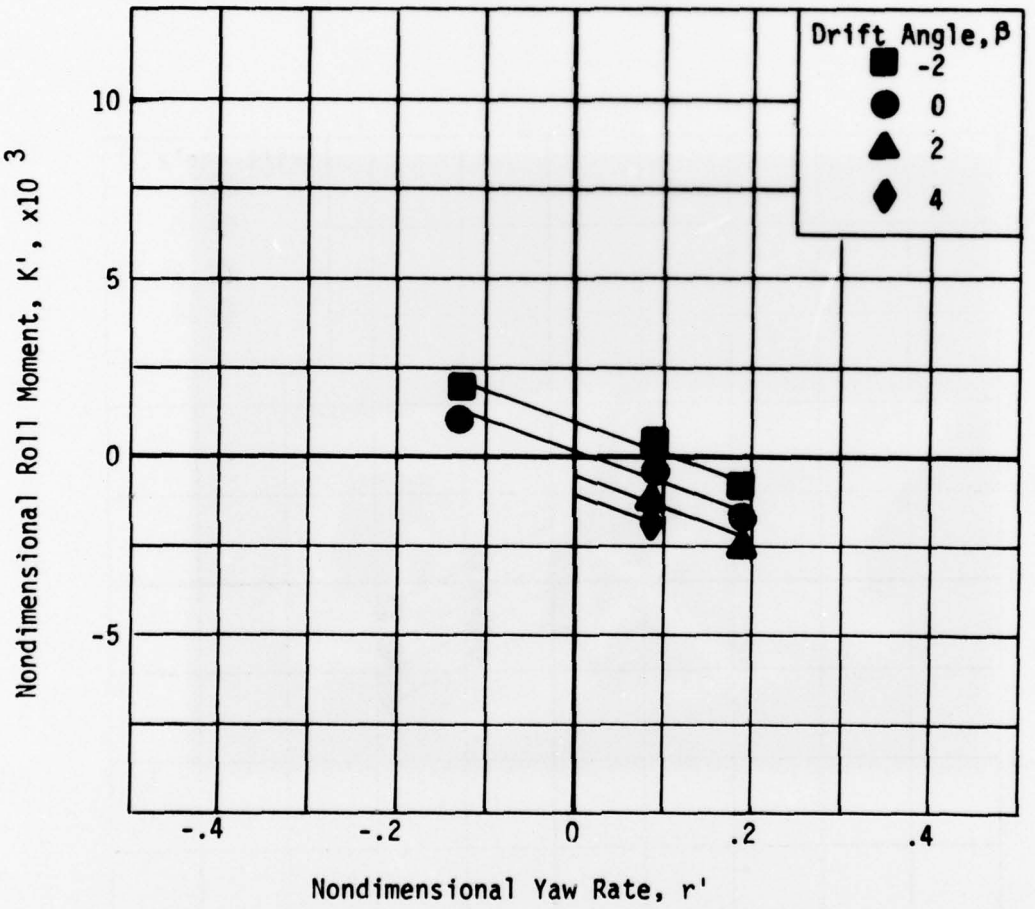

Figure 96 - Variation of Nondimensional Roll Moment with Nondimensional Yaw Rate for a Series of Drift Angles at a Full Scale Speed of 15 Knots at Deep Draft

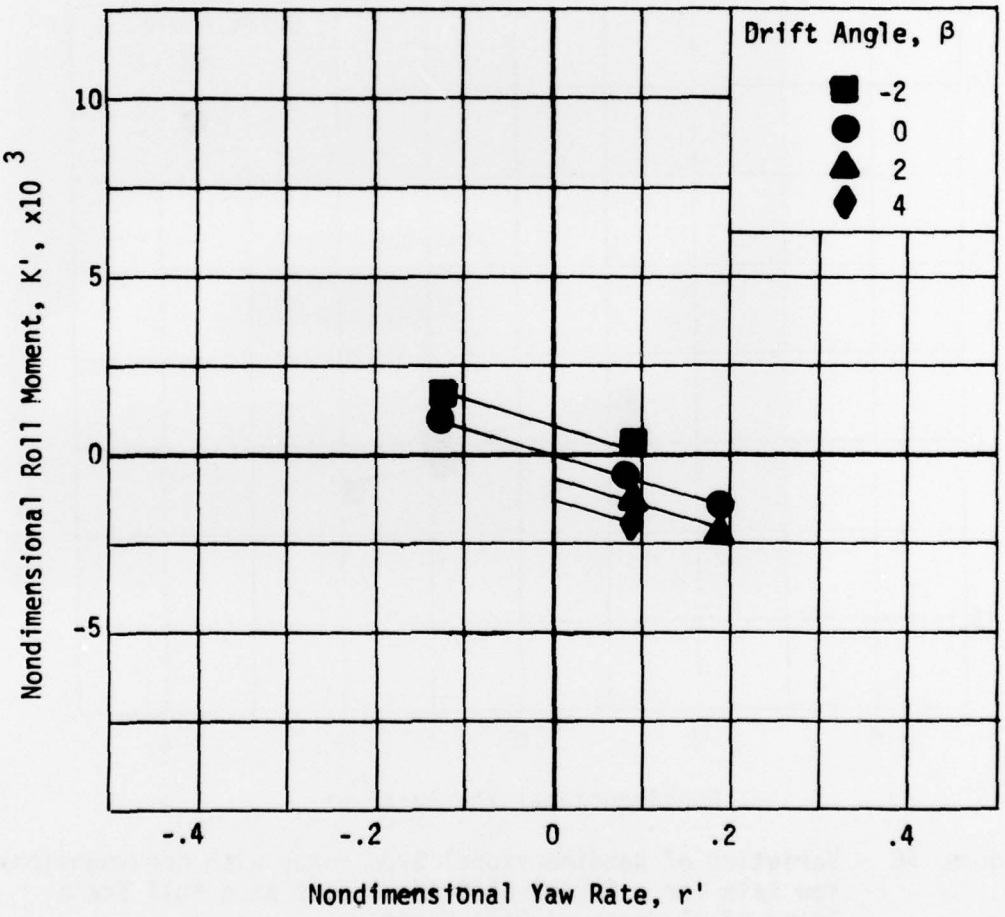

Figure 97 - Variation of Nondimensional Roll Moment with Nondimensional Yaw Rate for a Series of Drift Angles at a Full Scale Speed of 18 Knots at Deep Draft

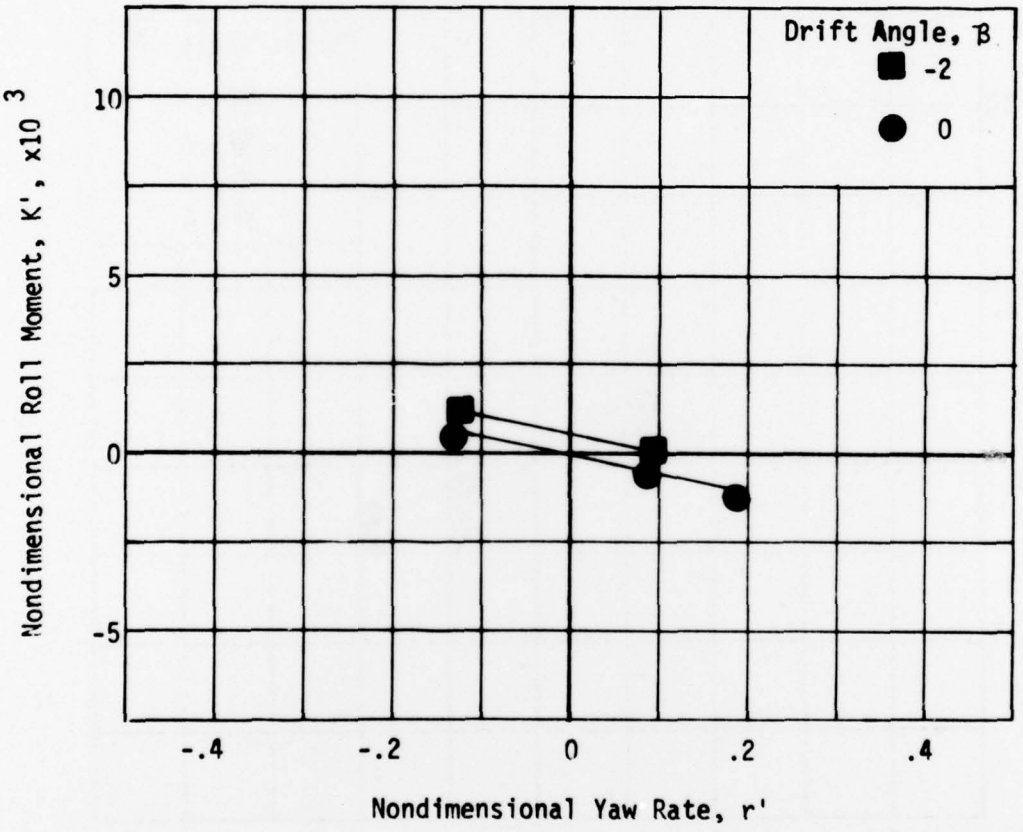

Figure 98 - Variation of Nondimensional Side Force with Nondimensional Yaw Rate for a Series of Drift Angles at a Full Scale Speed of 21 Knots at Deep Draft

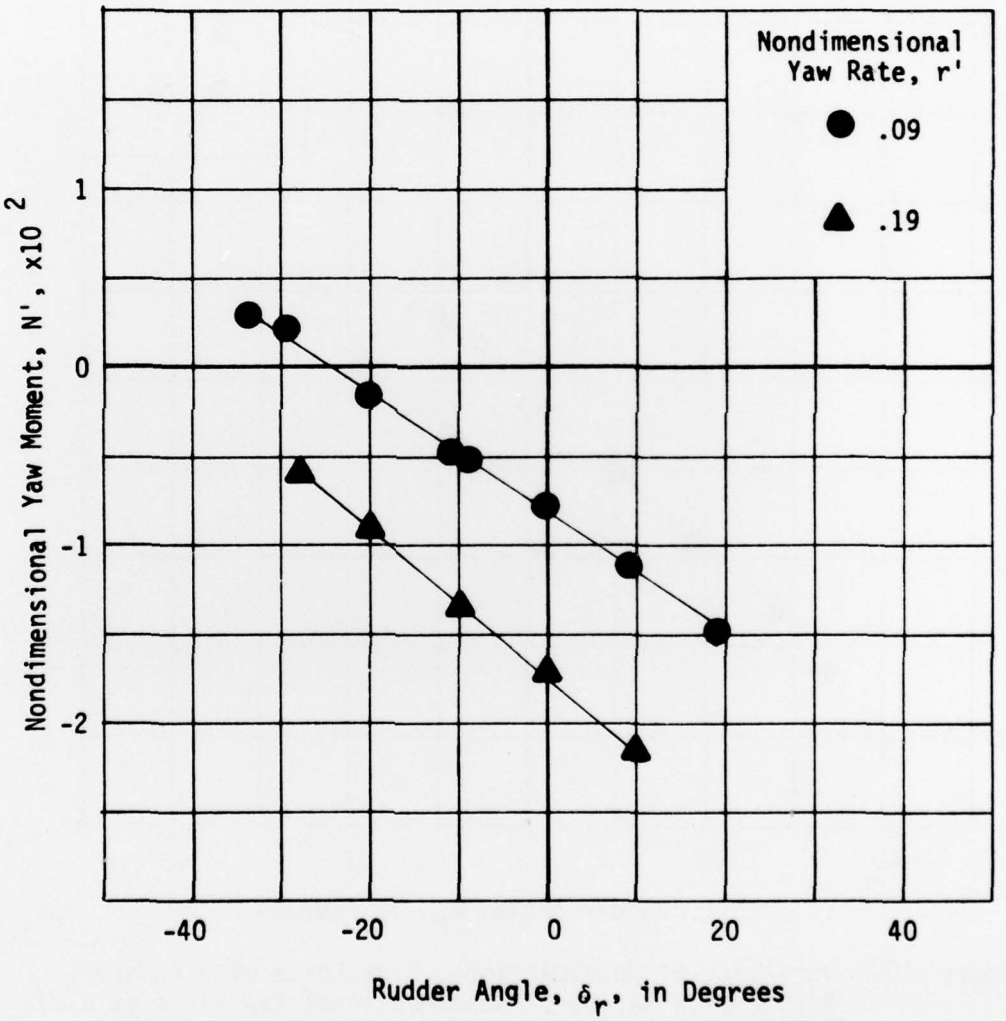

Figure 99 - Variation of Nondimensional Yaw Moment with Rudder Angle for a Series of Nondimensional Yaw Rates at a Full Scale Speed of 9 Knots at Deep Draft

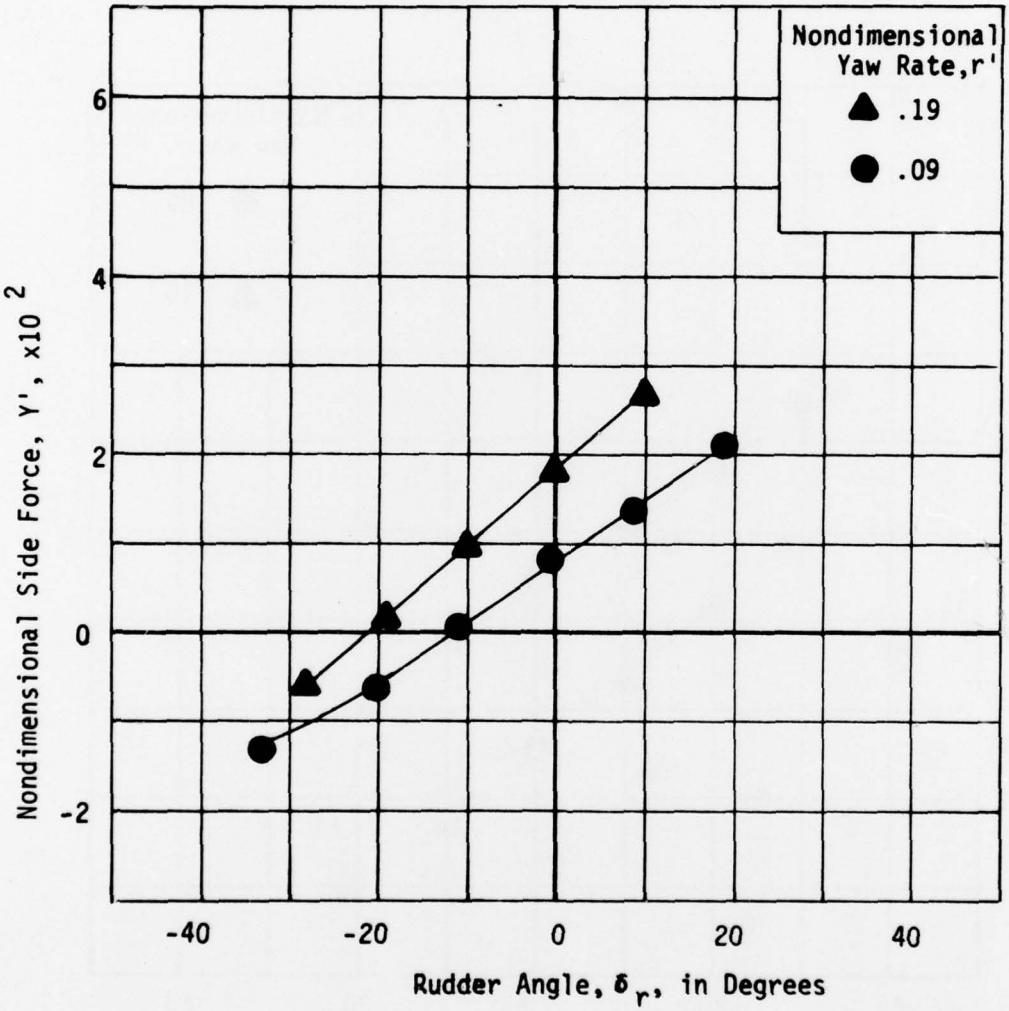

Figure 100 - Variation of Nondimensional Side Force with Rudder Angle for a Series of Nondimensional Yaw Rates at a Full Scale Speed of 9 Knots at Deep Draft

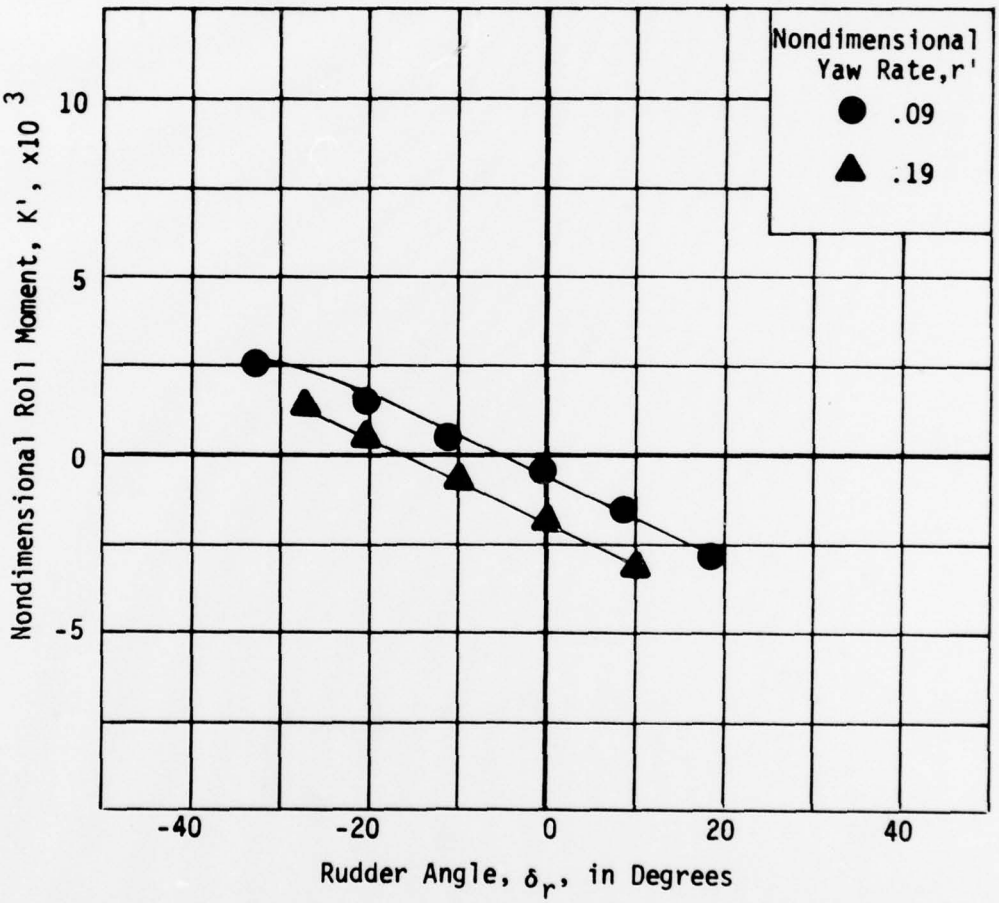

Figure 101 - Variation of Nondimensional Roll Moment with Rudder Angle for a Series of Nondimensional Yaw Rates at a Full Scale Speed of 9 Knots at Deep Draft

DTNSRDC ISSUES THREE TYPES OF REPORTS

1. DTNSRDC REPORTS, A FORMAL SERIES, CONTAIN INFORMATION OF PERMANENT TECHNICAL VALUE. THEY CARRY A CONSECUTIVE NUMERICAL IDENTIFICATION REGARDLESS OF THEIR CLASSIFICATION OR THE ORIGINATING DEPARTMENT.

2. DEPARTMENTAL REPORTS, A SEMIFORMAL SERIES, CONTAIN INFORMATION OF A PRELIMINARY, TEMPORARY, OR PROPRIETARY NATURE OR OF LIMITED INTEREST OR SIGNIFICANCE. THEY CARRY A DEPARTMENTAL ALPHANUMERICAL IDENTIFICATION.

3. TECHNICAL MEMORANDA, AN INFORMAL SERIES, CONTAIN TECHNICAL DOCUMENTATION OF LIMITED USE AND INTEREST. THEY ARE PRIMARILY WORKING PAPERS INTENDED FOR INTERNAL USE. THEY CARRY AN IDENTIFYING NUMBER WHICH INDICATES THEIR TYPE AND THE NUMERICAL CODE OF THE ORIGINATING DEPARTMENT. ANY DISTRIBUTION OUTSIDE DTNSRDC MUST BE APPROVED BY THE HEAD OF THE ORIGINATING DEPARTMENT ON A CASE-BY-CASE BASIS.